Stony Brook University

Generation of Conformation Sensor Recombinant Antibodies to Understand Redox Regulation of PTP1B

A Dissertation Presented

by

Aftabul Haque

to

The Graduate School

in Partial Fulfillment of the

Requirements

for the Degree of

Doctor of Philosophy

in

Molecular and Cellular Biology

Stony Brook University

December 2010

Stony Brook University

The Graduate School

Aftabul Haque

We, the dissertation committee for the above candidate for the Doctor of Philosophy Degree, hereby recommend acceptance of this dissertation.

Dr. Nicholas K. Tonks
Professor, Cold Spring Harbor Laboratory
Dissertation Advisor

Dr. Todd Miller
Professor, Department of Physiology and Biophysics, Stony Brook University, Chair of the Dissertation Committee

Dr. William P. Tansey
Ingram Professor of Cancer Research, Department of Cell and Developmental Biology, Vanderbilt University, Adjunct Professor, Cold Spring Harbor Laboratory

Dr. Raffaella Sordella
Assistant Professor, Cold Spring Harbor Laboratory

Dr. Nick Carpino
Assistant Professor
Department of Molecular Genetics and Microbiology, Stony Brook University

Dr. Toren Finkel
Chief, Translational medicine Branch, National Heart, Blood and Lung Institute (NHLBI), National Institute of Health (NIH), External Examiner

This dissertation is accepted by the Graduate School.

Lawrence Martin
Dean of the Graduate School

Abstract of the Dissertation

Generation of Conformation Sensor Recombinant Antibodies to Understand Redox Regulation of PTP1B

By

Aftabul Haque

Doctor of Philosophy

In

Molecular and Cellular Biology

Stony Brook University

2010

Protein tyrosine phosphatase 1B (PTP1B) plays important roles in down-regulation of insulin signaling. Although it has been established as a potential therapeutic target for the treatment of diabetes and obesity, the finding of pharmaceutically acceptable inhibitors remains challenging. PTP1B is regulated by reactive oxygen species (ROS) produced in response to insulin. The reversibly oxidized form of this enzyme (PTP1B-OX) is inhibited and undergoes profound conformational changes at the active site. We hypothesized that a conformation-sensor antibody that recognizes PTP1B-OX may stabilize the inactive state and inhibit phosphatase activity. We isolated PTP1B-OX-specific single chain variable fragments (scFvs) from an antibody phage display library. These scFvs displayed significant inhibition of the reactivation of PTP1B-OX by reducing agent, but did not directly inhibit the reduced, wild type enzyme. Selected scFvs bind to PTP1B-OX, but not to PTP1B in its reduced active state, both *in vitro* and when expressed in 293T cells as intracellular antibodies or “intrabodies”. Expression of the intrabody enhanced and extended insulin-induced tyrosyl phosphorylation of the β-subunit of the insulin receptor and its substrate IRS-1. PTP1B-OX-specific intrabody also caused significant enhancement of signaling downstream of the insulin receptor, as revealed by increased PKB/AKT phosphorylation in insulin-stimulated cells. These effects on signaling were diminished when catalase was ectopically co-expressed to quench cellular H_2O_2. Our data suggest that conformation-sensor scFvs can be used as potential inhibitors of PTP1B by stabilizing the transiently oxidized and inactivated form of the enzyme. Therefore, it may be possible to stabilize the oxidized, inactive form of PTP1B with appropriate therapeutic molecules that mimic the effects of these antibodies as a new approach for PTP-directed drug development.

to my parents

Contents

List of Figures

Figure Legends: Chapter 1

Figure Legends: Chapter 2

Figure Legends: Chapter 3

Figure Legends: Chapter 4

List of Tables

Acknowledgements

The research presented in this dissertation was carried out in the laboratory of my supervisor Nicholas K. Tonks at Cold Spring Harbor Laboratory. First and foremost, I would like to thank Nicholas Tonks for his advice, guidance, and support throughout my research project. I am grateful for his tireless supervision, constructive criticism, patience and understanding and most importantly for his constant encouragement at various steps of my thesis project, especially at times when it was needed the most. As a mentor he enabled me to develop an understanding of the subject and taught me to think independently about my research.

I acknowledge the members of my thesis committee, Todd Miller, William Tansey, Raffaella Sordella, Nick Carpino, and Michael Myers for their valuable insights and suggestions during the progress of my project. I would like to express my special appreciation to Toren Finkel for being the External Examiner of my Defense and for his valuable inputs in my project. I would like to thank MCB Graduate Program, its faculties and staff for providing me the opportunity to pursue my education and research at Stony Brook University.

I am heartily thankful to all the present members of Tonks Lab: Benoit Boivin, Li Li, Navasona Krishnan, Ulla Schwertassek, Gaofeng Fan, Gyula Bencze, Guang Lin, Fauzia Chaudhary, Mathangi Ramesh, Ming Yang, Xiaoqun (Catherine) Zhang, Xin Cheng, Paloma Anderson, Brady Patricia, and Margaret Wallace for their continuous support, helpful discussions and overall for creating a warm working environment in the lab. I also thank past members of the lab, with whom I worked for some time: Jannik Andersen**,** Deirdre Buckley, Robert Del Vecchio**,** Hsu-Hsin (May) Chen, Naira Gorovits, Shantá Hinton, Lifang Zhang, Antonella Piccini, and Jennifer Ye for their help and support. I would like to extend my special thanks to Jannik Andersen for his efforts and initiatives at the beginning of my project.

I am very thankful to all my friends in the MCB Program and at Cold Spring Harbor Laboratory for their encouragement and help in all aspects of life during the completion of my project. Finally I thank my family for being a constant source of inspiration in each and every step of my study and research.

Patents and Publications

Nicholas Tonks and Aftabul Haque (2010). US patent application C1300.70013WO00 “PTP1B Inhibitors”

Chapter 1

Redox Regulation of PTP1B: Therapeutic Implications

1.1 Protein Tyrosine Phosphatases

Reversible protein phosphorylation is an important post-translational modification involved in regulating a vast array of biological functions including cell growth and differentiation, cell motility, and proliferation (reviewed in (Tonks and Neel, 1996)). Fisher and Krebs first discovered this reversible protein phosphorylation in regulation of glycogen metabolism when they found that glycogen phosphorylase is activated by addition of a phosphate group (Fischer and Krebs, 1955; Krebs and Fischer, 1956). Protein phosphorylation is reversibly regulated by two broad groups of enzymes: the protein kinases and the proteins phosphatases. The kinases are the enzymes that transfer the phosphate groups from ATP to target proteins whereas the protein phosphatases remove the phosphate from substrate phospho-proteins by hydrolysis (Figure 1.1).

Based on substrate specificity, protein phosphatases are broadly divided into two groups: the protein tyrosine phosphatases (PTPs) and the protein serine/threonine phosphatases. There are other phosphatases with different structural and functional features such as acid phosphatases, alkaline phosphatases, lipid phosphatases etc. PTPs have the capacity to function as inhibitors of pTyr-dependent signaling as well as positive regulators in promoting signaling. The protein tyrosine phosphatase (PTP) superfamily of enzymes regulates a number of signaling pathways in a coordinated manner with protein tyrosine kinases to control an array of fundamental physiological processes. This important regulatory role of PTPs in biological systems is apparent in their involvement in the etiology of multiple diseases resulting from deregulated signaling for the lack or improper functioning of specific members of PTP family (Figure 1.2).

The protein tyrosine phosphatase (PTP) superfamily consists of two major groups: the classical PTPs, which target phosphotyrosyl residues on the substrate proteins and the dual specificity phosphatases (DSPs), which dephosphorylate both phosphotyrosyl and phosphoseryl/threonyl residues. All these different classes of PTPs share a common, evolutionarily conserved signature catalytic motif ($C(X)_5R$) in their

Figure 1.1

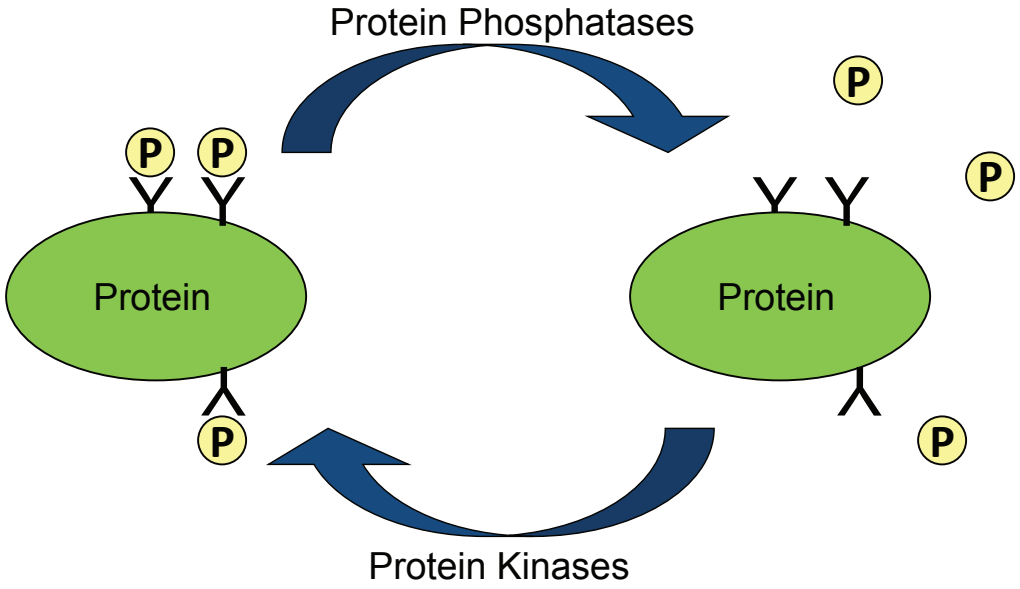

Figure 1.2

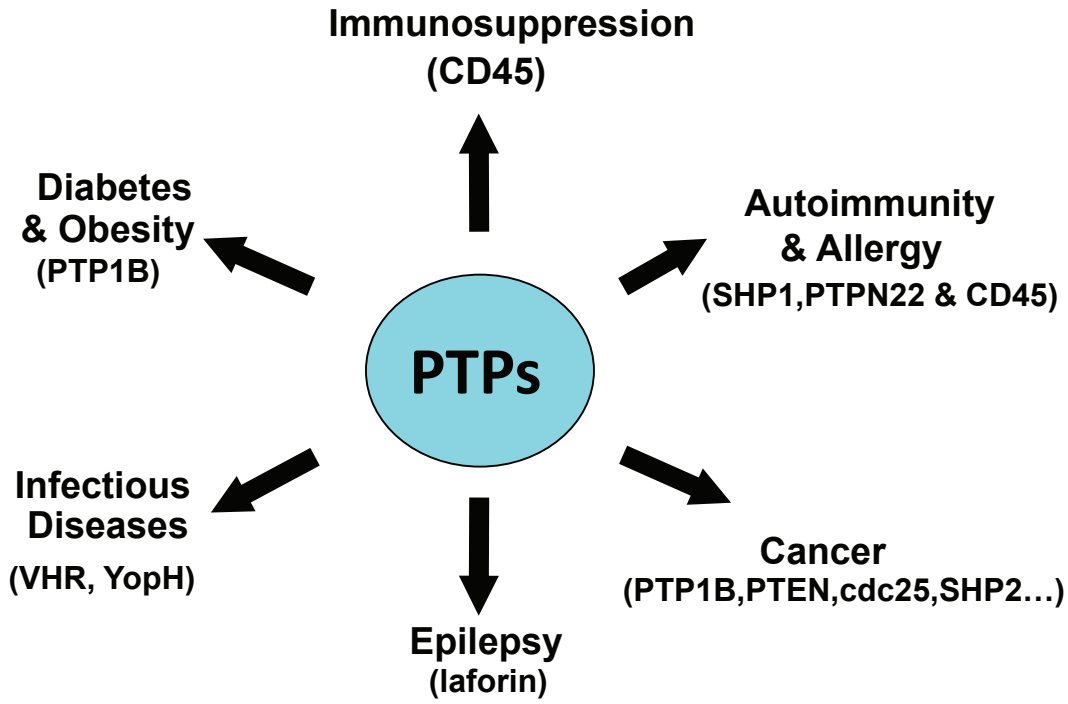

Figure1.1. Reversible Phosphorylation of Proteins.
Protein phosphorylation is one of the major signal transducing mechanisms in cells. Two groups of enzymes control the protein phosphorylation states: the protein kinases and the protein phosphatases. The kinases transfer phosphate groups from ATP to protein, whereas the protein phosphatases catalyze the removal of phosphate groups.

Figure 1.2. PTPs and Human Diseases.
Many PTPs have been implicated in various human diseases including cancer, diabetes, immune and infectious diseases. PTP1B has been well established as a bona fide target for treatment of diabetes and obesity. The phenotype of the PTP1B knockout mouse suggests that an inhibitor of this PTP will address both obesity and insulin resistance, thereby presenting a unique therapeutic opportunity.

primary sequence, in which the invariant Cys and Arg residues are essential for catalysis. The classical PTPs recognize phosphotyrosyl residues exclusively as their substrate. This group is further sub-classified on the basis of their cellular localization: the transmembrane PTPs and the cytosolic PTPs (Figure 1.3).

1.2 PTP1B Structure and Function

1.2.1 Structural Features of PTP1B Catalytic Domain

Protein tyrosine phosphatase 1B (PTP1B) is the prototypical member of the family of PTPs, and has been the most extensively studied within this group. It was the first identified member of the PTP superfamily and was purified to homogeneity from human placenta as a catalytic domain of 37 kDa (Tonks et al., 1988b). The purified protein demonstrated absolute specificity and high affinity for phospho-tyrosyl substrates and showed no activity on phosphoseryl/phosphothreonyl proteins. The activity of this protein was also found to be absolutely dependent on a catalytic cysteine residue (Tonks et al., 1988a). Later, it was characterized as a ~50 kDa protein (435 amino acids), consisting of a defined N-terminal catalytic domain (PTP domain) followed by a C-terminal segment that serves a regulatory function and anchors the protein at the cytoplasmic face on the ER membrane (Brown-Shimer et al., 1990; Chernoff et al., 1990; Frangioni et al., 1992; Guan et al., 1990) (Figure 1.4 A). PTP1B contains a signature catalytic motif (the PTP loop) consisting of 11 residues: (I/V)HCXAGXXR(S/T)G, a highly conserved structural feature among PTPs (Tonks, 2003). Cys215 and Arg221 within this motif are essential for its catalytic activity (Tonks, 2003). The crystal structure of the 37 kDa PTP1B catalytic domain shows that there is a single domain consisting of eight α-helices and 12 β-strands (Barford et al., 1994) (Figure 1.4 B). The signature motif is located at the base of the catalytic cleft. Three separate motifs, the WPD loop, the Q loop and the pTyr loop define the sides of the cleft. The WPD loop contains the invariant Asp residue, which is involved in the catalysis process by acting as both general acid and base in two separate steps of the phosphatase catalytic mechanism. The Q loop contains Gln262, which mediates release of phosphate from the substrate. Tyr46 in the pTyr loop defines the depth of the

Figure 1.3

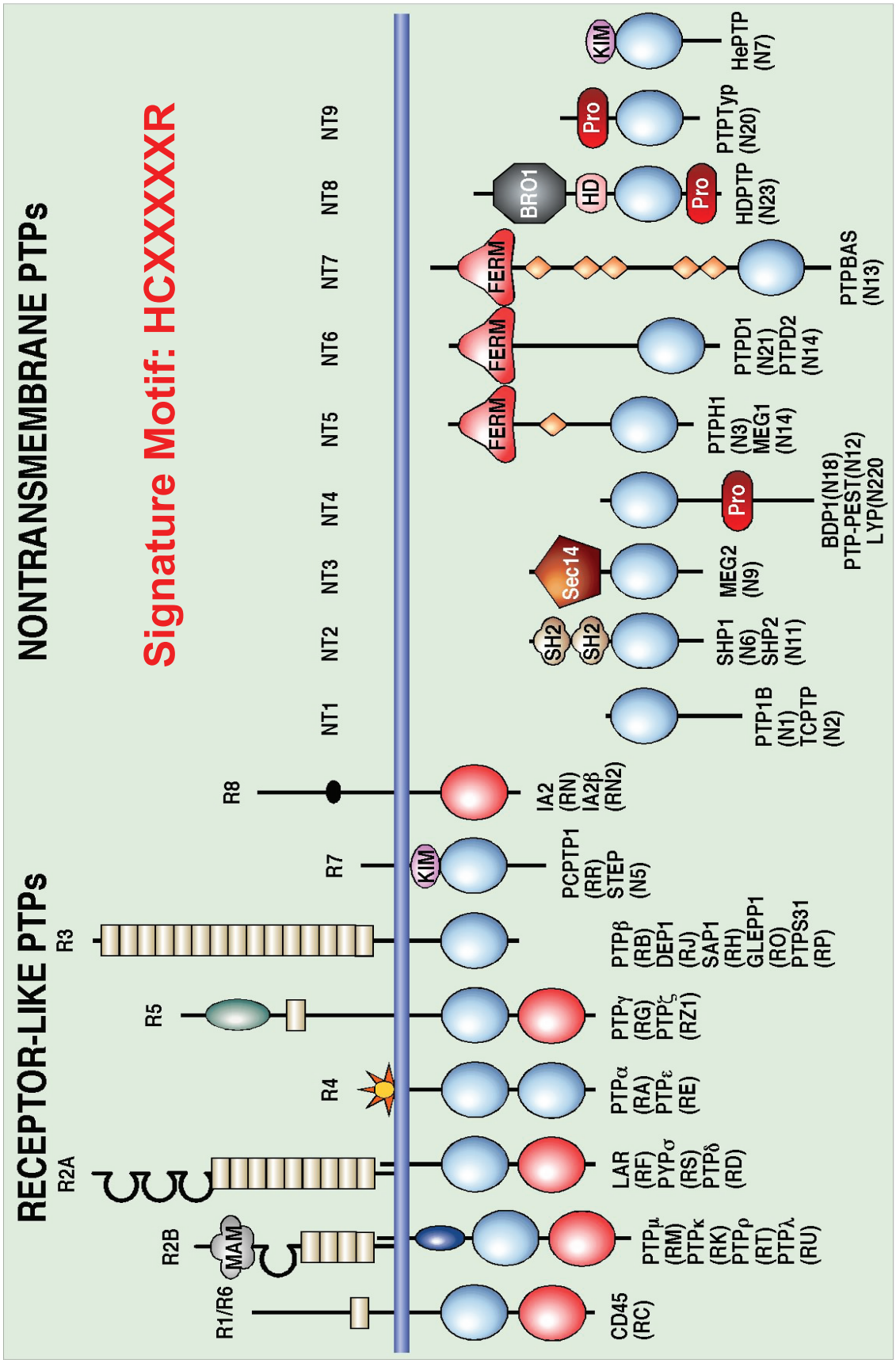
RECEPTOR-LIKE PTPs
NONTRANSMEMBRANE PTPs
Signature Motif: HCXXXXXR
R1/R6
R2A
R2B
MAM
R3
R4
R5
R7
R8
NT1
NT2
NT3
NT4
NT5
NT6
NT7
NT8
NT9
CD45 (RC)
PTPμ (RM) PTPκ (RK) PTPρ (RT) PTPλ (RU)
LAR (RF) PTPσ (RS) PTPδ (RD)
PTPα (RA) PTPε (RE)
PTPγ (RG) PTPζ (RZ1)
PTPβ (RB) DEP1 (RJ) SAP1 (RH) GLEPP1 (RO) PTPS31 (RP)
KIM
PCPTP1 (RR) STEP (N5)
IA2 (RN) IA2β (RN2)
PTP1B (N1) TCPTP (N2)
SH2
SH2
SHP1 (N6) SHP2 (N11)
Sec14
MEG2 (N9)
Pro
BDP1(N18) PTP-PEST(N12) LYP(N220
FERM
FERM
FERM
PTPH1 (N3) MEG1 (N14)
PTPD1 (N21) PTPD2 (N14)
PTPBAS (N13)
BRO1
HD
Pro
HDPTP (N23)
Pro
PTPTyp (N20)
KIM
HePTP (N7)

Figure 1.3. The classical protein tyrosine phosphatases (PTPs).
The classical PTPs are divided in two broad groups – the transmembrane receptor-like proteins (RPTPs) and non-transmembrane (NT) cytoplasmic proteins. The PTPs are structurally and functionally different from the Ser/Thr phosphatases. They are defined by the presence of a signature motif in the catalytic core, in which Cys and Arg are essential for catalysis. Receptor-like PTPs can regulate cellular signaling by ligand controlled dephosphorylation of the tyrosine residues of the substrate proteins whereas the non-transmembrane PTPs dephosphorylate their substrates at various locations in the cytoplasm. PTP1B is the prototypic member of the PTP superfamily. It is broadly classified in the non-transmembrane family of PTPs. Its localization in the cytoplasm, however, is unique as it is anchored in the ER membrane by a C-terminal transmembrane sequence with the catalytic domain facing the cytoplasm. [adopted from (Tonks, 2006)]

Figure 1.4

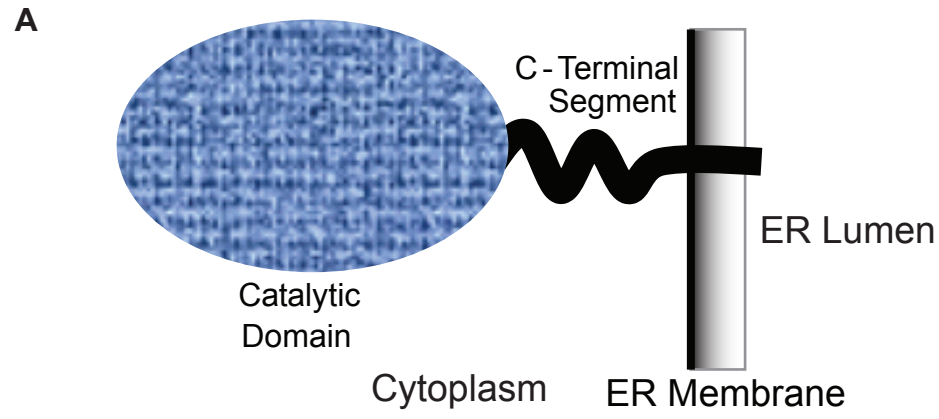
A
C - Terminal
Segment
ER Lumen
Catalytic
Domain
Cytoplasm
ER Membrane

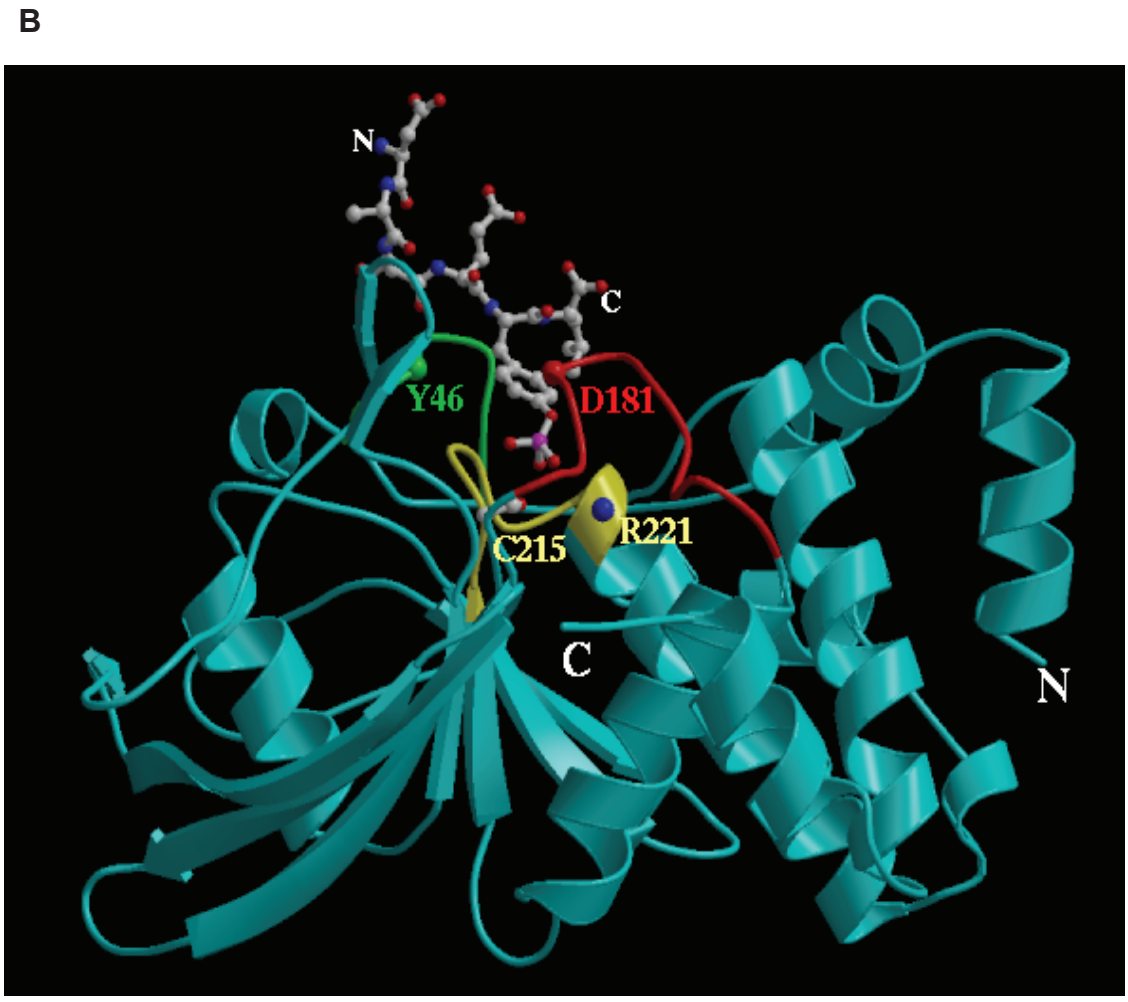
B
N
C
Y46
D181
C215
R221
C
N

Figure1.4. Structure of PTP1B.
(A) Schematic Representation of PTP1B Structure and Localization. The cytosolic catalytic domain (oval shaped) is anchored to the ER membrane by a hydrophobic ER anchoring motif at the very end of the C-terminal segment [adopted form (Flint et al., 1993)].
(B) Crystal Structure of the active site of PTP1B. Ribbon representation of the crystal structure of the 37 kDa catalytic domain of PTP1B in conjunction with a hexapeptide substrate, modeled on the basis of the autophosphorylated epidermal growth factor receptor (EGFR), which is a physiological substrate of PTP1B (Jia et al., 1995). Critical elements of the catalytic core – the signature motif (yellow), the WPD loop (red) and the pTyr loop (green) are shown.

cleft and along with the nearby residue Val49 contributes to the substrate specificity. There are two hydrogen bonds that stabilize the active site cleft – one is between the catalytic Cys215 and nearby Se222 and the other one is between Ser216 of the PTP loop and Tyr46 of the phosphotyrosine loop.

1.2.2 Catalytic Mechanism of PTP1B

The phosphatase mechanism of PTP1B involves a two-step process (Figure 1.5). In the first step, the cysteine in the active site acts as a nucleophile that attacks the incoming phosphate; the aspartate in the WPD loop functions as a general acid to form the cysteinyl phosphate as an intermediate, with release of the dephosphorylated substrate. In the second step, the cysteinyl phosphate intermediate is hydrolyzed to release free phosphate and to restore the active form of the enzyme. Biochemical studies and crystallographic analysis revealed a thorough mechanical insight of the phosphatase reaction (Barford et al., 1995; Jia et al., 1995), which is described below.

Tyr46 and Val49 of the recognition loop guide the phosphorylated tyrosine residue of the substrate for proper entry in the active site cleft. These two residues also aid in the retention of the phosphotyrosine molecule by providing a non-polar pocket for the phenol ring of the phosphotyrosine moiety while the phosphorylated end is securely placed in the polar catalytic cleft. Substrate entry in the catalytic site is accompanied by a major conformational change in the WPD loop. Crystallographic studies showed that PTP1B exists in 'open' and 'closed' conformations (Barford et al., 1994; Barford et al., 1995; Jia et al., 1995). The catalytic WPD loop (Trp179, Pro180 and Asp181) swings out to form a substrate accessible binding pocket in the open conformation. In the presence of substrate, the WPD loop closes over the Tyr(P)-binding pocket to facilitate cleavage of the Tyr(P) substrate by forming a catalytically competent closed conformation that promotes subsequent nucleophilic attack. In this closed conformation Asp181 moves close to the tyrosine phosphate and acts as a general acid during the reaction. Concurrent movement within the PTP loop allows Arg 221 to shift towards the phosphotyrosine to adjust its connection with the phosphate moiety and stabilize the closed conformation. At this optimized catalytic position the gamma sulfur atom of

Figure 1.5

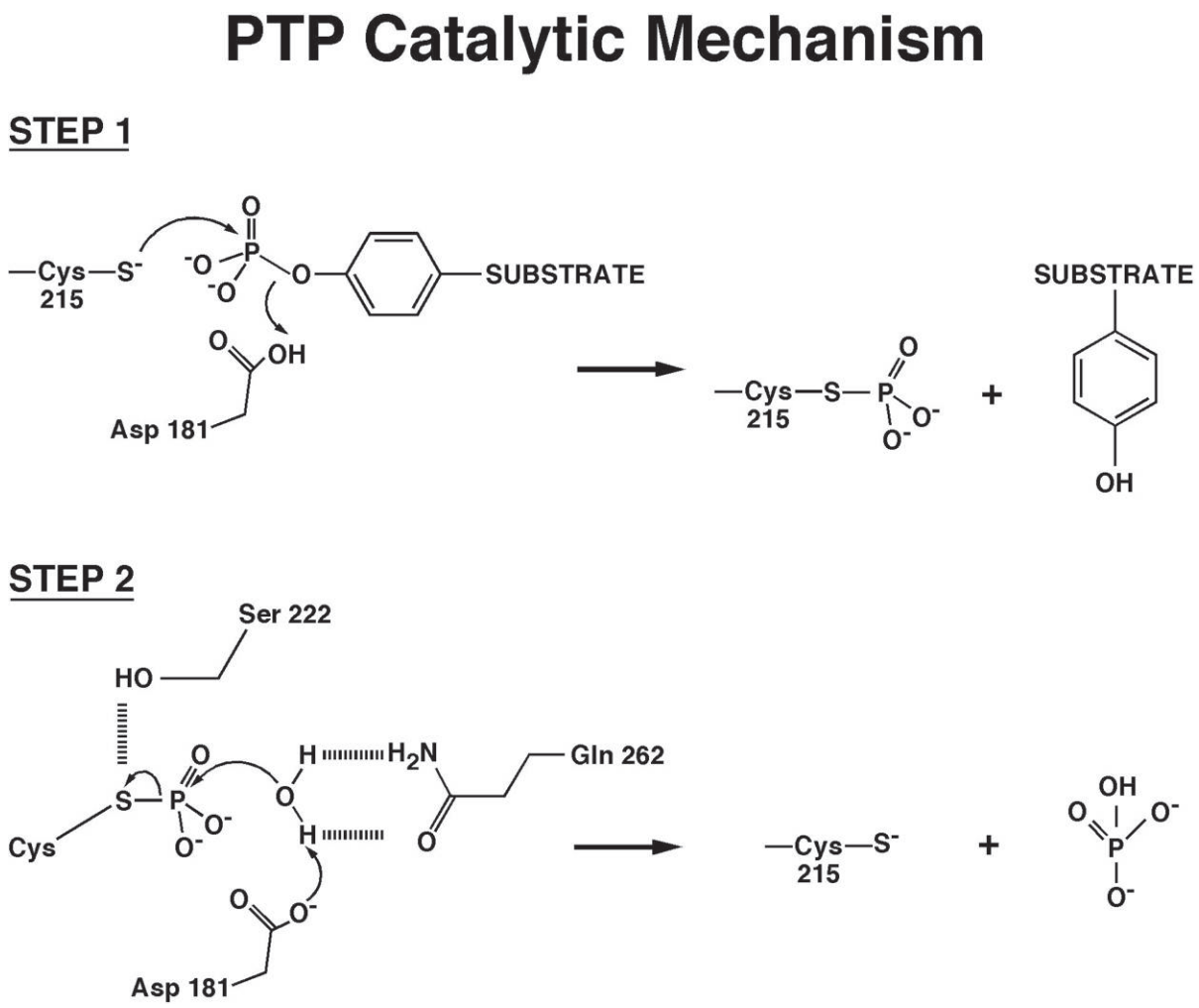
PTP Catalytic Mechanism
STEP 1
—Cys—S⁻
215
SUBSTRATE
Asp 181
SUBSTRATE
OH
STEP 2
Ser 222
HO
Cys
Gln 262
Asp 181
—Cys—S⁻
215
OH

Figure1.5. PTP Catalytic Mechanism.
The phosphatase mechanism involves a two-step process. In the first step the cysteine in the active site acts as a nucleophile that attacks the incoming phosphate; the aspartate in the WPD loop functions as a general acid to form the cysteinyl phosphate as an intermediate with release of the dephosphorylated substrate. In the second step, the cysteinyl phosphate intermediate is hydrolyzed to release free phosphate and to restore the active form of the enzyme [adopted from (Tonks, 2003)].

Cys215 and the phosphorus atom of the phosphotyrosine are juxtaposed and the Cys215 residue removes the phosphate group. The free phosphate is retained briefly in the cleft and binds to the sulfur of Cys215 to form the cysteinyl-phosphate intermediate. Asp181 protonates the dephosphorylated tyrosine causing its neutralization and diffusion away from the catalytic cleft. Mutation of Asp181 (generally to Ala) prevents the release of the dephosphorylated substrate and keeps the enzyme-substrate conjugate intact, an attribute that was later exploited to generate the substrate trapping strategy.

At this stage the WPD loop still maintains a closed conformation through the interaction of Arg221, Pro180, Trp179, and Phe182 residues with the cysteinyl phosphate. Gln262 and Asp181 position a H_2O molecule to carry out a nucleophilic attack on the cysteinyl-phosphate intermediate to ultimately remove the phosphate from the catalytic cysteine. After hydrolysis of the cysteinyl-phosphate intermediate the enzyme returns to its active conformation with the WPD loop in open position again to carry on another round of dephosphorylation reaction.

1.2.3 Function of PTP1B

Biochemical studies have implicated PTP1B in multiple signaling pathways, through the dephosphorylation of a variety of receptor tyrosine kinases, including the IR, EGFR, PDGFR, and IGF-IR (Ahmad et al., 1995; Buckley et al., 2002; Elchebly et al., 1999; Flint et al., 1997; Haj et al., 2002; Kenner et al., 1996). It also regulates non-transmembrane tyrosine kinases such as Src, p210Bcr-Abl, JAK2, TYK2, and transcription factor STAT5 (Aoki and Matsuda, 2000; Bjorge et al., 2000; Cheng et al., 2002; Gu et al., 2003; LaMontagne et al., 1998; Myers et al., 2001; Zabolotny et al., 2002). It plays an important role in the regulation of insulin (Elchebly et al., 1999) and leptin (Zabolotny et al., 2002) signaling and has been shown to influence growth factor (Haj et al., 2002) and integrin signaling (Arregui et al., 1998; Liang et al., 2005; Liu et al., 1998). PTP1B has been reported as an inhibitor of leptin signaling as depleting PTP1B in mice imparts resistance against diet induced obesity (Bjørbæk et al., 1998; Zabolotny et al., 2002).

1.3 Role of PTP1B in Insulin Signaling

PTP1B downregulates insulin and leptin signaling (Elchebly et al., 1999; Zabolotny et al., 2002). Activated insulin receptor is a substrate of PTP1B *in vitro* and in cells. Overexpression of PTP1B downregulates insulin signaling in various cellular systems (Ahmad et al., 1995; Kenner et al., 1996). Enhanced PTP1B expression has been reported in insulin-resistant patients (Drake and Posner, 1998). Gene-targeting studies with *ptp1B* knockout mice have established PTP1B as a major therapeutic target in diabetes and obesity as PTP1B-null mice do not develop type 2 diabetes and are obesity-resistant when fed with high-fat diet (Elchebly et al., 1999; Klaman et al., 2000). It has also been shown that mice lacking PTP1B have reduced weight and adiposity along with increased metabolic activity and energy expenditure (Cheng et al., 2002; Zabolotny et al., 2002; Kaszubska et al., 2002; Bence et al., 2006). Increased PTP1B expression has been reported in insulin resistant states and obesity (Ahmad et al., 1997). Hepatic expression of PTP1B has been shown to be increased in a fructose-fed hamster model of insulin resistance (Taghibiglou et al., 2002) whereas the level of expression is reduced in fasted mice (Gu et al., 2003).

Crystal structure and kinetic studies provide evidence that PTP1B preferentially dephosphorylates tyrosines 1162 and 1163 of the β subunit of the activated IR (Salmeen et al., 2000) (Figure 1.6). In addition to the IR, IRS-1 is also a potential substrate of PTP1B (Goldstein et al., 2000). Using substrate-trapping experiments Myers et al., first demonstrated that JAK2 and TYK2 are substrates of PTP1B suggesting its negative regulator role in leptin signaling (Myers et al., 2001). Applying similar substrate-trapping approach it was later reported that leptin-activated Jak2 is a substrate of PTP1B in the hypothalami of mice (Cheng et al., 2002; Zabolotny et al., 2002). Because of its negative regulatory roles in both insulin and leptin signaling, the development of inhibitors of PTP1B has become a high priority in the pharmaceutical industry for the treatment of diabetes and obesity (Tonks, 2003).

Figure 1.6

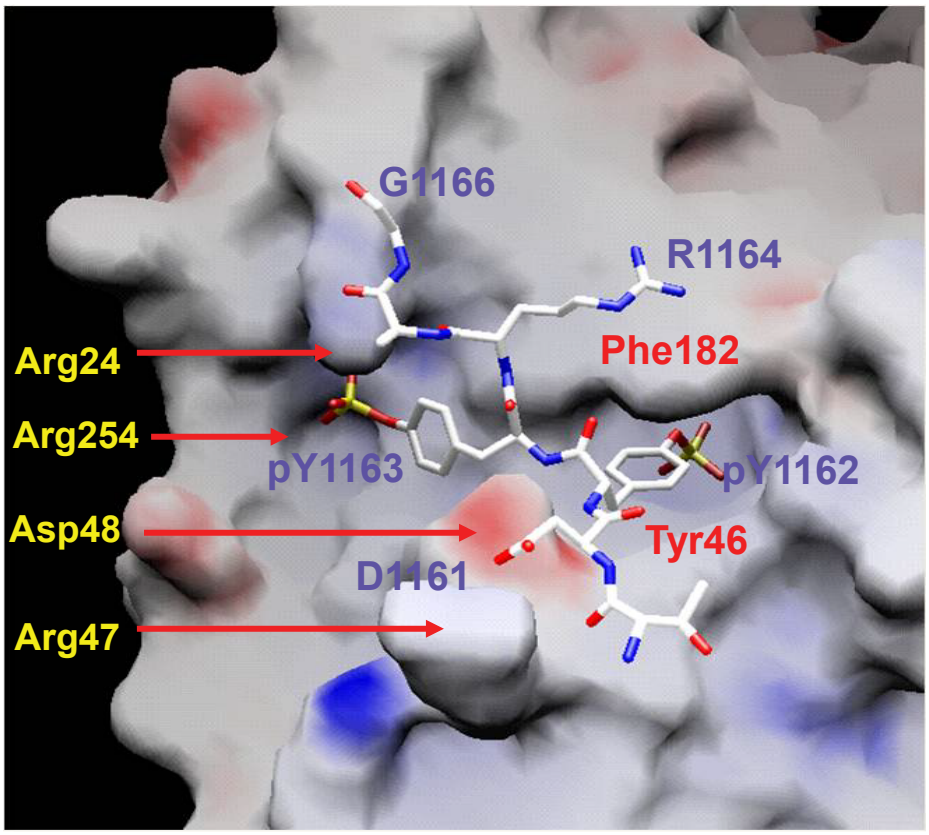
G1166
R1164
Phe182
Arg24
Arg254
pY1163
pY1162
Asp48
Tyr46
D1161
Arg47

Figure 1.6. Structure of PTP1B in Complex with the Insulin Receptor Activation Loop Peptide.
A surface representation of PTP1B active site in complex with the β subunit of the insulin receptor activation loop bis-phospho peptide is shown. Intimate recognition of the substrate phosphotyrosine 1162 is shown as the pTYr extends into the catalytic site inducing closure of the WPD loop with Phe182 and Tyr46 sandwiching the tyrosine ring of pTYr1162. The depth of the catalytic cleft is defined by Tyr 46 and the N-terminal acidic residues of the IR-β activation loop interact with positively charged residues presented around the PTP1B active site and orient the peptide for catalysis. Arg24 and Arg254 of PTP1B form a salt bridge interaction with the phosphoryl group of pTyr1163 and place it close to the catalytic core for subsequent dephosphorylation.

1.4 Redox Regulation of PTP1B

Redox regulation is emerging as a potential general mechanism for regulating PTP function in response to various physiological stimuli (Figure 1.7). It has been reported that several PTPs are transiently oxidized by H_2O_2 (Lee et al., 2002; Meng et al., 2002; Savitsky and Finkel, 2002) and also in response to certain physiological stimuli (Bae et al., 1997; Chiarugi and Cirri, 2003; Gross et al., 1999; Lee et al., 1998; Mahadev et al., 2001). The architecture of the PTP-active site is such that the cysteinyl residue has a pKa of 4.5–5.0 and is predominantly in the thiolate form, unlike the normal pKa of cysteine which is around 8 (Salmeen and Barford, 2005; Lohse et al., 1997). This property makes it a very good nucleophile but also renders it very prone to oxidation. Recently this unique property of the active site cysteine has been shown to underlie the oxidative regulation of PTPs. Several labs have demonstrated that PTPs are important targets of ROS in the induction of an optimal tyrosine phosphorylation response to a variety of physiological stimuli (reviewed in (Tonks, 2005)).

Mild oxidation of the active site cysteine of PTP1B produces a sulphenic acid intermediate that rapidly converts to a 5-atom cyclic sulphenyl-amide species, in which the sulfur atom of the catalytic cysteine is covalently linked to the main-chain nitrogen of the adjacent serine residue (Salmeen et al., 2003; Van Montfort et al., 2003). Formation of this sulphenyl-amide intermediate causes profound conformational changes in the catalytic site that transiently inhibit substrate binding and catalytic activity of the enzyme (Figure 1.9). These structural changes, however, are reversible under reducing conditions. In order to maintain reversibility, the active site Cys residue has to be oxidized no further than sulphenic acid (S-OH), as higher oxidation to sulphinic ($S\text{-}O_2H$) or sulphonic ($S\text{-}O_3H$) acid is generally irreversible (Salmeen et al., 2003; Van Montfort et al., 2003) (Figure 1.8). Our lab observed the formation of the sulphenyl-amide structure after soaking PTP1B crystal with stoichiometric amount of H_2O_2 (Salmeen et al., 2003). We reported that in presence of H_2O_2 the labile sulphenic acid form is rapidly converted to the sulphenyl-amide intermediate. On the other hand, Van Montfort et al., reported the formation of the same structure when PTP1B crystal was soaked with 2-phenyl-isoxazolidine-3, 5-dione, a previously identified PTP1B inhibitor. They suggested that

Figure 1.7

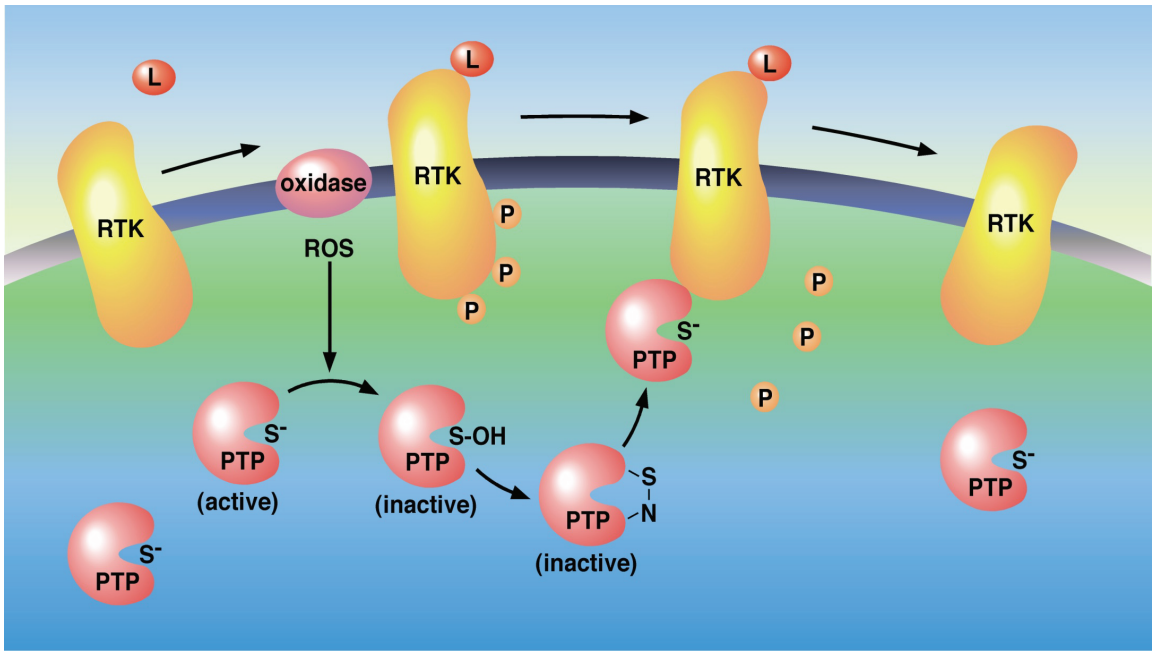

Figure 1.8

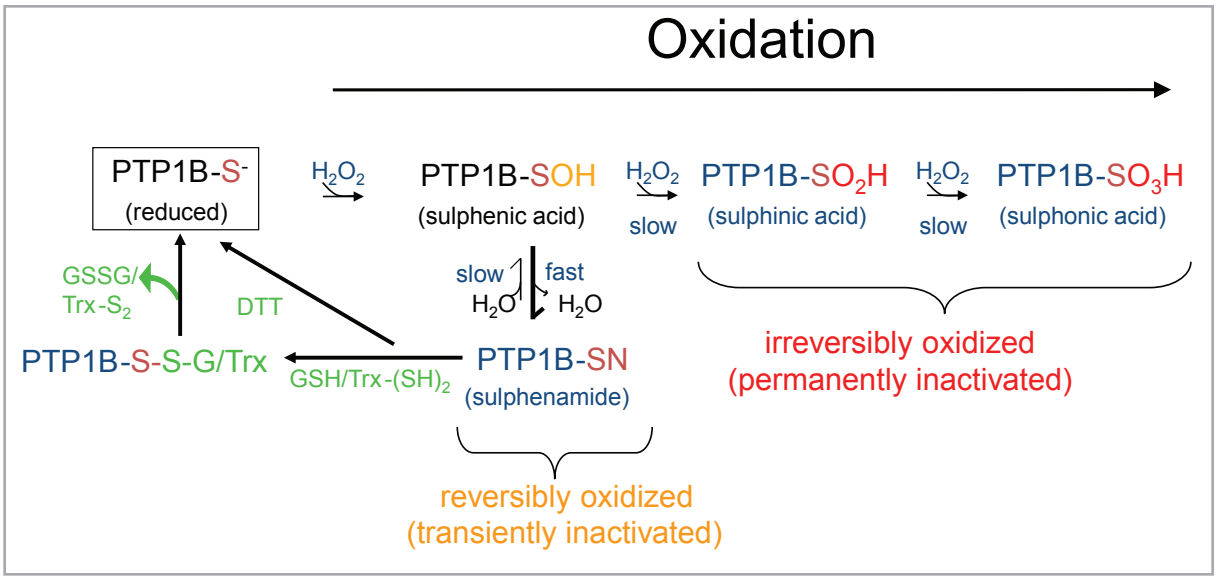

Figure 1.7. A Model for Regulation of PTP Activity by Reversible Oxidation. Ligand (L) dependent activation of a receptor tyrosine kinase (RTK) triggers the production of ROS through Rac-dependent NADPH oxidase assembly at the membrane. ROS oxidize the active site Cys residue of PTPs, converting it from a thiolate ion (the active form) to sulphenic acid (inactive form). Oxidation mediated inhibition of PTP activity promotes tyrosine phosphorylation. The sulphenic acid form of the active site Cys residue is rapidly converted to a sulphenyl-amide moiety, protecting it from irreversible oxidation. This oxidation of the PTPs is reversible and the enzymes are restored to their active conformation by cellular thioredoxin or glutathione (adopted from (Tonks, 2003).

Figure 1.8. PTP1B Function is Regulated by Oxidation.
The overall regulation of PTP1B function by oxidation is shown here. Reactive oxygen can modify the active site cysteine to a sulphenic form which no longer acts as a nucleophile and the enzyme is inactivated. This change, however, is reversible through the formation of a sulphenyl-amide intermediate. This regulatory mechanism not only protects the phosphatase from irreversible modification due to further oxidation to the sulphinic and sulphonic forms, which are permanently inactivated but it also keeps the option open for the transiently inactivated form of the enzyme to regain its active status.

Figure 1.9

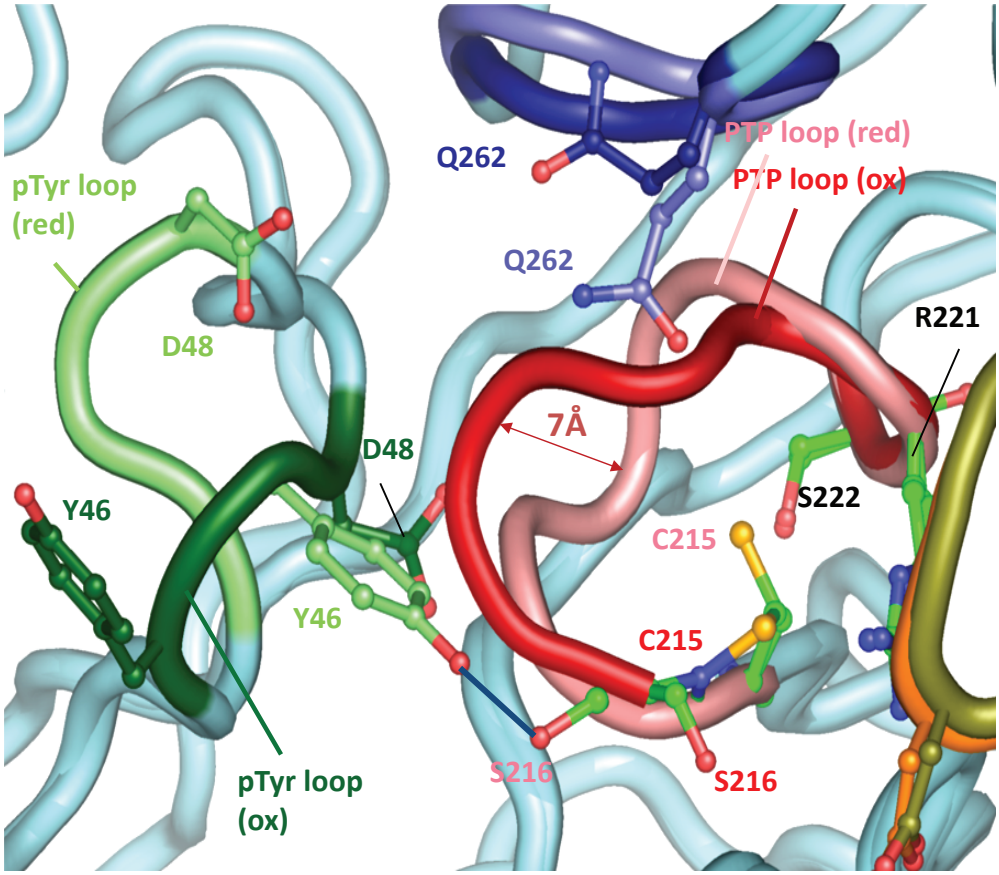
pTyr loop
(red)
D48
Y46
pTyr loop
(ox)
Q262
PTP loop (red)
PTP loop (ox)
Q262
R221
7Å
D48
S222
C215
Y46
C215
S216
S216

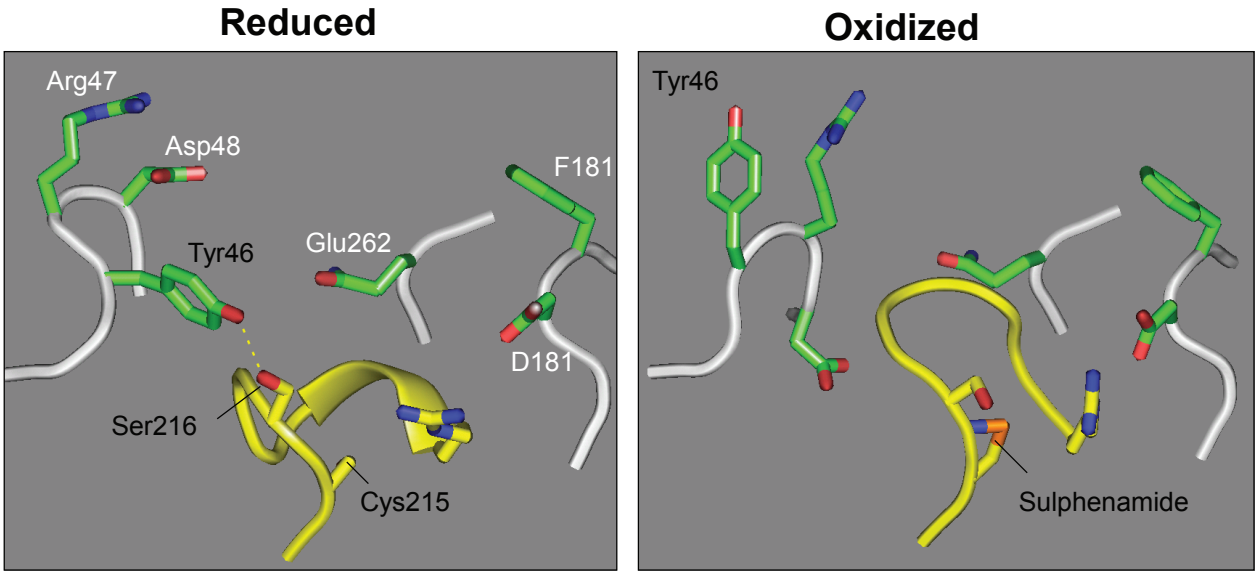
Reduced
Arg47
Asp48
F181
Tyr46
Glu262
D181
Ser216
Cys215
Oxidized
Tyr46
Sulphenamide

Figure 1.9. Oxidation Induced Conformational Change in PTP1B.
Oxidation of the catalytic Cys215 of PTP1B induces profound conformational changes at the catalytic site. Comparative structural features of the reduced and oxidized state of the catalytic site of PTP1B are depicted here ("red" = reduced, "ox" = oxidized). Formation of the sulphenyl-amide intermediate imposes conformational constraints on the main chain of the PTP loop and disruption of the Cys 215−Ser 222 hydrogen bond triggers dramatic structural changes in the catalytic site of the protein. Gly 218 shifts by about 7 Å, and the helical conformation of the PTP loop in reduced PTP1B (light red) converts to a reverse β-hairpin conformation in the oxidized state (dark red). Tyr46 of the phospho-tyrosine (pTyr) loop, which defines the depth of the catalytic cleft under reducing condition (light green), adopts a solvent accessible position in the oxidized state (dark green). Lower panels represent close-up view of the reduced, active and reversibly oxidized, inactive state of PTP1B catalytic core highlighting the conformational re-arrangements (adopted from (Salmeen et al., 2003))

mild oxidation was triggered by redox cycling of 2-phenyl-isoxazolidine-3, 5-dione to form the initial sulphenic acid form, which was then converted to a sulphenyl-amide structure. Similar oxidative modification of PTP1B has been reported in high throughput screening for inhibitors that tend to generate peroxides. Formation of this unique sulphenyl-amide structure in both these reports was described as a direct mechanism involving a nucleophilic attack of the backbone nitrogen of Ser 216 on the Sγ atom of Cys 215 and subsequent condensation. Reactivation of PTP1B is facilitated by the sulphenyl-amide and occurs via mixed disulphide formation with a thiol. These reports indicated that formation of this cyclic sulphenyl-amide intermediate may assist in the regulation of PTP1B in a bi-functional way - to protect the enzyme from being irreversibly modified by higher-order oxidation, and to facilitate a structural architecture amenable for reverting back to its active form by reducing agents (Tonks, 2005).

One of the ways by which the activity of PTPs, including PTP1B, is regulated *in vivo* is oxidation and reduction reactions that directly alter the redox status of the invariant cysteine in the catalytic domain and thereby profoundly influence its function. Insulin stimulation in insulin-sensitive hepatoma and adipose cells causes reversible oxidative inhibition of PTP activity, which is mediated by the enhanced production of intracellular hydrogen peroxide (H_2O_2) in these stimulated cells (Mahadev et al., 2001). Meng et al., later showed that insulin stimulation caused a rapid and transient oxidative inhibition of PTP1B and its close relative TCPTP in Rat1 cells (Meng et al., 2004).

Nox4, a member of the family of NADPH oxidases, was shown to mediate insulin-stimulated H_2O_2 generation and regulate the insulin signaling cascade (Mahadev et al., 2004; Goldstein et al., 2005). Mahadev et al. showed that overexpression of Nox4 significantly inhibits the catalytic activity of PTP1B and subsequently increases insulin-stimulated receptor tyrosine phosphorylation (Mahadev et al., 2004). That study provided initial information about the role of Nox4 as a molecular link between insulin-stimulated ROS and mechanisms involved in their modulation of insulin signal transduction. Interestingly it has also been shown that Nox4 and PTP1B co-localize on ER membrane (Chen et al., 2008; Martyn et al., 2006). In an insulin-induced cellular system it is possible that ROS produced locally by Nox4 inactivate PTP1B and

subsequently enhance insulin signaling. In such a scenario all the components in this regulation have to be in close proximity in a defined subcellular location where local production of ROS by Nox4 will be able to oxidize and inactivate PTP1B.

1.5 Role of PTP1B in Cancer

Apart from its negative regulatory role in insulin and leptin signaling PTP1B has been reported to have both positive and negative effects on various tyrosine phosphorylation-dependent signaling pathways. The genetic region that harbors *ptp1B* gene is frequently amplified in breast cancer and PTP1B is overexpressed in *erbB2*-transformed cell lines. It has been demonstrated that PTP1B acts as a positive regulator of signaling events associated with breast tumorigenesis (Tonks and Muthuswamy, 2007). Recent studies in mice have indicated a positive role of PTP1B in tumor development and metastasis (Bentires-Alj and Neel, 2007; Julien et al., 2007) and renewed interest in delineating the mechanistic role of PTP1B in cancer.

Julien et al. generated NDL2 mice that express an activated mutant of ErbB2 and show similar features of human breast cancer development. Upon targeted deletion of *ptp1B* in these NDL2 mice, tumor development was significantly delayed and incidence of lung metastases was reduced (Julien et al., 2007). Their study suggests a positive role of PTP1B in both tumor development and progression in a breast cancer model. In a related study by a separate group, *ptp1B* knockout mice that overexpress activated ERbB2 were generated using different genetic background (Betires-Alj and Neel, 2007). In this study the researchers found that the absence of PTP1B also caused a marked delay in tumor development and this effect was specific for the ErbB2-induced tumorigenesis. This study emphasizes a positive regulatory role of PTP1B specifically in ErbB2-induced tumorigenesis. Both the above-mentioned studies indicated that loss of PTP1B is accompanied by attenuated activation of the Ras/MAP kinase pathway but they differed in their findings regarding the mechanism by which PTP1B exerts its effects.

Although these studies established a vital positive regulatory role of PTP1B in ErbB2 signaling, the molecular mechanism of this regulation in the context of mammary tumorigenesis and malignancy remains unclear and controversial. Regardless of the mechanism underlying the positive regulatory role of PTP1B in breast cancer tumorigenesis and metastasis, these recent studies have emphasized the potential importance of PTP1B as a therapeutic target in cancer. PTP1B is reversibly oxidized and transiently inactivated by ROS, which is produced following RTK-ligand interaction (Tonks, 2005). However, the role of redox regulation of PTP1B in the context of cancer is not well-understood. Interestingly, in a recent study, Lou et al., examined the redox status of endogenous protein tyrosine phosphatases in HepG2 and A431 human cancer cells, in which reactive oxygen species are produced constitutively. They showed that the catalytic cysteine residue of PTP1B is oxidized to high stoichiometry in response to intrinsic reactive oxygen species production. In addition, when they inhibited the production of cellular ROS it coincided with decreased tyrosine phosphorylation of cellular proteins and inhibition of anchorage-independent cell growth suggesting a role of PTP1B redox regulation in the transformed phenotype of human cancer cells. It will be interesting to understand whether redox regulation of PTP1B is also involved in the intricate mechanism of ErbB2 induced tumorigenesis.

1.6 Role of PTP1B C-Terminal in Regulating its Function and Redox Status

Full length PTP1B consists of a defined and well-studied N-terminal catalytic domain (PTP domain) followed by a rather undefined and uncharacterized C-terminal segment (Figure 1.4 A). PTP1B is a tail-anchored protein localized to the cytoplasmic face of the ER membrane and it plays major regulatory roles in various cellular signaling pathways by dephosphorylating its substrates. Its activity, therefore, must be strictly regulated to avoid nonspecific dephosphorylation of cellular phospho-tyrosine proteins. Even though the catalytic site of the intracellular PTPs is highly conserved, protein sequences outside the catalytic domain, such as the C-terminal end of PTP1B, serve as 'zip codes' to locate this protein specifically to defined subcellular compartments (Mauro and Dixon, 1994). Interestingly physiological function of TCPTP, the closest relative of PTP1B, is also regulated by its cellular location. TC-PTP exists as two alternatively

spliced forms in cells: TC-PTP48 (48 kDa) and TC-PTP45 (45 kDa). The 48 kDa form contains a hydrophobic C-terminus that, like for PTP1B, anchors the protein to the cytoplasmic face of the ER. The 45 kDa form lacks the hydrophobic segment in the C-terminus and is capable of shuttling in and out of the nucleus in response to mitogenic stimulation through a bipartite nuclear localization signal (Lorenzen et al., 1995; Tiganis et al., 1997).

Controlled proteolytic cleavage of PTP1B by calpain in platelets generates a soluble 42 kDa form of the enzyme by cleaving a 75-residue long segment of the C-terminal segment including the ER-targeting motif (Frangioni et al., 1993). This truncated form of PTP1B demonstrates enhanced phosphatase activity, suggesting that the C-terminal end itself or the subcellular localization conferred by the C-terminal end may regulate the function and accessibility of PTP1B to its substrates. The C-terminal segment of TC-PTP, the closest relative of PTP1B also shows similar negative regulation towards enzymatic activity (Hao et al., 1997).

A long-standing conundrum in the field of PTP1B research is how the endoplasmic reticulum (ER)-localized PTP1B can interact with the activated IR (or other RTK substrates) on the plasma membrane. It has been reported that the ER can come into close proximity with the plasma membrane under some conditions (Gagnon et al., 2002), and it is possible that PTP1B under such conditions can access the IR for dephosphorylation to take place. It is also reported that the activated IR is internalized into endosomes, and it seems plausible that the endosome-bound IR can be directed to specific dephosphorylation compartment on the ER, where it becomes dephosphorylated by PTP1B, a mechanism that has also been suggested for the dephosphorylation of the activated PDGFR and EGFR by PTP1B (Haj et al., 2003; Haj et al., 2002). It has been reported that PTP1B mediated dephosphorylation of the receptor tyrosine kinases (EGFR and PDGFR) required endocytosis, and the PTP1B-RTK interaction occurred at specific sites on the cytoplasmic surface of the ER (Haj et al., 2002; Romsicki et al., 2004). It was observed that internalization of most of the activated RTKs is a prerequisite for interaction with PTP1B implying that RTK activation and inactivation (by PTP1B) are spatially and temporally partitioned within cells.

1.7 PTP1B Inhibitors: Prospect, Development and Challenges

Considerable interest has grown in the last decade for harnessing PTPs as therapeutic targets after their regulatory importance in several signaling pathways was elucidated. PTP1B, in particular, has been targeted for a long time for developing therapeutic remedies against diabetes and obesity, based on its important role in mediating insulin and leptin signaling.

Diabetes has become one of the major causes of premature illness and death in most countries, mainly through the increased risk of cardiovascular disease (CVD). Obesity is a major contributing factor for developing type 2 diabetes. The World Health Organization estimates that more than 180 million people worldwide have diabetes. This number is likely to double by 2030 (Figure 1.10). In 2005, an estimated 1.1 million people died from diabetes. Diabetes and its complications also impose significant economic consequences on individuals, families, health systems and countries. About 24 million people in the United States currently have diabetes. Diabetes was the seventh leading cause of death in 2007 and according to the Center for Disease Control (CDC), it's the leading cause of blindness, kidney failure, and other associated complications among adults. Treatment of diabetes is costly and an estimated $174 billion is spent annually to care for patient with this debilitating disease. What is even more alarming is that a recent analysis by CDC showed that as many as 1 in 3 American adults could have diabetes by the year 2050, which is a sharp rise from one in 10 adults currently living with the disease (Boyle et al., 2010). Effective treatments for diabetes are still lacking and currently the disease is only maintained by controlling the blood sugar level or by administering recombinant insulin in advanced cases. Most of the drugs for symptom maintenance, however, have serious side effects, which pose serious concern considering the chronic nature of the symptoms. Recently a widely-used diabetes drug Avandia (rosiglitazone) was pulled out from European market because it causes serious heart problem as a side effect and for many other currently available drug choices the benefits may no longer outweigh the risks.

Figure 1.10

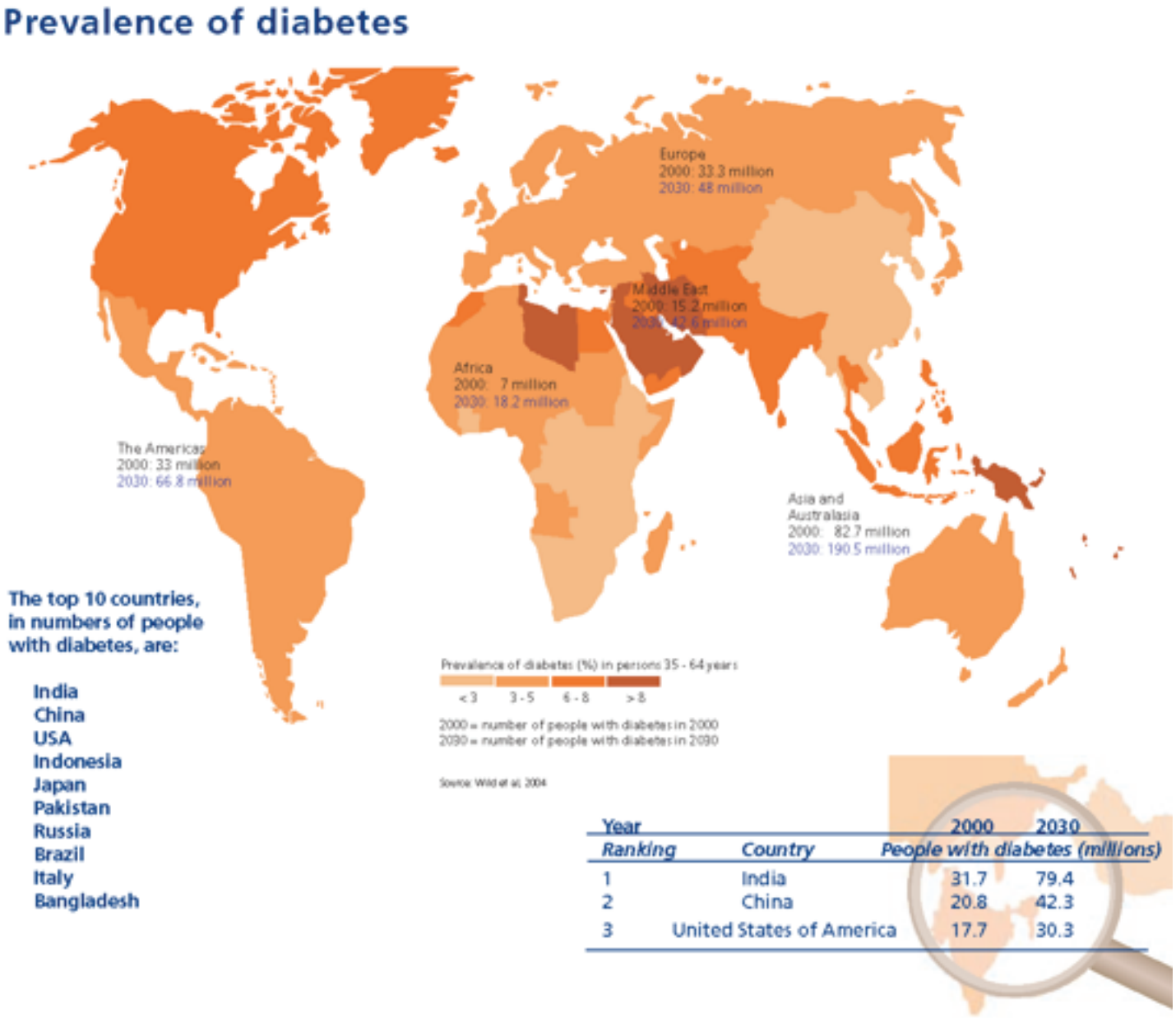

Year		2000	2030
Ranking	*Country*	*People with diabetes (millions)*	
1	India	31.7	79.4
2	China	20.8	42.3
3	United States of America	17.7	30.3

Figure1.10. Prevalence of Diabetes

The World Health Organization (WHO) estimates that more than 180 million people worldwide have diabetes. This number is likely to double by 2030. In 2005, an estimated 1.1 million people died from diabetes. Diabetes and its complications also impose significant economic consequences on individuals, families, health systems and countries. According to a new forecast by the Centers for Disease Control (CDC, USA) as many as 1 in 3 American adults could have diabetes by the year 2050. At present about 23.6 million people in the United States have diabetes.

An array of biochemical, structural and *in vivo* studies showed that PTP1B is an attractive target for therapeutic intervention of type 2 diabetes. PTP1B has been shown to be a negative regulator of insulin signaling by biochemical and cell-based studies (Ahmad et al., 1995; Chen et al., 1997; Kenner et al., 1996; Seely et al., 1996). Gene targeting studies in mice have shown that PTP1B-null mice do not develop type 2 diabetes and are resistant to obesity when fed with a high fat diet, yet they do not show any phenotypic abnormalities (Elchebly et al., 1999; Klaman et al., 2000). Additional linkage between type 2 diabetes and PTP1B has been reported by demonstrating that depletion of PTP1B expression with antisense oligonucleotides (Rondinone et al., 2002; Zinker et al., 2002) and inactivation of PTP1B catalytic activity by small molecule inhibitors [reviewed in (Johnson et al., 2002)] elicits anti-diabetic and anti-obesity effects.

There has been a considerable effort in developing potent inhibitors of PTP1B focused on the active site pocket. However, the discovery of pharmaceutically acceptable inhibitors directed to the active site of PTP1B remains elusive due to very complex structural and regulatory features of the catalytic site. Potential small molecule inhibitors have been reported by various research laboratories and pharmaceutical companies on the basis of *in vitro* studies (Combs, 2010). The normal strategy for selecting active site directed inhibitors is to develop pharmacophores in high throughput screening (HTS) to find scaffold-like compound from a library of small molecules. This is generally accompanied by structural analysis of the candidate molecules to drive chemical optimization for enhancing specificity and potency. Since most of the binding energy for the substrate comes from the phosphate group, the resulting candidate compounds from high throughput screening have been highly charged and very polar and consequently do not have favorable pharmacokinetic properties. Most of these potent molecules selected *in vitro* were found to be poorly bioavailable for oral administration in clinical trials and could not be advanced as pharmaceutically acceptable drugs. In addition designing active site directed selective inhibitors of PTPs including PTP1B could be difficult because of the high degree of homology among members of this enzyme family. Selectivity over other phosphatases involved in vital

regulatory functions in the cell is required to decrease the risk of undesirable side effects.

Wiesmann et al., has reported allosteric inhibition of PTP1B by small molecule inhibitor as a promising alternative strategy for the development of selective PTP inhibitors (Wiesmann et al., 2004). In that study crystal structure of PTP1B in complex with a small molecule allosteric inhibitor revealed a previously uncharacterized regulatory site located ~20 Å from the catalytic site. This allosteric inhibitor prevents formation of the active "closed" form and stabilized the open inactive conformation of the enzyme by blocking mobility of the catalytic loop. This allosteric site is amenable to binding small molecules and is not as well conserved among phosphatases as the catalytic site, thus affording an opportunity to circumvent the problems associated with inhibitors of the catalytic site. The kinetic, crystallographic and cell-based data presented in that work showed how one can inhibit PTP1B by compounds binding at a site different from the active site. The physiological relevance of this allosteric site, however, is unclear.

1.8 Rationale and Significance of the Project

Type 2 diabetes accounts for >90% of all diabetes, which is caused by insulin resistance resulting in loss of proper glucose homeostasis. Obesity is one of the major contributing factors for developing type 2 diabetes and possesses the risk of substantially increasing the number of cases all over the world (Saltiel, 2001). Therapeutic options for treating diabetes and obesity are inadequate and ineffective at this time and innovative and effective approaches to encounter the disease conditions are urgently needed. Studies on protein tyrosine phosphatase 1B (PTP1B) in the past decade have established this molecule as a validated target for the treatment of type II diabetes and obesity.

The highly charged catalytic core of the reduced active form of PTP1B has been the main obstacle for finding pharmaceutically appropriate inhibitors for this enzyme. This catalytic pocket is also very prone to oxidative inhibition. High throughput

screenings for inhibitors tend to detect many oxidizing agents (i.e., peroxide generators) and yield a lot of “false-positive” candidates. Reversible oxidation, however, causes profound conformational change at the active site and may present new sites for developing small molecule inhibitors. Thus, if this transiently inactive form of PTP1B can be stabilized by locking the reversibly oxidized inactive conformation of the active site, insulin signaling could be promoted, which could provide new hope in the fight against diabetes. A small molecule inhibitor that recognizes the reversibly oxidized conformation of PTP1B and locks it in that inactive state will be very useful for this purpose. It is believed that oxidation of PTPs in response to particular stimuli is a local event and only a pool of the relevant PTP, which is important for regulation of that particular signaling pathway, is inactivated. Targeting only the oxidized pool by specific molecules for selective inhibition will reduce complications of global effects from broad spectrum targeting and inhibition of the entire pool of the PTP.

An analogous example of inhibiting a target enzyme by stabilizing the inactive conformation is stabilization of p210 Bcr-Abl by Imatinib (Schindler et al., 2000). Imatinib (STI-571) is a 2-phenylaminopyrimidine class of pharmacophore that binds with high affinity and specificity to an inactive conformation of Bcr-Abl kinase, in which a centrally located activation loop is not phosphorylated. This is a notable example for the application of a small inhibitory compound to exploit a distinctive inactivated conformation of a target enzyme to achieve high degree of inhibition that can be subsequently translated into pharmaceutically applicable drug.

The overall aim of my project is to generate conformation sensor antibodies to the reversibly oxidized form of PTP1B to understand its redox regulation, particularly in response to H_2O_2 and to physiological stimuli such as insulin. In this project I proposed to design and isolate conformation-specific recombinant antibodies specific for the reversibly oxidized form of PTP1B by the antibody phage display technique. Reversible oxidation of PTP1B causes profound conformational change at the active site of the enzyme causing its transient inactivation. The core hypothesis of this project is, if this reversibly inactivated conformation of PTP1B can be stabilized by a conformation sensor antibody, the physiological role of PTP1B in key signaling pathways can be

manipulated. PTP1B is particularly known for its negative regulatory role in insulin signaling and it is reversibly oxidized by insulin-induced ROS in cells. The focus of my project is, therefore, to characterize of the interaction between such conformation sensor antibodies and reversibly oxidized PTP1B and to investigate their application as an alternative approach to develop inhibitors against PTP1B.

The scope of my thesis is as follows:

1. Construction of a large, diverse antibody library by the phage display technique in order to screen conformation-specific antibodies that will be able to recognize the reversibly oxidized form of PTP1B
2. Characterization of selected conformation-specific antibodies for the detection of reversibly oxidized PTP1B *in vitro* and in mammalian cells.
3. Understanding the redox regulation of PTP1B *in vitro* and in mammalian cells in response to H_2O_2 and insulin.
4. Application of the conformation sensor antibody to manipulate PTP1B-mediated regulation of insulin signaling

Chapter 2

Construction of Antibody Phage Display Library to Target PTP1B-OX

2.1 Basic Structure of Antibody

Antibodies are glycoproteins that belong to the immunoglobulin superfamily found in all vertebrates. Antibodies are classified in five different types – IgG, IgM, IgD, IgA and IgE on the basis of the variation in the constant regions. IgGs are the major antibody found in serum and the most commonly used in biomedical and pharmaceutical applications.

Each antibody molecule contains variable (V), diversity (D, heavy chain only), joining (J) and constant (C) regions (reviewed in (Burton, 2001)) (Figure 2.1). The modular structure of an IgG molecule is composed of four polypeptide chains: two identical light chains (25 kD each) and two identical heavy chains (50-70 kD each). Inter chain disulfide bridges link each light chain to a heavy chain and the two heavy chains to one another. There are also intra-chain disulfide bonds and non-covalent interactions that contribute to the tertiary structure of antibody. Both the heavy and light chain contain two distinct regions with different variability in the amino acid sequences: the variable regions (V_H and $V_{L,}$ for variable heavy and variable light, respectively) and the constant regions (C_H and C_L, for constant heavy and constant light, respectively). The heavy chain has multiple constant regions (C_{H1}-C_{H3}/C_{H4}). There is a hinge region with some rotational flexibility in the middle of the heavy chain domains that links C_{H1} to C_{H2}-C_{H3} regions.

Variable domains at each N-terminal of both light and heavy chains (V_H and V_L) form the antigen binding region. Each variable light and heavy chain contains, in alternate fashion, three hypervariable regions of varying amino acid sequences, and three frame-work regions of relatively conserved amino acid sequence. The hypervariable regions are known as the complementarity determining regions (CDRs), which confers specificity to antibody-antigen interaction (Wu and Kabat, 1970).

Antibody molecules contain discrete protein domains or fragments that can be separated by controlled protease digestion or produced by recombinant techniques

(Figure 2.1). Papain cleaves the immunoglobulin molecule in the hinge region to produce two identical fragments containing the entire light chain and the V_H and C_{H1} domains of the heavy chain. These fragments are called the Fab fragments as they preserve the antigen binding sites. This digestion also produces the Fc region with the rest of the heavy chain (C_{H2} and C_{H3} domain), which has no antigen binding property (Roitt and Delves, 2006). Treatment with pepsin generates a divalent fragment that contains the antigen binding sites of both of the heavy and light chains and called $F(ab')_2$. The Fc region of the molecule is digested into small peptides by pepsin. Generation of the smallest functional antigen binding fragment Fv (fragment variable) of antibody molecule by proteolytic cleavage is very rare (Givol, 1991). Two functional antigen-binding fragments, designated Fab and Fv (Figure 2.1), have been cloned and displayed on phage (reviewed in (Burton, 2001)). We used the smaller Fv (fragment variable), which is composed of the variable light (V_L) and variable heavy (V_H) regions to generate the library. In a single chain variable fragment (scFv), the two variable regions are artificially joined with a flexible peptide linker of varied length (Figure 2.1) and expressed as a recombinant polypeptide chain fused to the surface protein pIII of phage particles (Bird et al., 1988).

2.2 Antibody Phage Display

Antibody phage display is a powerful and effective technique for generation and selection of specific antibodies from a large and diverse collection of functional antibody fragments displayed on the surface of bacteriophage. Smith first described the use of phage display for the display of specific binding peptides fused to the phage coat protein (Smith, 1985). Later Winter and Wells demonstrated that functional folded proteins, such as an antibody fragment or a hormone, can be displayed on the phage surface. In the phage display technique a functional polypeptide responsible for a phenotype (i.e., specific binding to an antigen or ligand) is displayed on the phage surface following introduction of the gene coding for the polypeptide into the phage genome (Figure 2.2) (Lowman et al., 1991; McCafferty et al., 1990). This technique, therefore, physically links the phenotype with the genotype and offers advantages and flexibility in term of *in vitro* manipulation. Winter and coworkers first developed the

Figure 2.1

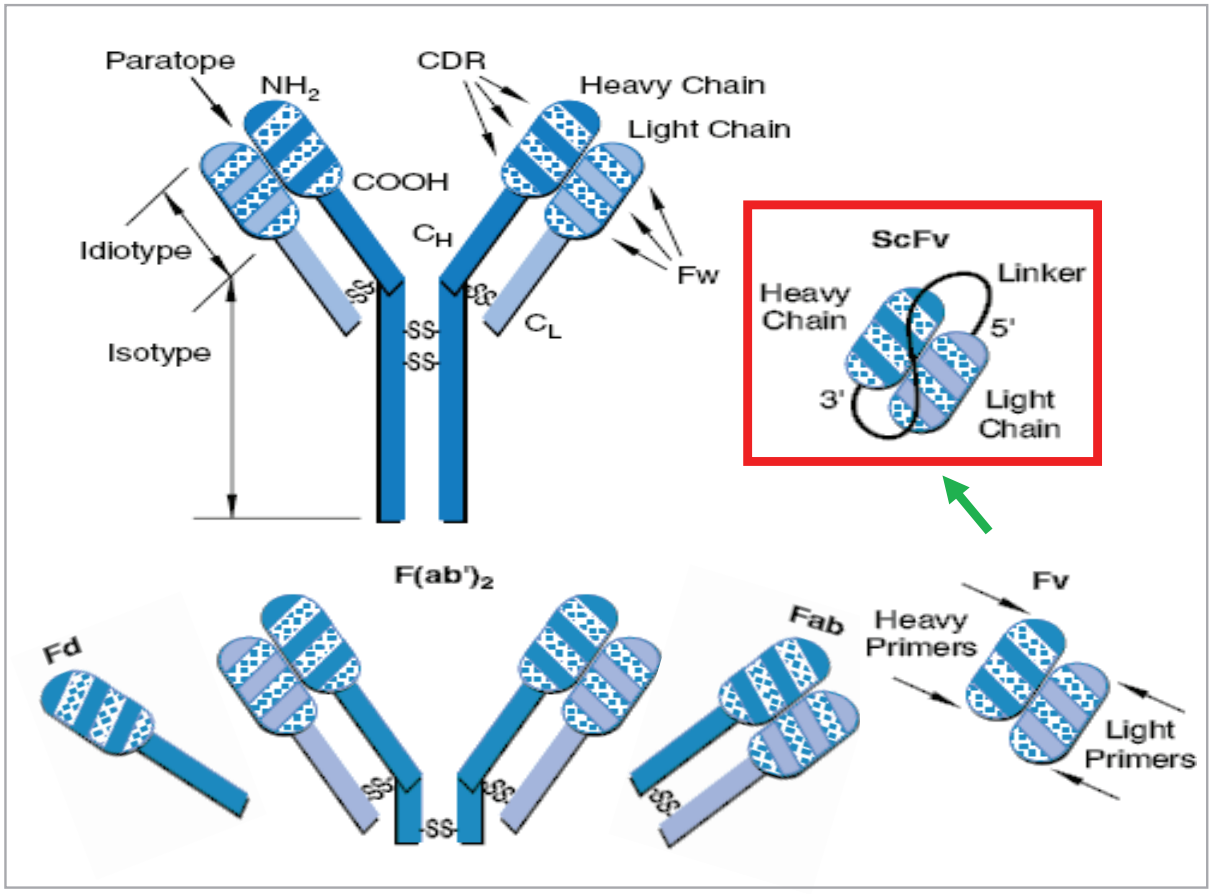

Figure 2.2

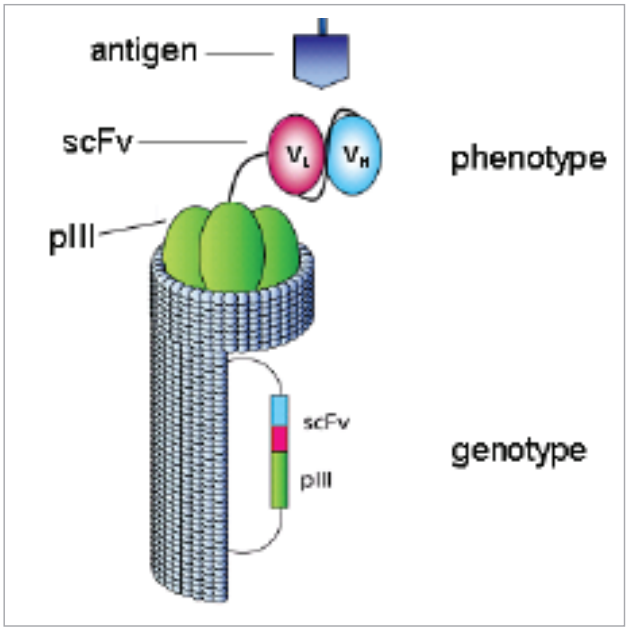

Figure 2.1. Basic Antibody Structure and Subunit Composition.
The C region of an antibody is relatively conserved while the V region is antigen-specific. The V region consists of alternating framework (FW) and hyper variable complementarity-determining regions (CDR). Antibody molecules contain discrete protein domains or fragments (showed in the shaded area) that can be isolated by protease digestion or produced by recombinant techniques. We used the smaller Fv (fragment variable), which is composed of the VL and VH regions only. In scFv, the two variable regions are artificially joined with a neutral linker and expressed as a single polypeptide chain adopted from (Amersham, 2000).

Figure 2.2. Antibody Phage Display.
This cartoon shows a phage particle displaying a functional antibody fragment in the form of single chain variable fragment or scFv as fusion protein with a minor coat protein pIII. In antibody phage display a functional antibody elements (capable of binding target antigen) is displayed on the phage surface by introducing the antibody gene coding for the functional element into the phage genome or into engineered recombinant phagemid vector (adopted from (Sommavilla, 2010).

antibody phage display method to express diverse population of antibody-fragments on the surface of bacteriophage. The antibody fragment expressing genes can be produced from naive source (Hoogenboom and Winter, 1992), or derived after immunization (Clackson et al., 1991), or they can be produced by introducing random mutations *in vitro* in one or more complementarity determining regions (CDRs) (Griffiths et al., 1994).

Antibody phage display library refers to a collection of phage particles that display recombinant antibody fragment fused to the surface proteins. The number of phage particles displaying antibody fragments in the repertoire defines the size of the library. The larger the library, the greater is the chance of isolating specific high affinity antibodies to an epitope (Perelson and Oster, 1979). The diversity of the amino acid sequences of the antibodies in the library is another defining parameter for library performance. Most diversity is found in the CDRs, whereas the frame work regions provide the structural scaffold of the antibodies. In nature, diversity is mainly concentrated in CDR3 loops.

A bacteriophage is a virus that only infects bacteria. It is made up of simple genetic material (a circular, single-stranded DNA molecule), which is enveloped in a protein coat. The phage genome causes infected bacteria to amplify progeny phage. The most common bacteriophage used for phage display is a filamentous phage that infects strains of *E. coli* harboring the F pilus, which translocates the phage genome into the bacterial cytoplasm. Both phage- and host-derived proteins help to replicate the phage genome, which is used to produce all phage structural proteins, and finally the genome is packaged into functional phage particles efficient for further round of infection.

The protein core of filamentous phage particles is composed of multiple copies of major and minor coat proteins. Several thousand copies of a small major coat protein, pVIII, make the bulk of the outer protein envelope, whereas few copies of the minor coat

proteins pIII and pVI, are displayed at one end and pVII and pIX are present at the opposite extremity of the phage outer protein structure. Recombinant proteins and peptides are commonly displayed as fusions with pIII (Parmley and Smith, 1988; Smith, 1985) or pVIII (Greenwood et al., 1991). However, proteins as fusion with the minor coat protein pVI have also been reported (Greenwood et al., 1991). Initially polypeptides were displayed on phage using phage vectors containing the entire phage genome with cloning sites for fusion of the protein of interest with pIII or pVIII. However, over time the use of phagemid vector was adopted for its simple and easy maneuvering during cloning and other practical manipulation.

A phagemid is a circular plasmid that carries the gene III of phage with cloning sites for recombinant gene insertion and a packaging signal (Hoogenboom et al., 1991). Upon transformation of bacteria with phagemid containing the gene of interest the bacteria are infected with helper phage carrying a complete phage genome, to aid the production of functional phage particles harboring the phagemid. The helper phage (M13K07 or VCS-M13) genome has slightly defective origin of replication and therefore the phagemid vectors are preferentially packaged into the progeny phage particles. Peptides displayed from vectors containing the entire phage genome are polyvalent (i.e. 3 to 5 identical polypeptides displayed on one phage particle), which selects for lower affinity binders. The phagemid vectors on the other hand produce monovalent display of the recombinant protein-pIII chimera, an attribute that is essential for isolating high-affinity binders.

For generating the antibody phage display library against PTP1B_CASA, we used a phagemid, which is a plasmid that carries the recombinant coat protein gene III as well as a phage origin of replication. The genes of interest, in this case the genes for the single chain variable fragments (scFvs), are inserted into this phagemid. The recombinant phagemid is transformed to a male strain of *E. coli,* which is susceptible to phage infection. The phagemid is then amplified by the *E. coli* without making any functional new phage particle. A helper phage (VCS-M13) with all other necessary phage proteins, is used to infect the already transformed bacteria to make functional phage particles that express the scFv antibody fused to the surface protein pIII. A

collection of phage displaying a population of related but diverse recombinant antibody (phage antibody library) is produced from the infected bacteria. The library is next exposed to the target antigen, which is PTP1B-CASA in our case. Unbound and weakly bound phage are washed away and only the tightly bound phage are selected. The captured phage is eluted and re-amplified after re-infecting bacteria. Multiple rounds of selection can be performed (in general 2-4 rounds) in this way resulting in very high degree of selection and amplification of the desired phenotype from a background of phage carrying undesired phenotypes. The displayed scFv from this amplified pool are then characterized as functional antibodies. ScFv fragments generally have a molecular weight of ~ 30 k and are not glycosylated. Use of scFvs as intracellular antibodies, or intrabodies, to target intracellular proteins has been reported (Biocca and Cattaneo, 1995) and represents a powerful aspect of the technology for my study.

Many highly conserved mammalian proteins are less conserved or absent in non-mammalian species, making avian species, such as chickens, a useful source for producing high level of immune genes against the antigen of interest. Chickens generally produce higher level of immune response, to an extent that is difficult to achieve with mice and rabbits (Andris-Widhopf et al., 2000; Davies et al., 1995). Generation of antibody phage display libraries from animals already immunized with the antigen is advantageous because diversity for the antigen is already created *in vivo* by the immune system (Burton et al., 1991; Clackson et al., 1991). This diversity is further increased during the generation of scFvs, by varying the order of the V domains at either the N-terminus or at the C-terminus (Bird et al., 1988; Huston et al., 1988) or by changing the length of the polypeptide linker between the two variable domains (Huston and Haber, 1996). The resulting libraries are enriched in antigen-specific antibody domains, and may therefore yield high-affinity antibodies.

2.3 Advantages of Antibody Phage Display

Antibody phage display technology generates high complexity (>10^6) libraries, which ensure higher probability for the most specific or highest affinity interactions to be resolved. It also enables successive rounds of selection or panning to identify conformation-specific antigens (Hoogenboom and Chames, 2000; Burton, 2001)). Phage display technique enables *in vitro* selection of antibodies for antigens that are poor immunogens in conventional approaches of antibody production. Expressing the recombinant antibody fragments in bacteria offers the additional advantage of producing short antibody fragments for structural studies on a large scale (Skerra, 1993). Shortening of the size of the antibody molecule to Fv has practical benefits. Use of a short single chain fragments makes the construction of a large and diverse library easier and has very high yield in *E. coli* as recombinant protein.

Single chain variable fragment (scFv) of recombinant antibodies presented at the surface of bacteriophage (Winter et al., 1994; Smothers et al., 2002) can be selected from combinatorial libraries *in vitro* under extensively controlled selection conditions. Specific biochemical conditions during the selection steps of the phage display technique allow selection of highly specific antibodies even in the presence of competitive molecules. This *in vitro* process of antibody selection does not involve any natural immune system and, therefore, antibodies to toxic compounds, lethal pathogens and highly conserved antigens can be obtained. In comparison with classical, animal-based approaches, this has the major advantage of preserving the native conformation of target antigens to allow the generation of conformation specific antibodies. Amongst several different methods for antibody selection, including yeast, bacteria or ribosomal display (reviewed in (Bradbury et al., 2003)), antibody phage display has been proven to be the most robust, versatile and most widely used technique. This *in vitro* selection technique was employed systematically to find conformation-specific antibodies to the reversibly oxidized form of PTP1B (PTP1B-OX).

Results: Chapter 2

2. 4 PTP1B-CASA is Structurally Similar to PTP1B-OX

From comparative analysis of the crystal structure of PTP1B in the reduced and oxidized state, it was observed that mutation of the catalytic cysteine 215 and serine 216, both to alanine, would break two critical hydrogen-bonds and thereby reorganize the conformation of the active site. The crystal structures of this doubly mutated form of PTP1B and the reversibly oxidized form are identical. The surface representation of the crystal structures of both the oxidized and mutated PTP1B shows that the tyr46 of the pTyr loop becomes solvent exposed and the PTP loop is also presented on the protein surface (Figure 2.3). This mutated form was therefore used as a stable antigen to generate conformation-specific antibodies that would eventually recognize the oxidized form of PTP1B.

2.5 Construction of Antibody Phage Display Library

We have generated a phage display library displaying single chain variable fragments (scFvs) fused to phage surface protein pIII, from immune genes collected from spleen and bone marrow of chicken immunized with PTP1B (1-321)-CASA (Figure 2.4 A and B). To increase the diversity of the antibody library even further we constructed two different types of scFv constructs, one with a short linker sequence (GGSSRSS) and one with a long linker (GGSSRSSSSGGGGSGGGG) and mixed them together for generating a complex and diverse scFv library. The final library size was ~2 $x10^7$.

To select for scFvs specific for the PTP1B-CASA mutant from the antibody library we employed a subtractive panning strategy. Addition of molar excess of reduced wild type PTP1B (1-321) to the library in solution would enrich specific CASA-specific pools, whereas pools that recognize and detect the common epitopes on both the oxidized and the reduced form of the enzyme would be excluded. Specific scFv expressing phage particles were isolated with biotinylated PTP1B-CASA and subsequent capturing of the antigen-antibody complex with streptavidin coated magnetic beads.

Figure 2.3

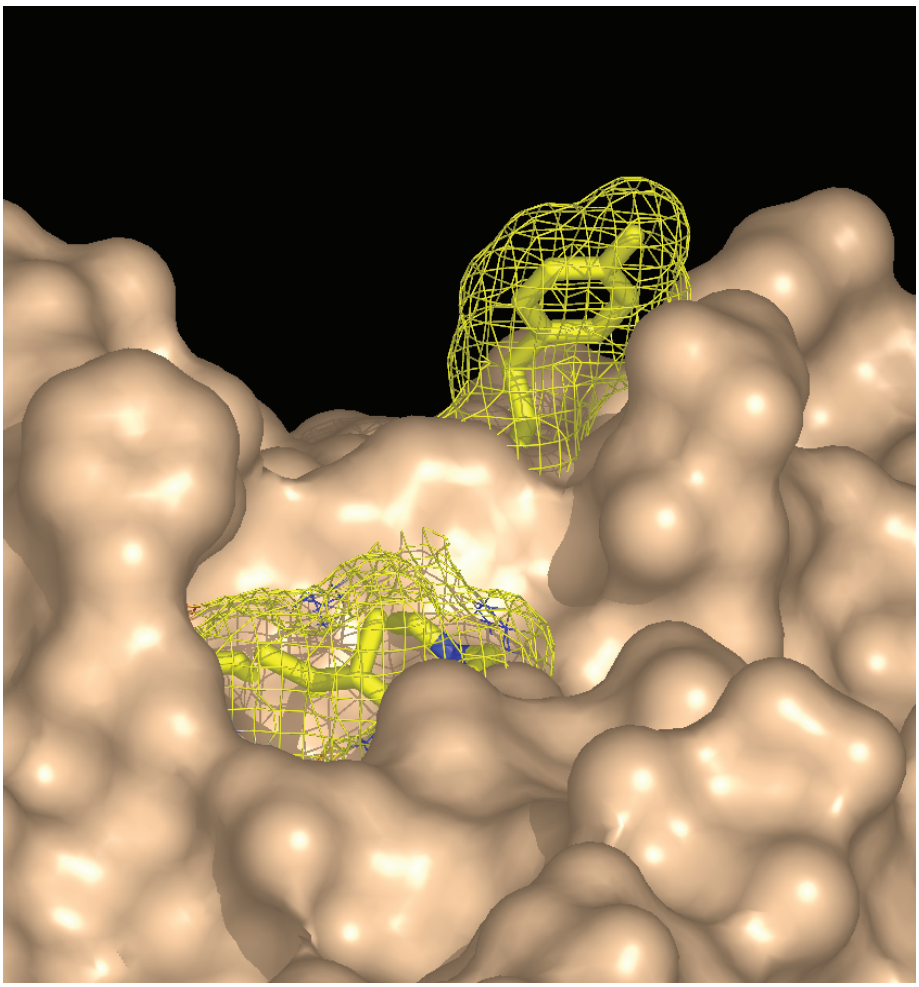

PTP1B-OX

PTP1B-WT: **VHCSAGIGRSG**

PTP1B-CASA: **VHAAAGIGRSG**

Figure 2.3. PTP1B-OX and PTP1B-CASA are Structurally Identical.
In PTP-CASA, mutation of the catalytic cysteine 215 and serine 216, both to alanine, reorganizes the active site conformation by breaking the hydrogen bonds, which are required for holding the active site together. The crystal structures of this doubly mutated form of PTP1B and the oxidized form exactly resemble each other. The PTP loop and tyr46 of the pTyr loop become solvent exposed as a result of the lack of hydrogen bonds.

Figure 2.4

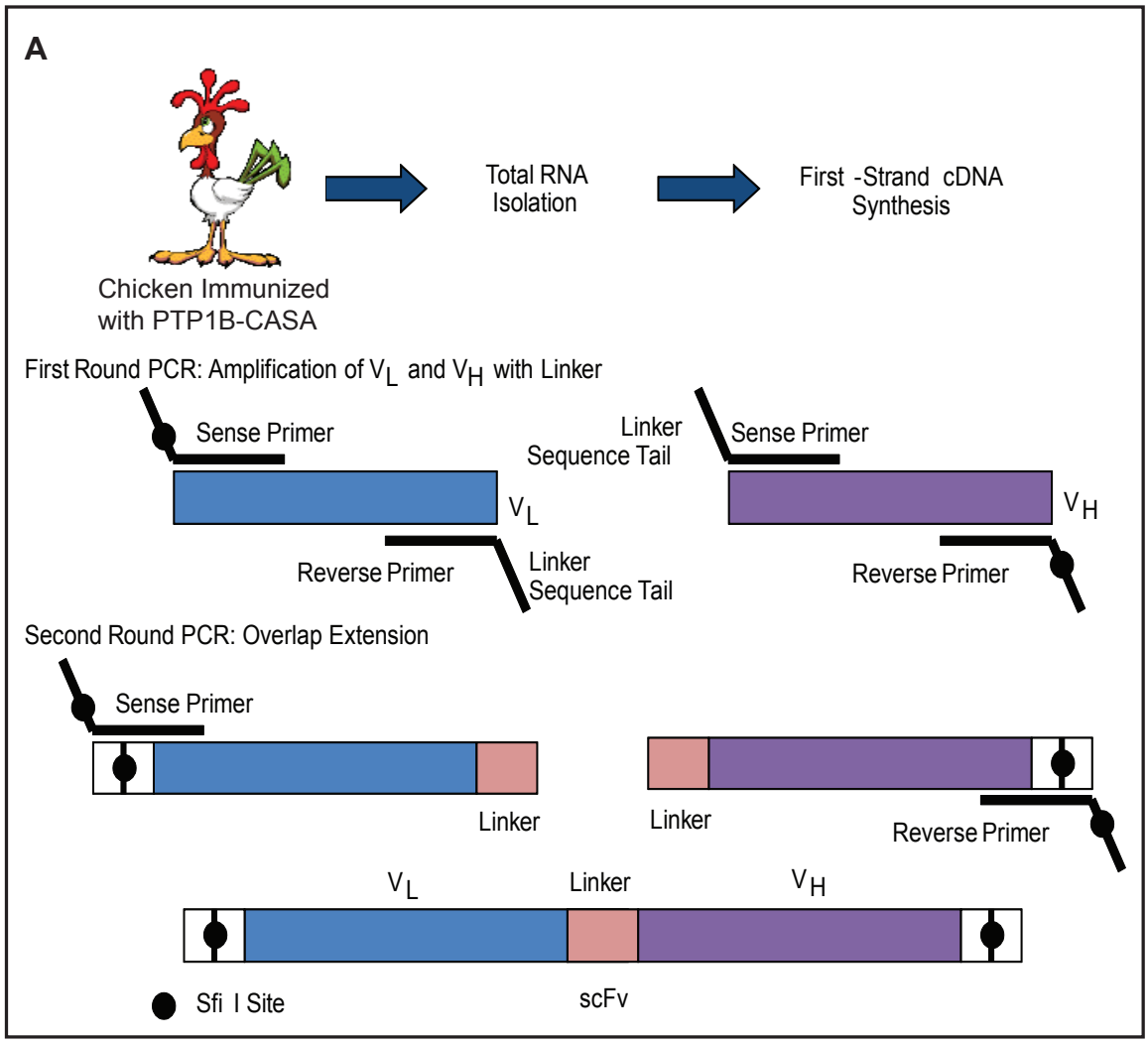
A
Chicken Immunized with PTP1B-CASA
Total RNA Isolation
First -Strand cDNA Synthesis
First Round PCR: Amplification of V_L and V_H with Linker
Sense Primer
V_L
Reverse Primer
Linker Sequence Tail
Linker Sequence Tail
Sense Primer
V_H
Reverse Primer
Second Round PCR: Overlap Extension
Sense Primer
Linker
Linker
Reverse Primer
V_L
Linker
V_H
scFv
Sfi I Site

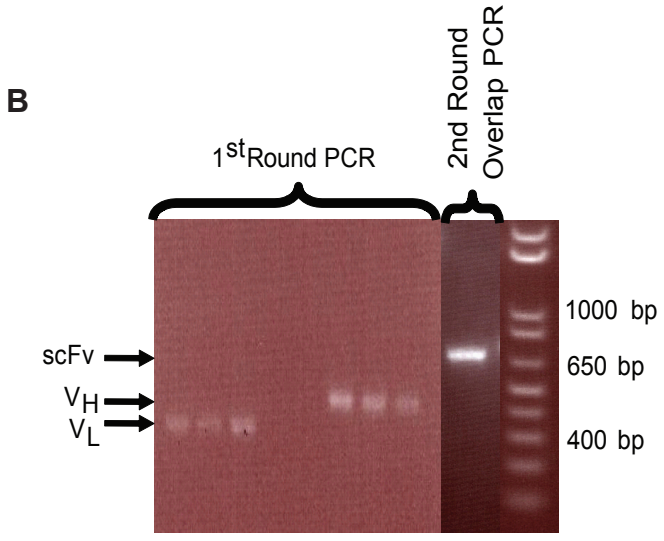
B
1st Round PCR
2nd Round Overlap PCR
scFv
V_H
V_L
1000 bp
650 bp
400 bp

Figure 2.4. Generation of single chain Variable fragments (scFvs)
A) First-strand cDNA from chicken immunized with PTP1B-CASA was used to amplify individual variable light (V_L) and variable heavy (V_H) regions in the primary amplification step. The final scFv products were generated by mixing equimolar ratios of the individual products from the first step with appropriate oligonucleotide primers. Short regions of complementary sequence were introduced into both primary products through the primers for creating an overlapping region to link the individual products for the amplification of scFvs with short and long linker.
(B) The V_L and V_H chain genes were amplified from the cDNA of the bone marrow and spleen of an immunized chicken by PCR using DNA polymerase. The final scFv DNA constructs were generated by taking equimolar amount of V_L and V_H products and linking them together in an overlap PCR. The phagemid vector and these scFv constructs were then digested by Sfi 1 restriction enzyme, gel purified and ligated to generate scFv containing phagemid constructs. Ligated phagemid constructs were electroporated into *E. coli* (XL-1 Blue) to generate the scFv library.

2.6 Effect of Biotinylation (*in vitro* chemical vs. *in vivo* site-specific) on PTP1B Function

Initially we generated biotinylated CASA mutant for using in the subtractive panning by an *in vitro* chemical modification (Figure 2.5A). We used three different protein:biotin ratios (1:10, 1:20, and 1:30) at pH 7.0 to add the biotin moiety to the free amine group of purified PTP1B-WT and PTP1B-CASA and determined biotin incorporation by the HABA (4´-hydroxyazobenzene-2-carboxylic acid) assay. It was estimated that 1-2 mol biotin per mol PTP1B were incorporated when the biotinylation reaction was performed at a 1:10 protein to biotin ratio at pH 7.0. The number of incorporated biotin group increased as we increased the ratio of the biotinylation reagent and at 1:30 ratio ~10 biotin molecules were incorporated per molecule of PTP1B. Biotinylation was also confirmed by standard Western blot analysis of the biotinylated proteins using streptavidin-HRP (Figure 2.5B). This biotinylation method, however, adds biotin to any free amine group of PTP1B at random and thereby could alter the conformation of the target antigen. To test the possibility that this random chemical biotinylation had any effect on the conformation of PTP1B (in particular at the catalytic site) we tested the phosphatase activity of the biotinylated PTP1B-WT and found that chemical biotinylation caused significant reduction of activity. Higher levels of biotinylation, at 1:20 enzyme to biotinylation reagent ratio and beyond, reduced the catalytic activity of PTP1B even more significantly (Figure 2.7 B).

To overcome this problem we took the approach of site specific homogenous biotinylation of PTP1B (1-321) in *E. coli* by virtue of a biotinylation tag (Schatz, 1993) that we fused to the N-terminus of recombinant PTP1B (Figure 2.6 A and B). N-terminally biotinylated PTP1B-CASA and –WT (NBT-PTP1B-CASA and NBT-PTP1B-WT) were purified to homogeneity from *E. coli* that co-expressed excess recombinant biotin ligase (Figure 2.7 C, D, E, and F). We optimized the expression conditions for this co-expression system and found that expression of NBT-PTP1B and its biotinylation in *E. coli* was optimal with 1 M IPTG for 4 hours at 37ºC in presence of 50 µM biotin in the growth media (Figure 2.7). Biotinylation of PTP1B by this method caused no reduction in activity when compared to the phosphatase activity of the wild type non-modified enzyme (Figure 2.7 B). When tested side by side in the same assay, phosphatase

Figure 2.5

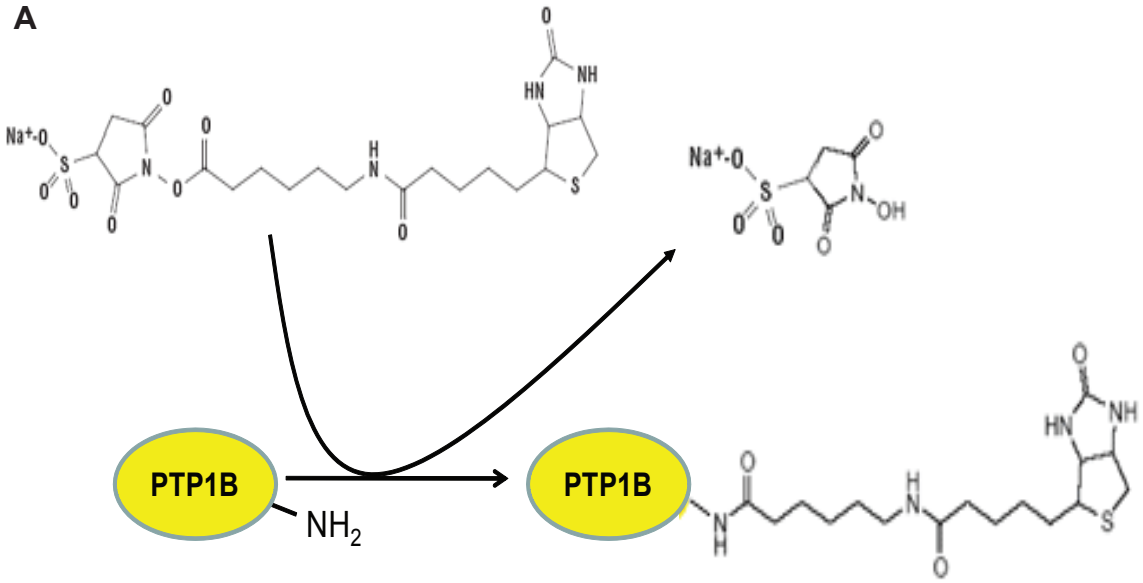
A
PTP1B
NH2
PTP1B

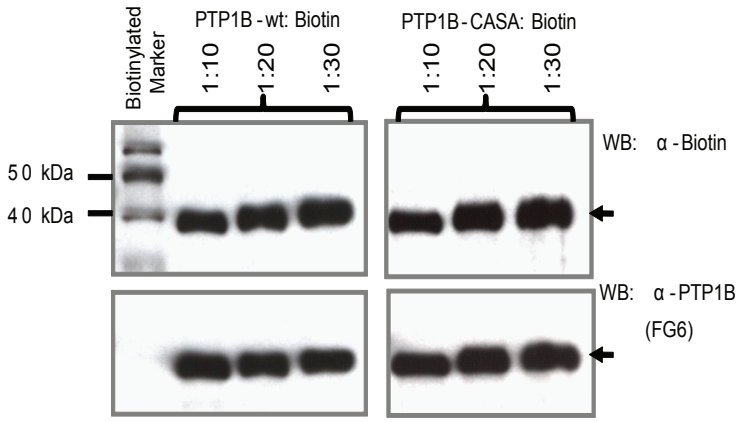
B
Biotinylated Marker
PTP1B - wt: Biotin
PTP1B - CASA: Biotin
1:10
1:20
1:30
1:10
1:20
1:30
50 kDa
40 kDa
WB: α - Biotin
WB: α - PTP1B
(FG6)

Figure 2.5. Biotinylation of PTP1B_wt and PTP1B_CASA *in vitro*
(A) N-hydroxysuccinimide (NHS) ester-activated biotin (sulfosuccinimidyl-6-[biotin-amido]hexanoate) reacts with primary amine groups of proteins at pH 7-9 to form stable amide bonds. The N-terminus and the primary amine groups of the accessible lysines of a protein are labeled with biotin by this reaction and NHS is produced as the leaving group, which along with excess biotin reagent is removed by buffer exchange.
(B) Purified PTP1B-WT (37 kDa) and PTP1B-CASA (37 kDa) were biotinylated by sulfo-NHS-LC-Biotin at three different protein to biotin molar ratio at pH 7.0. Biotinylation was confirmed by western blot with anti-biotin-HRP antibody for detecting the biotinylated proteins and with anti-PTP1B antibody for detecting PTP1B-wt/PTP1B-CASA.

Figure 2.6

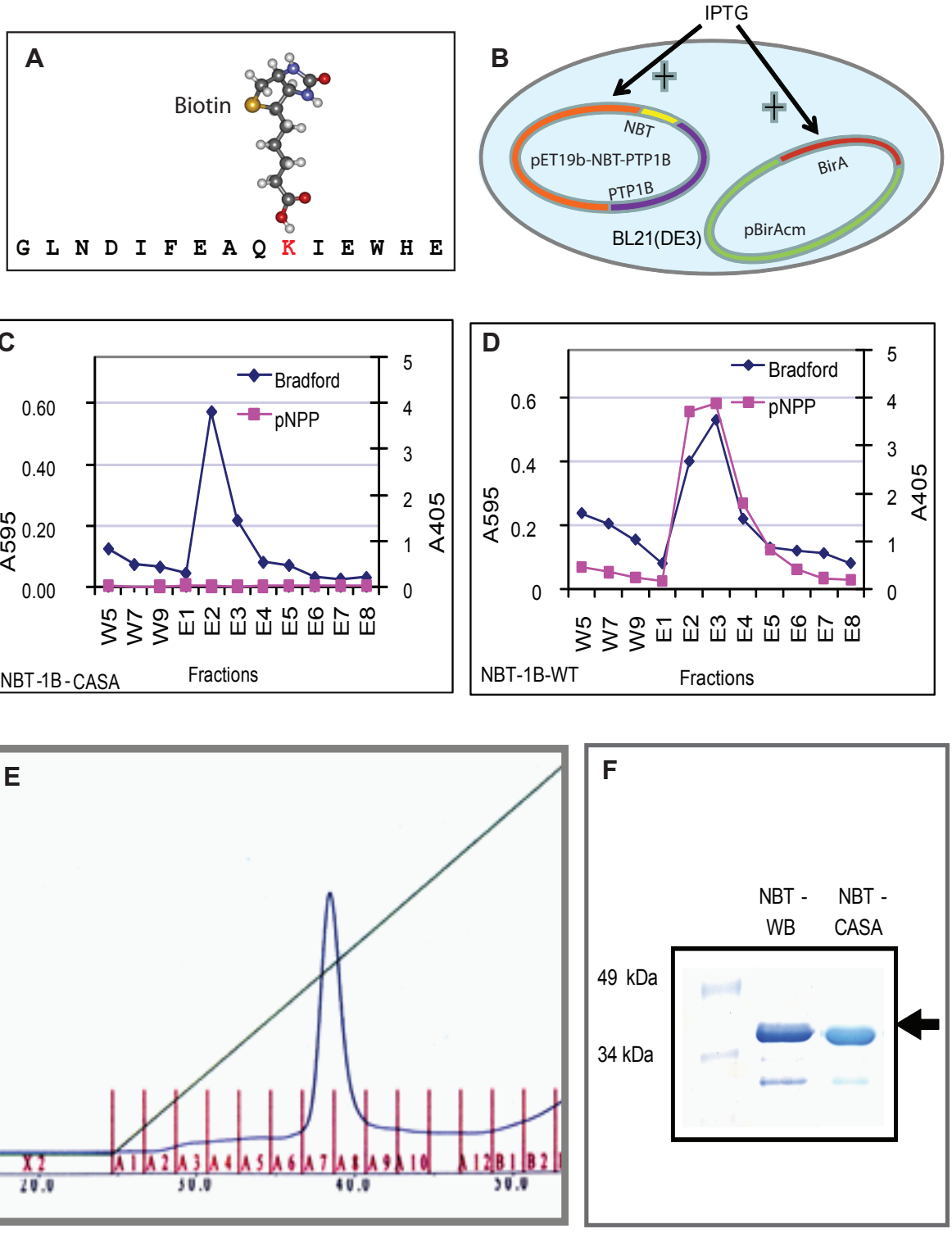
A
Biotin
G L N D I F E A Q K I E W H E
B
IPTG
NBT
pET19b-NBT-PTP1B
PTP1B
BirA
pBirAcm
BL21(DE3)
C
Bradford
pNPP
A595
A405
NBT-1B-CASA
Fractions
W5 W7 W9 E1 E2 E3 E4 E5 E6 E7 E8
D
Bradford
pNPP
A595
A405
NBT-1B-WT
Fractions
W5 W7 W9 E1 E2 E3 E4 E5 E6 E7 E8
E
F
NBT - WB
NBT - CASA
49 kDa
34 kDa

Figure 2.6. Site-Specific Biotinylation of PTP1B (WT/CASA) *in vivo*
(A) The biotinylation sequence is a 15-residue long unique peptide, which is recognized by biotin ligase. In the presence of ATP, the ligase specifically attaches biotin to the lysine residue in this sequence. This tag enables homogenous, site-specific *in vivo* biotinylation (Schatz, 1993).
(B) The biotinylation tag was fused to the N-terminal of PTP1B in pET19b vector and co-expressed in *E. coli* with the recombinant biotin ligase (pBirAcm) by IPTG induction. Biotin ligase in presence of ATP activates biotin to form biotinyl 5' adenylate and transfers the biotin to biotin-accepting proteins or proteins containing the tag. Addition of biotin during the time of induction ensures complete biotinylation of the tagged protein. Using an *E. coli* strain that over-expresses biotin ligase, up to 95% biotinylation of substrate proteins is possible.
(C, D, E, F) Recombinant PTP1B (1-321, WT and CASA) biotinylated *in vivo* in *E. coli* was purified in a two-step purification scheme. In the first step the biotinylated recombinant protein was separated by monomeric avidin beads. Biotinylated proteins were eluted with 5 mM biotin and the fractions were collected (panel C and D are showing purification of NBT-PTP1B-CASA and NBT-PTP1B-WT, respectively). For PTP1B-WT the corresponding protein fractions also showed phosphatase activity as measured by pNPP, whereas the fractions for the CASA mutant showed no activity. In the second step (E) the protein was further purified by an anion exchange column (Q column) and eluted with salt gradient as described in the material and method section. Purified biotinylated proteins were analyzed by SDS-PAGE and Coomassie Blue staining (F).

Figure 2.7

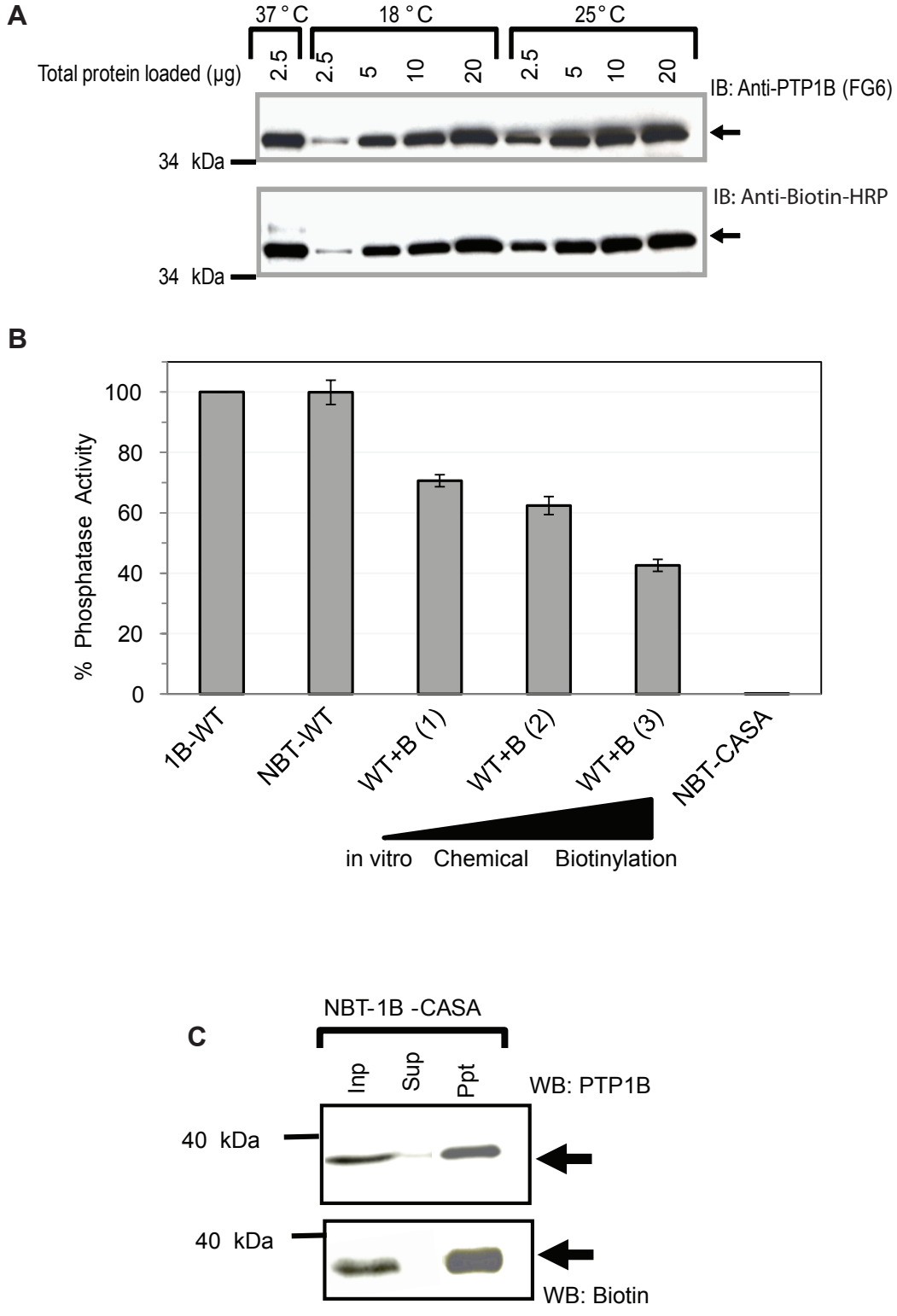
A
37 ° C
18 ° C
25° C
Total protein loaded (µg)
2.5
2.5
5
10
20
2.5
5
10
20
IB: Anti-PTP1B (FG6)
34 kDa
IB: Anti-Biotin-HRP
34 kDa
B
% Phosphatase Activity
100
80
60
40
20
0
1B-WT
NBT-WT
WT+B (1)
WT+B (2)
WT+B (3)
NBT-CASA
in vitro
Chemical
Biotinylation
C
NBT-1B -CASA
Inp
Sup
Ppt
WB: PTP1B
40 kDa
40 kDa
WB: Biotin

Figure 2.7. Site-Specific Biotinylation of PTP1B (WT/CASA) is Efficient and does not affect PTP1B Activity

(A) Conditions for *in vivo* biotinylation were optimized. *E. coli* transformed with pET-NBT-CASA was grown at three different temperatures after IPTG (1 mM) induction. Different amount of total bacterial lysate, as indicated in the figure legend, were separated on SDS-PAGE. PTP1B and biotinylation were detected by anti-PTP1B and anti-biotin-HRP antibodies, respectively.

(B) Phosphatase activity of recombinant PTP1B (1-321), biotinylated *in vivo* (NBT-WT or NBT-CASA) or *in vitro* (WT+B) was measured using ^{32}P-RCML as the substrate as described in the method section. Chemical biotinylation of PTP1B-WT was done at three different protein: biotin ratio [(1) = 1:10, (2) = 1:20 and (3) = 1:30]. The activity of the different PTP1B preps was compared to that of the untagged wild type enzyme (1-321), which was set as 100%. Error bar represents standard deviation from 4 separate phosphatase reactions.

(C) The efficiency of biotinylation and the recovery of the biotinylated protein by Streptavidin coated magnetic beads were tested under experimental conditions similar to those used in the subtractive panning steps for enrichment of antibody phage display library. NBT-CASA (10 nm) was captured with Streptavidin coated magnetic beads (25 µl) and presence of biotinylated protein (and PTP1B) was detected in input, supernatant and precipitated sample by western blot using anti-biotin-HRP antibody (and anti-PTP1B antibody)..

activity of the chemically biotinylated PTP1B was found to be significantly decreased with increasing level of biotinylation. This suggests that the *in vivo* biotinylation does not add biotin non-specifically to important residues in or around the catalytic site of PTP1B and NBT-PTP1B-CASA was amenable to be used for screening specific conformation sensor antibodies. We also observed that NBT-PTP1B-CASA can be completely recovered in solution by streptavidin coated magnetic beads, which was an important prerequisite for its use in the subtractive panning (Figure 2.7 C).

2. 7 Library Enrichment, Validation and Pilot Screening

2.7.1 Significant Enrichment of PTP1B-CASA-Specific scFv-Expressing Phage: We performed five rounds of subtractive panning using NBT-PTP1B-CASA in presence of molar excess of PTP1B-WT (not biotinylated) (Figure 2.8A). We gradually increased the molar ratio of untagged wild type enzyme in the panning steps. We used 10X molar excess of wild type enzyme under reducing conditions, in the first round, 25X in the second round and 50X for the subsequent rounds. Selective enrichment of phage expressing PTP1B-CASA-specific scFvs was observed in terms of increased phage output/input ratio after each round of panning or selection against NBT-PTB1B-CASA. We observed more than 1000-fold enrichment of specific scFv-expressing phage particles after 4^{th} round of panning (Figure 2.8B).

Initially we used ELISA by immobilizing PTP1B-CASA or –WT on the plate surface, to assess whether these enriched pools of phage-scFvs after each round of panning were binding PTP1B-CASA specifically. We have observed that after second round of panning the enriched pools did display moderate preference to CASA over WT PTP1B (Figure 2.8 C). Phage pools at this stage, however, may still yield a mixed population of scFvs. Some of these will be specific for the CASA mutant because of its profound conformational difference from the active reduced form of the enzyme in and around the catalytic site whereas others may recognize the common epitopes of both CASA and WT that are dispersed throughout regions of the proteins other than the active site.

Figure 2.8

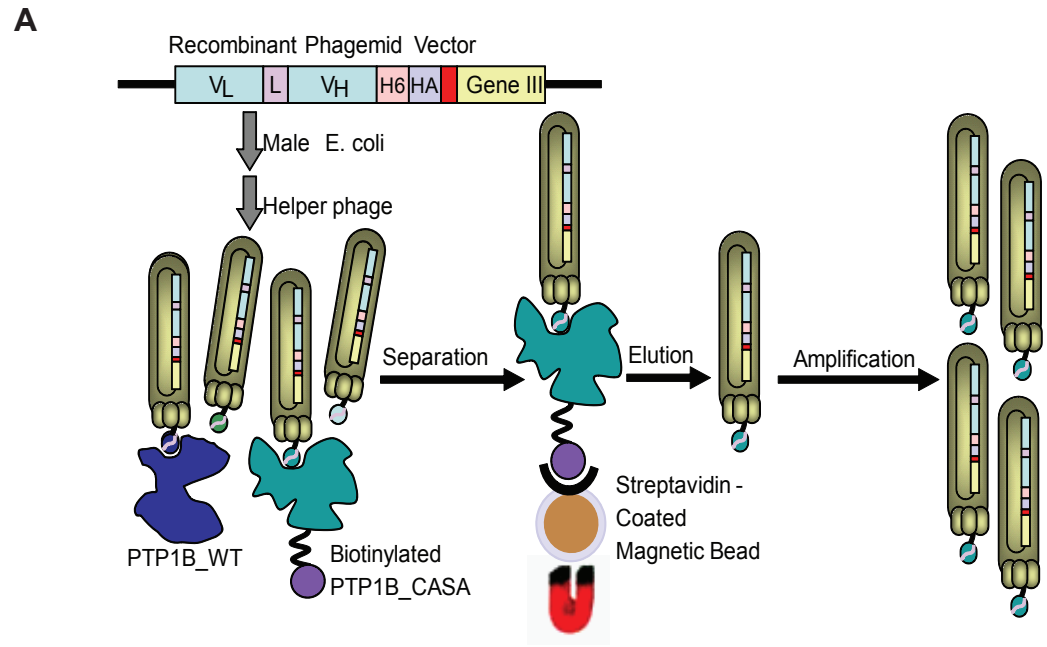
A
Recombinant Phagemid Vector
VL
L
VH
H6
HA
Gene III
Male E. coli
Helper phage
Separation
Elution
Amplification
Streptavidin -
Coated
Magnetic Bead
PTP1B_WT
Biotinylated
PTP1B_CASA

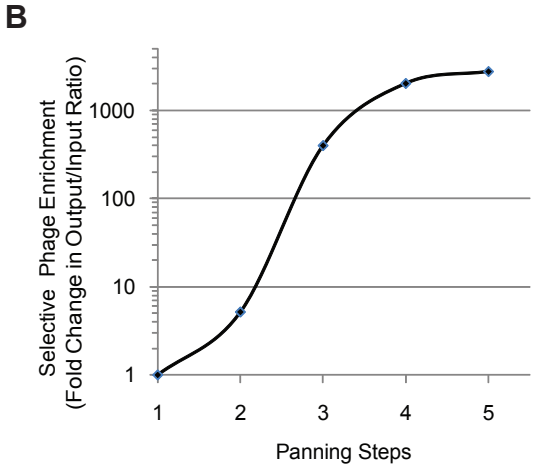
B
Selective Phage Enrichment
(Fold Change in Output/Input Ratio)
1000
100
10
1
1
2
3
4
5
Panning Steps

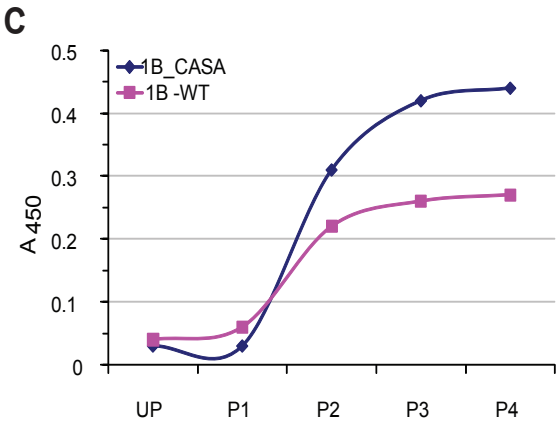
C
1B_CASA
1B -WT
A 450
0.5
0.4
0.3
0.2
0.1
0
UP
P1
P2
P3
P4

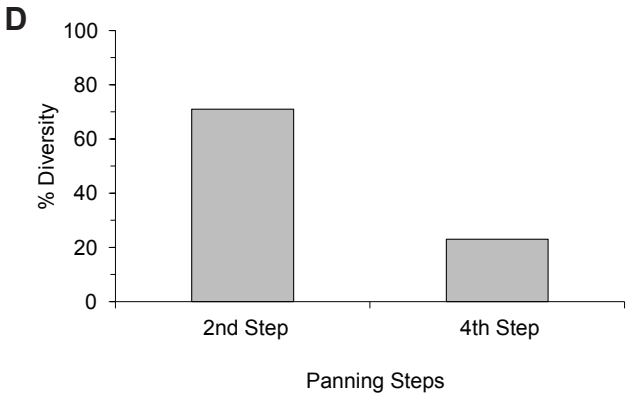
D
% Diversity
100
80
60
40
20
0
2nd Step
4th Step
Panning Steps

Figure 2.8. Subtractive Panning to Enrich PTP1B-OX-Specific scFvs
(A) Single chain variable fragments (scFvs) were inserted into the phagemid that carries a recombinant phage coat protein gene III (at the C-terminal of the scFvs) and was transformed to a male strain of *E. coli* (XL1-Blue). Infection of this transformed bacteria with a helper phage (VCSM13) enabled it to make a collection of functional phage particles expressing the scFvs fused to the surface protein pIII. In the subtractive panning, molar excess (up to 50X) of wild type PTP1B is added under reducing condition (5 mM TCEP). Then biotinylated PTP1B-CASA is added and specific phage-scFvs are isolated by magnetic separation. The phage-scFvs are eluted by glycine-HCl, pH 2.2, amplified in bacteria and used for subsequent rounds of panning. A total of five rounds of panning were performed to enrich the library pool with CASA-specific scFvs.
(B) Enrichment of phage expressing PTP1B-CASA scFvs was estimated in terms of phage output/input ratio by counting phage particles from infected bacteria before and after selection in terms of plaque forming units in each round of panning.
(C) Phage pools from original unpanned scFv library and from each panning step were tested for binding to the immobilized target antigens (PTP1B-CASA and PTP1B-WT) by ELISA. Antigen-bound scFvs displayed on the phage were detected with an HRP-conjugated antibody against the phage coat protein (M13).
(D) As the library was enriched, the diversity decreased. Diversity was determined by checking the variation in the CDR regions of sequenced scFvs from different round of panning.

2.7.2 Enriched Phage Pool Contains Diverge scFvs with Complete Functional Sequences: To isolate individual phage particles expressing functional scFvs we sequenced ~400 phagemid constructs. Bacterial clones from the 4^{th} and 2^{nd} round of panning were sequenced using phagemid-specific primers. Sequences were analyzed using Vector NTI software (Invitrogen). More than 95% of the sequences were full-length functional scFvs, indicating that the cloning strategy and library display worked. Interestingly, diversity among the functional scFv sequences was found to be ~70% after the 2^{nd} round of panning, whereas after the 4^{th} round of panning it was 20% (Figure 2.8 D), suggesting that the library was enriched with specific scFvs after the panning steps. Sequences were sorted into groups on the basis of their differences in the hypervariable regions. Selection of functional scFv sequences was confirmed by checking whether the sequences are of chicken origin. All the selected sequences in this case aligned with the amino acid sequence of light and heavy chains of chicken IgG, except for the differences in the hypervariable regions. As expected, the CDR3 region of the heavy chain was found to be the most variable segment in the scFvs. The selected scFv sequences also contain the 6-His and HA tags at the C-terminal. A portion of the analyzed sequences is shown in Figure 2.9.

2.7.3 Solid-Phase ELISA is not Suitable for Screening Conformation-Sensor scFvs: Analysis of individual clones from a panned pool can be performed either with antibody fragment displaying phage prepared from a single clone or with a single antibody fragment expressed and prepared from IPTG induced phage infected bacterial culture (Figure 2.10 A and B). To isolate PTP1B-CASA-specific scFv from this enriched pool of library we initially used a phage-ELISA technique by immobilizing PTP1B-CASA or –WT on plate surface and using individually grown phage particles with different scFvs expressed on their surface. We were not successful in isolating significant numbers of scFvs specific for CASA mutant by this method (Figure 2.8 C). At this stage the scFvs, however, are still attached to the entire phage particle through the surface protein pIII and this may cause some steric hindrance, restricting specificity to a particular conformation. Therefore, we decided to express all these pre-sorted individual scFvs as soluble proteins in bacteria without the pIII fusion. We screened ~1000 individual bacterially expressed scFvs (~400 with known sequence and ~600 by

Figure 2.9

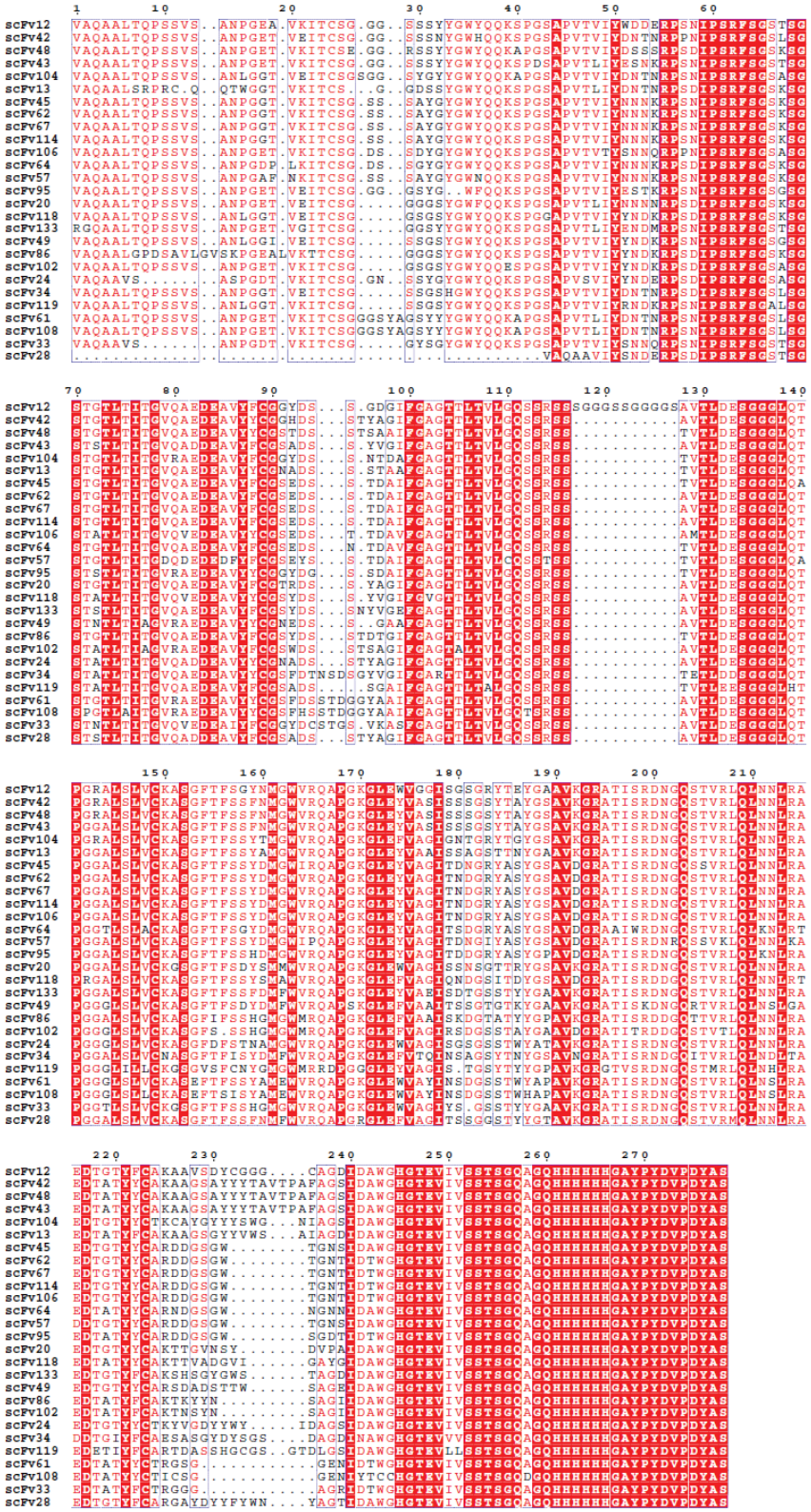
scFv12
scFv42
scFv48
scFv43
scFv104
scFv13
scFv45
scFv62
scFv67
scFv114
scFv106
scFv64
scFv57
scFv95
scFv20
scFv118
scFv133
scFv49
scFv86
scFv102
scFv24
scFv34
scFv119
scFv61
scFv108
scFv33
scFv28

Figure 2.9. Multiple Sequence Alignment of Selected scFvs
A representation of multiple sequence alignment of the selected scFvs is presented here. All scFvs in this alignment are characterized either *in vitro* or expressed as intrabodies and their binding with PTP1B-OX was determined.

Figure 2.10

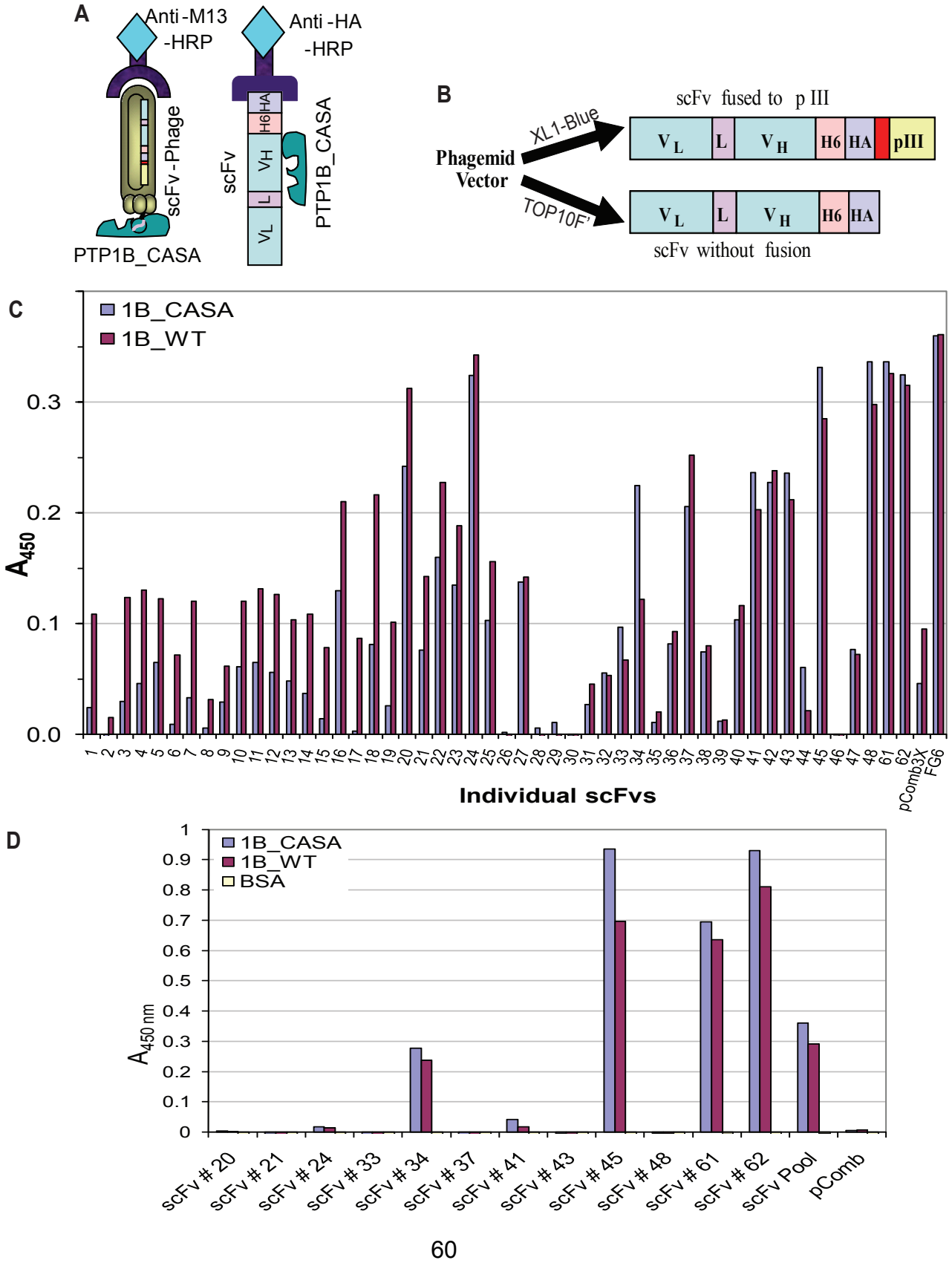
A
Anti-M13
-HRP
scFv-Phage
PTP1B_CASA
Anti-HA
-HRP
H6
HA
scFv
VH
L
VL
PTP1B_CASA
B
scFv fused to p III
Phagemid
Vector
XL1-Blue
TOP10F'
VL
L
VH
H6
HA
pIII
scFv without fusion
C
1B_CASA
1B_WT
A450
0.0
0.1
0.2
0.3
Individual scFvs
pComb3X
FG6
D
1B_CASA
1B_WT
BSA
A450 nm
0
0.1
0.2
0.3
0.4
0.5
0.6
0.7
0.8
0.9
1
scFv # 20
scFv # 21
scFv # 24
scFv # 33
scFv # 34
scFv # 37
scFv # 41
scFv # 43
scFv # 45
scFv # 48
scFv # 61
scFv # 62
scFv Pool
pComb

Figure 2.10. Screening for PTP1B-CASA-Specific scFvs by ELISA
(A) This panel shows the scheme for screening individual scFvs by Phage ELISA or by ELISA using soluble scFvs expressed in bacteria. The target antigen (PTP1B-CASA) was immobilized on ELISA plate and bound scFv was detected by using a phage coat protein specific antibody (anti-M13-HRP) in case of phase ELISA. For detecting bacterially expressed scFvs bound to the immobilized antigen we used an anti-HA-HRP antibody, which recognizes the C-terminal HA tag of the associated scFv molecule.
(B) Soluble scFvs can be expressed in bacteria in two ways. There is an amber codon between the HA tag and the pIII surface protein of phage particle. When expressed in non-suppressor bacterial strains (XL1-Blue) that do not recognize this stop codon scFvs are produced as a fused chimera with the pIII protein. However, in suppressor strains, such as TOP10F´, this amber codon allows expression of soluble protein by excising the gene III fragment. We have used scFvs without pIII fusion for *in vitro* screening and characterization of PTP1B-OX specific antibodies.
(C) A representation of phage ELISA shows binding of 50 pre-sorted individual phage particles expressing different scFvs to PTP1B-CASA or –WT immobilized on plate surface. Bound scFv was detected by recognizing the associated phage by anti-M13-HRP antibody. Phage preparation from phagemid without any insert was used as a negative control and anti-PTP1B antibody (FG6) was used to measure the bound antigen on plate surface.
(D) Individual scFvs were expressed in TOP10F´ as soluble protein and extracts from infected bacteria were screened against immobilized PTP1B CASA/WT by ELISA. Bound scFvs were detected by anti-HA-HRP antibody. Bacterial extract infected with the phage particle containing only the phagemid without any scFv insert was used as a negative control.

randomly selecting scFvs from 2nd and 4th round of panning) by ELISA with immobilized CASA mutant. In these initial screenings we were unable to find scFvs displaying significant preferential binding to CASA over the reduced wild type form of the enzyme (Figure 2.8 D).

We have performed the panning process in solution, but all our screening to this step was done with immobilized PTP1B-CASA/PTP1B-WT. The immobilization was performed by coating PTP1B randomly on plastic surfaces without any uniform directional orientation. Immobilization of antigens on plastic causes partial denaturation (Nizak et al., 2005) and the conformational difference at the active site between the reduced WT and CASA mutant forms of PTP1B may not be preserved under these conditions. In the ELISA protocol, we attached the antigen by initially treating it with 100 mM sodium bicarbonate at pH 8.6 as the coating buffer. This elevated pH may also cause alteration at the active site and denaturation of the protein, which is evident in significant reduction of phosphatase activity at this high pH. Moreover, PTP1B, like many other PTPs, is very prone to oxidation. All the ELISA experiments were done under non-controlled environment without protecting the WT enzyme from oxidation. During the process of surface coating and subsequent washes, the WT enzyme may be oxidized and associate with the scFvs making screening and isolation of CASA-specific scFvs quite challenging.

2.8 Isolation of Candidate scFvs Specific to PTP1B-OX

To analyze systematically individual scFvs from enriched pools of phage particles after the subtractive panning, we adopted two approaches to conduct the screen in solution in order to preserve the conformational integrity of PTP1B-OX. In the first approach we employed a phosphatase assay in solution to detect whether any scFvs bound to reversibly oxidized PTP1B and inhibit its reactivation. In the second approach we expressed a number of different scFvs in mammalian cells and assessed their binding in solution to endogenous PTP1B under oxidizing conditions. Testing individual scFvs directly in cells also provided us with immediate important information about the specificity of the antibody in a cellular context.

To screen for PTP1B-OX-specific scFvs using reversibly oxidized recombinant PTP1B (1-321), we first established conditions under which PTP1B was reversibly oxidized by H_2O_2 in solution. We found that PTP1B (15 nM) can be reversibly oxidized when treated with 50 μM to 1 mM H_2O_2 followed by addition of the reducing agent (5 mM TCEP) to reactivate the enzyme under the conditions described (Figure 2.11 B). The ability of individual scFvs to stabilize the reversibly oxidized, inactive conformation of the PTP1B was assessed by the ability of the scFv to inhibit the reactivation of the enzyme by reducing agent (Figure 2.11 A).

At first we wanted to see whether any of the scFvs used in this screen had direct inhibitory effect on phosphatase activity of PTP1B under reducing or non-oxidizing conditions. None of the scFvs from a batch of randomly selected 12 scFvs had any effect on PTP1B activity, under reducing or non-oxidizing conditions (Figure 2.11 A).

Some of the scFvs (45, 57, 64 and 106), when incubated with reversibly oxidized PTP1B, showed substantial inhibition of the restoration of PTP1B activity with the addition of reducing agent (Figure 2.11 D). In particular, scFvs 45 and 57, inhibited the reactivation by ≥70% (IC_{50} 19 nM and 10 nM, respectively) (Figure 2.12 and Table 1). These results reflected the ability of these scFvs to stabilize PTP1B-OX conformation *in vitro* and inhibit the reactivation to an active, reduced form of the enzyme.

Figure 2.11

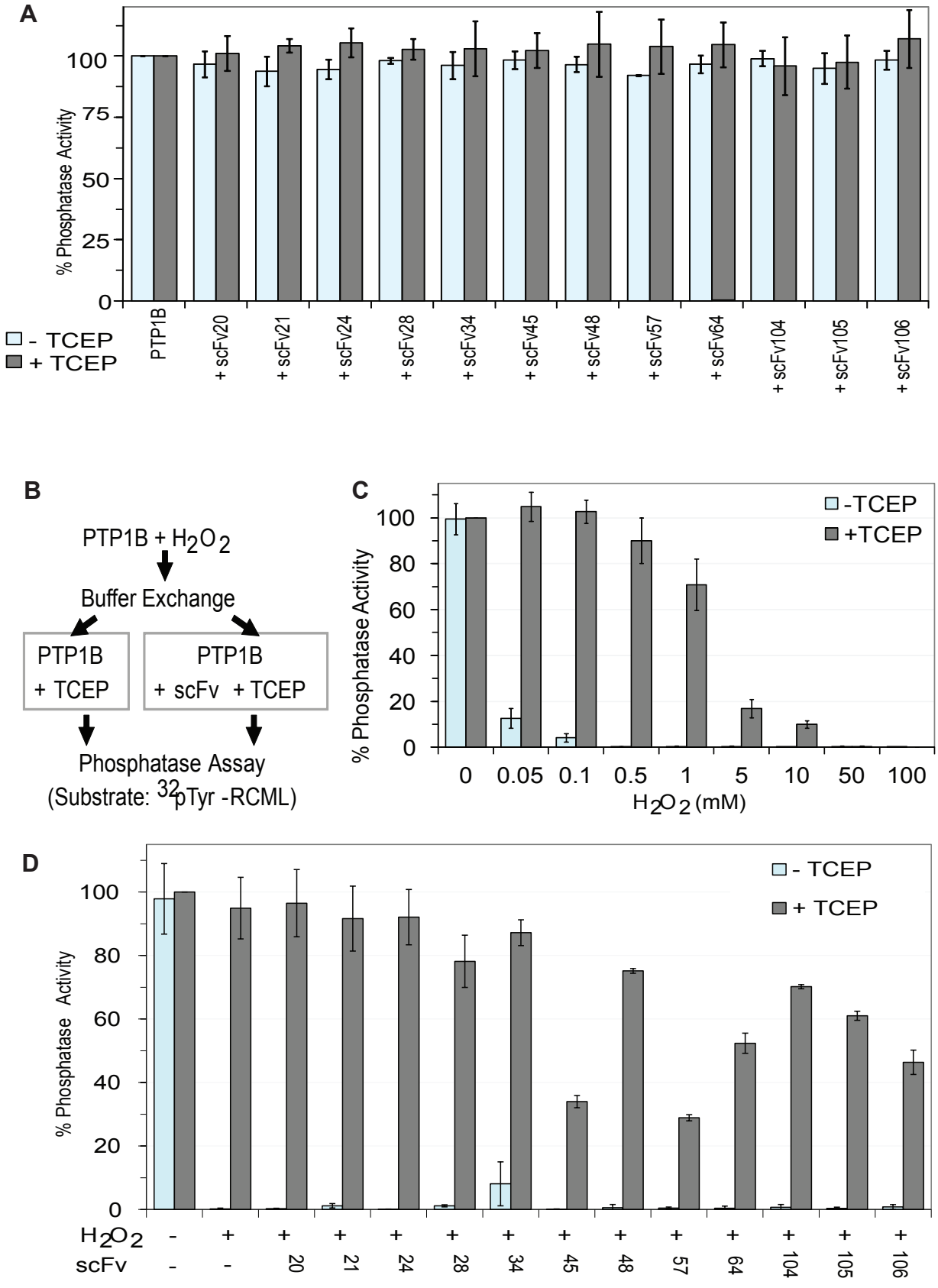
A
% Phosphatase Activity
100
75
50
25
0
- TCEP
+ TCEP
PTP1B
+ scFv20
+ scFv21
+ scFv24
+ scFv28
+ scFv34
+ scFv45
+ scFv48
+ scFv57
+ scFv64
+ scFv104
+ scFv105
+ scFv106
B
PTP1B + H2O2
Buffer Exchange
PTP1B
+ TCEP
PTP1B
+ scFv + TCEP
Phosphatase Assay
(Substrate: 32pTyr -RCML)
C
-TCEP
+TCEP
% Phosphatase Activity
100
80
60
40
20
0
0 0.05 0.1 0.5 1 5 10 50 100
H2O2 (mM)
D
- TCEP
+ TCEP
% Phosphatase Activity
100
80
60
40
20
0
H2O2 - + + + + + + + + + + + + +
scFv - - 20 21 24 28 34 45 48 57 64 104 105 106

Figure 2.11. Screening for PTP1B-OX-Specific scFvs by PTP1B Reactivation Assay

(A) Purified individual scFvs (750 nM) were incubated with PTP1B (7.5 nM) with or without reducing agent TCEP (5 mM). Aliquots from these samples were used to measure phosphatase activity of PTP1B. An artificial protein substrate RCML in which tyrosine was phosphorylated with ^{32}P was used in this assay to measure the phosphatase activity as described in the method section. The final PTP1B and scFv concentrations during the phosphatase reaction were 5 nM and 500 nM, respectively.

(B) Flow chart shows the steps for screening conformation sensor scFvs against PTP1B-OX. Recombinant PTP1B (1-321) was reversibly inactivated by H_2O_2, which was removed by quick buffer exchange. Oxidized PTP1B was incubated with or without scFvs and finally phosphatase activity was measured after reactivating the enzyme with reducing agent (TCEP).

(C) Conditions for reversible oxidation of PTP1B by H_2O_2 was established. In this assay 15 nM of PTP1B was incubated with increasing concentration of H_2O_2 as indicated in the figure legend. H_2O_2 was removed by buffer exchange and aliquots of H_2O_2-treated protein (5 nM final) were used in the phosphatase assay without or with TCEP to observe the inactivation and reactivation of the enzyme, respectively.

(D) PTP1B (15 nM) was reversibly oxidized by H_2O_2 (75 µM) and aliquots (7.5 nM) from this reversibly oxidized PTP1B were incubated with purified scFvs (750 nM) at RT for 30 minutes. Reactivation of enzyme activity with or without the presence of different scFvs was measured by phosphatase assay in presence of TCEP. The final enzyme and scFv concentrations in the phosphatase assay were adjusted to 5 nM and 500 nM, respectively. (in A, C, and D error bar shows standard deviation from three phosphatase assays).

Figure 2.12

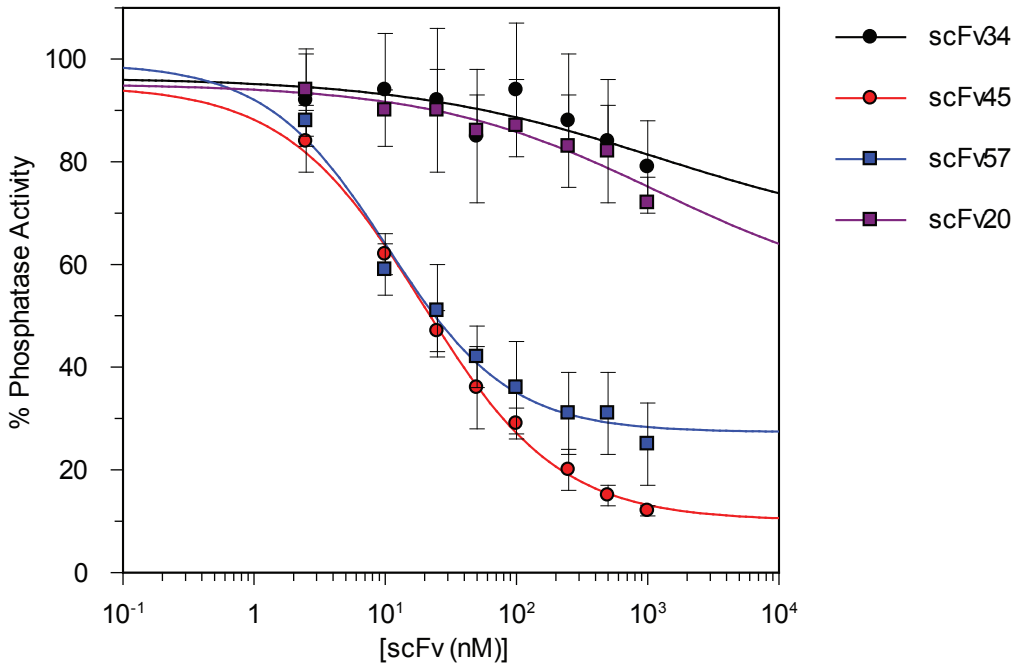

Table 1

scFv	IC50 (nM)
scFv45	19.0 ± 1.9
scFv57	10.2 ± 1.7
scFv34	1217.7 ± 1737.1
scFv20	1203.9 ± 757.4

Figure 2.12. Conformation Sensor scFv efficiently inhibits PTP1B-OX Reactivation PTP1B was reversibly oxidized by H_2O_2 as in Figure 3.1 and as indicated in the method section. Increasing concentrations of scFvs 45, 57, 34, and 20 (2.5 nM to 1 mM) were incubated with PTP1B-OX at RT for 30 minutes and phosphatase activity was measured after adding TCEP (5 mM).

Table 1. IC_{50} of scFvs for inhibiting the reactivation of PTP1B-OX. IC_{50} value for the inhibition of PTP1B reactivation was determined by fitting the % phosphatase activity with increasing concentration of scFvs (nM) using the Grafit software (Leatherbarrow, 2009). This software fits the inhibition data to a 4-parameter IC_{50} equation:

$$y = \frac{Range}{1 + \left(\frac{x}{IC_{50}}\right)^{s}} + Background$$

In this equation, *Range* is the fitted uninhibited value minus the Background, and *s* is a slope factor. The equation assumes that *y* (response, activity etc.) falls with increasing *x* (concentration).

Materials and Methods: Chapter 2

2.9 Construction of scFv Phage Display Library

A phage display library displaying single chain variable fragments (scFvs) fused to its surface protein pIII with a size of ~2 x 10^7 was constructed from the immune genes extracted from the spleen and bone marrow of chickens immunized with PTP1B-CASA (mutant structurally identical to reversibly oxidized PTP1B). Different steps of the library construction are described here.

2.9.1 Expression and Purification of Recombinant PTP1B: The catalytic domain (37 kDa) of wild type PTP1B (PTP1B-WT) or PTP1B-CASA was constructed in a pET19b vector (#69677-3, EMD Biosciences) and expressed in BL21 *E. coli*. Single colonies harboring the expression plasmid were grown in LB + Ampicillin (50 μg/ml) overnight. The overnight culture was diluted 1:50 in LB + Ampicillin (50 μg/ml) at 37°C until OD_{600nm} became 0.6. Expression of recombinant PTP1B was induced with 0.3 mM IPTG at 37°C, 250 rpm for 4 hours. Cells were harvested and resuspended in Lysis Buffer (25 mM NaH_2PO_4, pH 6.5, 10 mM NaCl, 1 mM EDTA, 5 mM DTT, 1 mM PMSF, 2 mM benzamidine and protease inhibitor cocktail). The suspension was incubated with 0.5 mg/ml lysozyme at 4°C for 30 minutes and sonicated to extract the soluble protein. The sample was then centrifuged at 50,000 g at 4°C for 30 minutes and supernatant was collected for purification of the recombinant PTP1B. The first purification step was a cation exchange column (SP Sepharose HP, # 17-1152-01) using 25 mM NaH_2PO_4, pH 6.5, 10 mM NaCl, 1 mM EDTA, 5 mM DTT as the binding buffer and the protein was eluted by a gradient elution with 10-500 mM NaCl. Fractions containing PTP1B were pooled together and used for a final purification step by an anion exchange column (Q Sepharose HP; # 17-1153-01, GE Healthcare) using 25 mM Tris-Hcl, pH 7.5, 1mM EDTA, 5 mM DTT as the binding buffer. The purified protein was eluted with 0-500 mM NaCl gradient.

2.9.2 Chicken Immunizations: Chickens (Pocono Rabbit Farm and Laboratory, PA, USA) were immunized with purified PTP1B-CASA. Blood from each immunized chicken was titrated by ELISA to determine the presence of an antigen-specific immune response. Detection of a strong serum antibody titer was an early indication of the presence of an enriched pool of PTP1B-CASA-binding immunoglobulin genes that make up the building blocks of combinatorial antibody library.

2.9.3 Total RNA Extraction: Spleen and bone marrow are the major repository of plasma cells that secrete antibodies against the antigen of interest and contain the highest levels of specific mRNA. Therefore, spleen and bone marrow from immunized animals were harvested. Total RNA was isolated from the spleen and bone marrow using TRI-Reagent (AM9738, Applied Biosystems) and isopropanol precipitation.

2.9.4 First-strand cDNA Synthesis from the Total RNA: First-strand cDNA was synthesized from the total RNA extracted from both bone marrow and spleen by reverse transcription-polymerase chain reaction (RT-PCR) using an oligo (dT) primer. This first-strand cDNA was directly used for PCR amplification of the V_L and V_H genes.

2.9.5 Generation of Recombinant scFvs: A peptide linker of varying length between the V_L and the V_H domains of immunoglobulin molecule generates recombinant single chain variable fragments (scFvs). An equimolar mixture of first-strand cDNA derived from the spleen and bone marrow of the PTP1B-CASA-immunized chickens was used to amplify V_L and V_H genes for the construction of combinatorial scFv antibody libraries. Two scFv constructs were produced, one with a 7 amino acid linker sequence (GQSSRSS) and one with an 18 amino acid linker (GQSSRSSSGGGGSGGGGS). Two PCR steps were performed in order to generate scFv constructs. In the first PCR step V_L and V_H gene segments were amplified separately with the addition of the linker sequence (short or long) in the forward primer for the V_H gene amplification. In the second overlap PCR V_L and V_H were combined via the linker sequence to form a full-length scFv construct. The primer pairs for the amplification were:

V_L: 5′ GTGGCCCAGGCGGCCCTGACTCAGCCGTCCTCGGTGTC 3′ (sense) and
5’ GGAAGATCTAGAGGACTGACCTAGGACGGTCAGG 3’ (reverse)
V_H: 5’ GGTCAGTCCTCTAGATCTTCCGCCGTGACGTTGGACGAG 3’ (sense) for short linker and
5’GGTCAGTCCTCTAGATCTTCCGGCGGTGGTGGCAGCTCCGGTGGTGGCGGTTC CGCCGTGACGTTGGACGAG 3’ (sense) for long linker and
5’ CTGGCCGGCCTGGCCACTAGTGGAGGAGACGATGACTTCGGTCC 3’ (reverse)

scFv: 5’ GAGGAGGAGGAGGAGGAGGTGGCCCAGGCGGCCCTGACTCAG 3’ (sense) and
5’GAGGAGGAGGAGGAGGAGGAGCTGGCCGGCCTGGCCACTAGTGGAGG 3’ (reverse)
All the PCRs were performed using Amplitaq DNA Polymerase (Applied Biosystems) following the manufacturer’s protocol. The final scFv PCR products were pooled together, ethanol precipitated and quantified.

2.9.6 The Phagemid Vector: A modified version of the pComb3XSS phagemid vector was used for the construction of the scFv antibody libraries. This vector allows uniform directional cloning that utilizes a single restriction endonuclease, Sfi I, based on asymmetry of the two sites. This vector contains the amber codon, inserted between the 3′ Sfi I restriction site and the 5′ end of phage gene III fragment. This allows for expression of soluble antibody fragments in nonsuppressor strains of bacteria without excising the gene III fragment. The pComb3XSS also contains two peptide tags, the histidine (H6) tag and the hemagglutinin (HA) tag for purification of soluble proteins and for immunodetection. This phagemid was modified in such a way that it has a reduced potential for recombination and deletion within the vector. In addition the vector contains an ampicillin resistant gene for selection purposes.

2.9.7 Construction of the scFv Library: Both the scFv PCR products and phagemid were prepared for cloning by restriction endonuclease digestion with Sfi I. The digested products were gel purified and the cloning efficiency of the linearized

vectors and scFv inserts was tested using small scale ligations and found to be in the range of 10^7 to 10^8 cfu/μg of DNA, with minimal background (less than 5%). Two ligation reactions were performed in parallel with a 2:1 molar ratio of insert:vector, 1X ligase buffer, 10 μl (1 U/μl) T4 DNA ligase, in a 200-μl reaction. The ligations were incubated overnight at room temperature, ethanol precipitated and resuspended in water. The ligated DNA was transformed into 300 μl of electrocompetent XL-1 Blue cells. This *E. coli* is a male strain that harbors F´ pili, through which the filamentous bacteriophage infect the bacteria. The F´ factor-containing XL-1 Blue cells are maintained by the selection pressure of tetracycline. The library size (expressed as the transformation efficiency of the ligated library construct) was determined by plating the transformed cells on LB/carbenicillin plates. The size of each library was found to be ~10^7. The culture was then grown under the selection of carbenicillin to select for transformed bacterial cells. To induce the production of functional phage particles by the infected *E. coli* culture, preparation of a filamentous helper phage VCSM13 (10^{12} PFU/ml) was added and selected with kanamycin (there is a kanamycin resistant gene in the genome of the helper phage). After overnight incubation at 37°C with shaking, the culture supernatant containing the phage particles was harvested by centrifugation. The bacterial pellet was used to purify phagemid DNA (the library DNA preparation) using the Qiagen Maxiprep kit. The phage particles displaying scFv fused to its pIII coat protein were finally harvested from the supernatants by PEG precipitation. PEG precipitated phage from each library were mixed together to generate an antibody phage display library with a size of ~2 x 10^7, which was used for panning to enrich PTP1B-CASA-specific scFvs.

2.10 Subtractive Panning for Isolating PTP1B-CASA Specific Antibody Fragments

A subtractive panning protocol was designed to isolate scFvs selective for the PTP1B-CASA mutant, while removing the pools that recognize and detect the common epitopes on both the oxidized and the reduced form of the enzyme. Addition of molar excess wild type PTP1B in its reduced active conformation to the library in solution will reduce the level of scFvs that recognize the common structural epitopes of the two

forms of the enzyme. Specific scFvs can be isolated with biotinylated PTP1B-CASA and subsequent capturing of the antigen-antibody complex with streptavidin coated magnetic beads. Several rounds of panning will enrich the CASA-specific scFvs. Different steps of the subtractive panning protocol are described below:

2.10.1 PTP1B Biotinylation *in vitro:* Purified PTP1B and PTP1B-CASA were biotinylated by using EZ-Link Sulfo-NHS-LC Biotinylation Kit (#21425, Thermo Scientific) according to the manufacturer's protocol. Excess biotinylation reagents were removed from the protein solution by buffer exchange with Zeba Desalting Columns (#89882, Thermo Scientific). The extent of biotinylation of purified proteins (moles of biotin/mole of protein) were measured by HABA (2-[4´-hydroxyazobenzene]-benzoic acid) assay (comes with the biotinylation kit) according to the manufacturer's protocol.

2.10.2 PTP1B Biotinylation *in vivo* and Purification of Biotinylated PTP1B: The biotinylation sequence is a unique peptide, 15 residues long (GLNDIFEAQKIEWHE), which is recognized by biotin ligase. In the presence of ATP, the ligase specifically attaches biotin to the lysine residue in this sequence. This tag was fused to the N-terminal of PTP1B in pET19b vector and the recombinant protein was co-expressed in *E. coli* [BL21(DE3)] with another plasmid that harbors recombinant biotin ligase. To co-express biotin ligase in E. coli we used pBirAcm plasmid, which was isolated from Dnase deficient K-12 *E. coli* strain (AVB99, Avidity). The pBirAcm plasmid is an engineered pACYC184 plasmid (ColEI compatible) with an IPTG inducible birA gene to over-express biotin ligase.

To make the expression construct for NBT-PTP1B (N-terminally biotinylated PTP1B), the 1-321 catalytic domain of the WT or CASA mutant was PCR amplified using forward primer with the entire biotinylation tag with additional Nco I restriction site and cloned in pET19b plasmid. The primers used for this amplification are– 5´GGGGAACCATGGGCCTGAACGACATCTTCG AGGCTCAGAAAATCGAATGGCACGAAATGGAGATGGAAAAGGAGTTCG3´ (sense) and 5´AGCAGCCGGATCCCCCGGGCTGCAGGAATTCTCTAGACTAGAG3´ (reverse).

The bacterial expression strain *E. coli* [BL21(DE3)] was first transformed with the recombinant biotin ligase (BirA) contain plasmid pBirAcm and maintained under the selection of chloramphenicol (10 µg/ml). This bacteria was made chemically competent again and transformed with pET19b containing the PTP1B (1-321) gene with N-terminal biotin tag fusion. We optimized the conditions for expression of both the recombinant proteins and the extent of biotinylation of the target protein by biotin ligase in bacteria by varying the IPTG concentration, induction temperature and time. Expression of recombinant proteins in bacteria was induced optimally with 1 mM IPTG in presence of 50 µM biotin in the growth medium for 4 hours at 37°C. Biotin-protein ligase activates biotin to form biotinyl 5' adenylate and transfers the biotin to biotin-accepting proteins. Addition of biotin during the time of induction ensures complete biotinylation of the tagged protein. Using an *E. coli* strain that over-expresses biotin ligase, up to 95% biotinylation of substrate proteins is possible. The *in vivo* biotinylated PTP1B (both CASA and wild type) was purified in a two-step purification scheme. In the first step the biotinylated recombinant protein was separated by Immobilized Monomeric Avidin resin (#20267, Thermo Scientific) following the manufacturer's protocol and eluted with 5 mM biotin in PBS. In the second step the protein was further purified by an anion exchange column (HiTrap Q FF, # 17-5053-01, GE Health Sciences) and eluted in 25 mM Tris-HCl, pH 7.5, 1 M NaCl, 1 mM EDTA, 5 mM DTT and dialyzed in 25 mM Tris-HCl, pH 7.0, 50 mM NaCl, 5 mM DTT, 0.1 mM PMSF (added before freezing), 0.02% NaN_3, 50% Glycerol.

To ensure that efficient recovery of the antigen would be achieved under the screening conditions and to assess the efficiency of the biotinylation in vivo we have performed a Streptavidin pull down experiment using the NBT-CASA or NBT-WT. In brief, 10 nm of the biotinylated proteins were mixed with 25 µl of Streptavidin coated magnetic bead in 1 ml of TBS containing 2% BSA, 5 mM DTT, 0.5% Tween-20 and 0.02% NaN3 and incubated with gentle rotation at 4ºC for 2 hours. The beads were washed 3X with cold TBS and associated complex was separated by SDS-PAGE.

PTP1B was detected by anti-PTP1B antibody (FG6) and biotinylated protein was detected by anti-biotin-HRP antibody.

The activity of the *in vivo* biotinylated protein along with the enzyme that was initially biotinylated *in vitro* by chemical modification was measured by an RCML phosphatase assay. The catalytic activity of PTP1B was found to be conserved by the specific *in vivo* modification whereas the chemically biotinylated protein showed reduced activity. This implies that the N-terminal site-specific biotinylation *in vivo* does not cause structural modification at the catalytic site of the enzyme. The *in vivo* biotinylated protein was used for panning.

2.10.3 Phosphatase Assay: Reduced carboxamidomethylated and maleylated lysozyme (RCML) was labeled with ^{32}P using recombinant GST-FER kinase to stoichiometry up to 0.8 (mol ^{32}P incorporated/mol of protein) as described by the method in (Meng et al., 2005). PTP1B (1-321)-WT without any modification, PTP1B (1-321)-WT/CASA with N-terminal biotinylation *in vivo* in E. coli, and *in vitro* biotinylated untagged PTP1B (1-321)-WT (5 nM PTP1B final concentration) was mixed with 500 nM ^{32}P-RCML in phosphatase **a**ssay buffer (50 mM HEPES, pH 7.0, 100 mM NaCl, 0.1% BSA, 5 mM TCEP) and incubated at 30°C for 10'. The reaction was stopped with 10% TCA (final) with 2.5% (w/v) BSA, incubated at -80°C for 30', and thawed at room temperature. The supernatant was collected and the CPM was determined by scintillation counting. Specific Activity of the protein preps was compared with that of the untagged PTP1B (1-321), activity of which was set as 100%.

2.10.4 Subtractive Panning: The scFv library was mixed in solution with 10-50 times molar excess of wild type PTP1B than the biotinylated PTP1B-CASA under reducing conditions for 4 hours at 4°C to exclude the pools of antibodies that recognize the common epitopes on both the oxidized and the reduced form of PTP1B. Biotinylated PTP1B-CASA was mixed to this solution and incubated for another 4 hours at 4°C. From this mixture, scFv displaying phage bound to this biotinylated PTP1B-CASA were captured by streptavidin coated magnetic beads. After magnetic separation

of the antibody-antigen complex captured on the beads, non-specific binders were removed by repeated washing. Bound phage displaying specific scFvs on their surface were eluted under acidic (glycine-HCl, pH 2.2) conditions, neutralized and amplified. Amplified phage from the first round of panning were used for the second round selection and a total of four rounds of panning were performed accordingly under the same conditions. The input phage were pre-incubated with the streptavidin coated beads before each round of panning to eliminate the bead- and streptavidin binding phage. Input and output phage were estimated to determine whether selective enrichment of specific scFv-displaying phage occurred during the panning steps. The detailed step by step protocol for the subtractive panning is described below:

1. The streptavidin (SA) coated magnetic beads were prewashed with 10 volumes of TBS containing 2% BSA and 0.02% NaN3 by mixing and centrifuging at 12,000 rpm for 30 seconds. The washed beads were resuspended in TBS containing 2% BSA, 5 mM DTT and 0.02% NaN3 to make the final SA concentration to 10 mg/ml.
2. The binding capacity of the beads is 5-10 μg (30-60 pmole) of biotinylated antibody (IgG) per mg of SA beads. Therefore, 25 μl of SA beads at 10 mg/ml, should bind 7.5-15.0 pmole of biotinylated protein. We used 400 ng of biotinylated PTP1B-CASA (~10 pmoles). In the first and second panning steps we used 4 μg (10X molar access) and 10 μg (25X molar access) of untagged wild type PTP1B (PTP1B-WT), respectively. In both the 3rd and 4th round of panning we used 20 μg of untagged wild type PTP1B, which is 50X molar access of the biotinylated PTP1B-CASA.
3. The scFv library was pre-adsorbed by SA beads in 400 μl final volume in 1.5 ml microcentrifuge tube by mixing 2 x 10^{12} phage particles in 400 μl of 2% BSA in TBS plus 1% Tween 20, 10 mM DTT and finally adding 25 μl of prewashed SA beads and incubating for 2 hours at 4°C.
4. Recombinant 37-kDa wild type PTP1B (4 μg) was added in 400 μl 1X TBS, 2% BSA, 0.5% T20 and 5 mM DTT to 200 μl of pre-adsorbed phage (10^{12} phage

particles) and incubated for 4 hours at 4°C. The biotinylated PTP1B-CASA (400 ng) was added in 400 μl 1X TBS, 2% BSA, 0.5% T20 and 5 mM DTT to this mixture and incubated at 4°C for 4 hours in a humidified box.

5. Pre-washed SA beads (25 μl) were added to the phage/screening molecules reaction in the tubes and incubated for 15 minutes at RT on a rocking platform.
6. To block the additional streptavidin binding sites on the beads 100 μl of 1 mM biotin (~0.1 mM final) was added in TBS containing 2% BSA and 5 mM DTT to the solution and incubated for 5 minutes at RT.
7. The supernatant was aspirated after the incubation and the beads were washed 3X by resuspending the beads in 1 ml of TBS and centrifuging at 12,000 rpm.
8. The phage particles associated with the SA-biotinylated PTP1B-CASA complex were eluted after adding 100 μl of elution buffer (0.2 M glycine-HCl, pH 2.2, 1 mg/ml BSA), pipetting up and down to mix the beads in the elution buffer and incubating for 10 minutes at RT. The beads were held at the bottom of the tube with the magnet, the sup was collected and transferred to a new microfuge tube and neutralized with 20 μl of neutralization buffer (1 M Tris base, pH 9.1).
9. The eluates were added to infect 2-ml overnight culture of XL-1 Blue strain of *E. coli* in SB medium and incubated at room temperature for 15 minutes. To this 6 ml of pre-warmed (at 37°C) SB medium (+ 1.6 μl of 100 mg/ml carbenicillin + 12 μl of 5 mg/ml tetracycline) was added and the culture was transferred to a 50-ml tube and shaken at 250 rpm for 1 hour at 250 rpm. Then 2.4 μl of 100 mg/ml carbenicillin was added to the culture and shaken for an additional hour at 250 rpm and 37°C.
10. Input and Output titering:

    a. Five μl of the infected culture was diluted in 500 μl of SB medium and 10 and 100 μl of this dilution were plated on LB/Amp or LB/Carbenicillin plates for output tittering.

    b. One hundred μl of the prepared *E. coli* culture was infected with 2 μl of a 10^{-8} dilution of the phage preparation [1 μl in 1000 μl SB (a 10^{-3} dilution); mix, 1 μl of the 10^{-3} dilution in 1000 μl of SB (a 10^{-6} dilution), mix and dilute 10 μl of the 10^{-}

^{6} dilution in 1000 μl of SB (a 10^{-8} dilution)]. The infected culture was incubated for 15 minutes at RT and plated on an LB/Amp plate.

c. The output and input plates were incubated at 37°C overnight.

11. The helper phage VCSM13 (10^{12} pfu) was added to the 8-ml culture and transferred to a 500-ml flask. To this 91 ml of pre-warmed (37°C) of SB medium (with 46 μl of 100 mg/ml carbenicillin and 184 μl of 5 mg/ml tetracycline) was added and finally the culture was shaken at 300 rpm for 2 hours at 37°C. Then 140 μl of 50 mg/ml Kanamycin was added and shaking was continued overnight at 300 rpm and 37 °C.
12. The culture was centrifuged at 3000 x g for 15 minutes at 4°C. The supernatant was transferred to a clean 500-ml centrifuge bottle and 25 ml 5X PEG/NaCl (final 20% w/v PEG, 2.5 M NaCl) was added, mixed and incubated on ice for 30 minutes.
13. Phage particles were precipitated by centrifuging at 15,000g for 15 minutes at 4°C. The supernatant was drained and the phage particles were resuspended in 2 ml of 1% BSA in TBS. Finally the phage preparation was filtered using 0.45 μm disc filters and stored at 4ºC.

The amplified phage particles form the first round of panning were used for the second round and a total number of four rounds of panning were performed. After each round of panning the output phage titers were determined on LB + carbenicillin plates and these output titer plates are the source of individual phage particles expressing scFv fused to the surface protein PIII.

2.11 Screening Phage Pools

The phage pools were screened after each round of panning to assess whether the subtractive panning experiment was successful and to select antibody pools displaying the desired specificity and affinity. Most protocols for evaluating phage display libraries recommend ELISA for isolation of positive clones. However, protocols using antigens

coated on plastic lead to partial antigen denaturation, which is not an ideal experiment for screening conformation specific antibodies. It has been reported in some studies that scFvs directed against denatured proteins are less efficient than those against unaltered protein conformations in solution, in immunofluorescence and *in vivo* expression (Nizak et al., 2003). We had similar experience in our initial screening experiments, in which we used ELISA by immobilizing CASA mutant or wild type PTP1B on plate surfaces. We did not find any significant binding preference of the panned phage pool or individual scFv expressing phage for CASA mutant over the wild type using this immobilized screening approach. So screening against denatured antigen should not be adapted to the selection of conformation sensitive scFvs.

Selected pools of antibody-fragment displaying phage were analyzed after several rounds of panning as a pool, as well as individually as separate clones. Even if a pool of selected phage shows specificity to the reversibly oxidized form of PTP1B, it still can have some high affinity individual scFvs which are directed to the epitope(s) other than the altered active site and may not be eliminated by the subtractive panning. We systematically analyzed individual scFvs from initial selection after the subtractive panning. Testing clones directly also gives us an immediate idea of the specificity and applicability of the antibody in a cellular context. Analysis of individual clones from a panned pool can be performed either with antibody fragment displaying phage prepared from a single clone or with a single antibody fragment prepared from IPTG induced culture as described later.

2.11.1 Phage ELISA: PTP1B-CASA or PTP1B-WT or purified BSA was diluted to10 ng/μl in plate coating buffer (0.1M Sodium bicarbonate, pH 8.6). The wells of an ELISA plate (Coster 96-well, flat bottom EIA/RIA plate, Corning # 9018) were coated with 100 μl of the diluted antigens (1 μg/well) and incubated at 37ºC for 1 hour. Coated wells were washed 2X with ddH_2O and blocked with 200 μl 3% BSA in TBST (25 mM Tris pH 7.2, 150 mM NaCl, 0.1% BSA, 0.05% Tween-20) for 1 hour at 37 ºC. Phage particles expressing ScFv on the surface were diluted in 3% BSA in TBST in equivalent amount (10^{13} particles/well for different pools of library and 10^{12} particles/well for

individual clone) and incubated for 2 hours at RT. Wells were washed 6X with ddH_2O. To each well 200 µl of α-M13-HRP (27-9421-01, GE Healthcare; 1:4000 in 3% BSA/TBST) was added and incubated for 1 hour at 37°C. Wells containing immune complex were washed 6X with ddH_2O. Finally 125 µl of a chromogenic substrate of HRP (3,3´,5,5´-tetramentylbenzidine or TMB) (slow TMB-ELISA Substrate, 34024, Thermo Scientific) was added to the well and incubated for 30 min at 30°C. The reaction was stopped by adding 125 µl of ELISA stop solution (1.5 M H_2SO_4) and the plate was read at 450 nm using an automated multi-well plate reader (SpectraMax 190 Absorbance Microplate Reader, Molecular Devices).

2.11.2 scFv ELISA: PTP1B-CASA or PTP1B-WT or purified BSA was coated to the wells (1 µg/well) of an ELISA plate as before. Coated wells were washed 2X with ddH_2O and blocked with 200 µl 3% BSA in TBST (25 mM Tris pH 7.2, 150 mM NaCl, 0.1% BSA, 0.05% Tween®-20) for 1 hour at 37 ºC. ScFv sups from bacteria were diluted in 5% milk in TBST and incubated for 1 hour at RT. Wells were washed 6X with ddH_2O. To each well 150 µl of α-HA-HRP [Anti-HA (clone12CA5)-HRP, #11667475001, Roche; 1:1000 in 5% milk/TBST) was added and incubated for 1 hour at 37°C. wells were washed again 6X with ddH_2O. Finally 100 µl of substrate (Ultra TMB-ELISA Substrate, #34028, Thermo Scientific) was added to the well and incubated for 10 min at RT. the reaction was stopped by adding 150 µl of stop solution (1.5 M H_2SO_4) and the plate was read at 450 nm.

2.12 Sequence Analysis of Individual scFv Clones

Individual clones from the subtractive panning steps were sequenced. Analysis of the scFv sequences made it possible to identify at a clonal level different individual antibodies, which are of special interest as the unique sequences of the antibodies might contribute to the specificity to the individual clones. The sequences were aligned with a chicken Ig VL + VH sequence for selecting functional scFv sequences and sorting them in groups of identical sequences.

Individual clones selected randomly from the enriched scFv pools from the subtractive panning steps were sequenced and aligned by multiple sequence alignment, MultAlin (http://multalin.toulouse.inra.fr;) (Corpet, 1988) for selecting functional scFv sequences. After initial ELISA screening of 576 individual scFv clones 116 candidate PTP1B-binders were shortlisted for a final "in-solution" screening to isolate the conformation sensor scFvs.

2.13 Screening Individual scFvs as Conformation-Sensor Antibodies to PTP-OX

After panning and initial screening against PTP1B-CASA by ELISA, potential individual scFv clones were selected and their ability to bind specifically to oxidized PTP1B was investigated by both *in vitro* and *in vivo* assays. For purification of individual scFv as functional antibody fragment, single scFv was expressed without pIII fusion in a nonsuppressor strain of *E. coli* (e.g. TOP10F' cells) by IPTG induction.

2.13.1 Expression and Purification of Soluble scFvs: Selected scFv clones were expressed under IPTG induction in TOP10F´ *E. coli* and purified from the culture supernatant with Ni-NTA resin exploiting the C-terminal His tag and subsequent elution with imidazole.

TOP10F´ E. coli cells were grown from single colonies in Super Broth (SB) medium (1% MOPS, pH 7.0, 3% tryptone, 2% yeast extract) at 37°C with shaking at 250 rpm overnight. This overnight culture was diluted 1:50 in SB medium and incubated at 37°C at 250 rpm until the OD_{600nm} became 0.8. This culture was then shaken slowly at 100 rpm at 37°C for 15 minutes to regenerate the sheared F´ pili of the TOP10F´ strain. This TOP10F´ cells were then infected with phage particles expressing individual scFvs by adding 10^{12} phage particles/ml of bacterial culture and incubating at room temperature for 15 minutes with occasional gentle shaking. The infected culture was diluted 1:50 in SB medium with 50 μg/ml of Carbenicillin and incubated at 37°C and 250 rpm until the OD_{600nm} reached to 0.5. The culture was induced with 1.5 mM IPTG at 30°C and 250 rpm for 16 hours. The cells were harvested and resuspended in Lysis

Buffer (50 mM NaH_2PO_4, pH 8.0, 500 mM NaCl, 10 mM imidazole, 1mM PMSF and EDTA free protease inhibitor cocktail, # 11873580001, Roche). Resuspended culture was incubated with lysozyme (0.5 mg/ml) for 30 minutes at 4°C. The suspension was sonicated and centrifuged at 50,000 g for 30 minutes at 4°C. The supernatant was used to purify the soluble scFv by using Ni-NTA (Ni-NTA superflow agarose, # 30410, Qiagen) gravity columns. After adding the supernatant to the column it was washed with 20 column volume of Wash Buffer (50 mM NaH_2PO_4, pH 8.0, 500 mM NaCl, 20 mM imidazole). The bound protein was finally eluted with the Elution Buffer (50 mM NaH_2PO_4, pH 8.0, 500 mM NaCl, 250 mM imidazole).

2.13.2 Purification of PTP1B (C-Terminal His-tagged) from *E. coli*: PTP1B constructs with C-terminal 6His tag (1-321-6His and 1-394-6His) in pET21b vector (#69741-3, EMD Biosciences) were expressed and purified from BL21(DE3) expression strain of *E. coli*. Single bacterial colonies harboring the expression construct were inoculated in LB + Amp (50 μg/ml) and grown overnight at 37°C. This starter culture was inoculated (1:50) in LB + Amp (50 μg/ml) and incubated at 37°C, 250 rpm for 3-4 hours (until $A_{600\ nm}$ = 0.6). The culture was then induced with 0.3 M IPTG for 4 hours at 37°C, 250 rpm. The cells (from 1 liter culture) were harvested by centrifugation at 4,000 rpm for 20 minutes at 4°C and washed with 250 ml of PBS. Washed cell pellet was collected by centrifugation at 4,000 rpm for 15 minutes at 4°C. Cells were resuspended in lysis buffer (25 mM Na_2HPO_4, pH 7.4, 600 mM NaCl, 10 mM Imidazole, 5 mM TCEP with EDTA free complete protease inhibitor from Roche, 5 μg/ml aprotinin, 5 μg/ml leupeptin, 1 mM PMSF, 2 mM Benzamidine and 0.5 mg/ml lysozyme) and incubated with gentle rotation at 4ºC for 30 minutes. Finally resuspended cells were lysed by sonication on ice. Soluble protein extract was harvested in the supernatant by centrifugation at 50,000 rpm at 4°C for 1 hour and filtered with 0.45 μM syringe filter. Recombinant PTP1Bs with C-terminal 6His tag were purified by a two-step purification protocol using AKTA FPLC system (GE Healthcare). In the first step the His tag protein was purified with a Ni-NTA column (HisTrap HP, GE #17-5247-01) using His-tag specific binding buffer (25 mM Na_2HPO_4, pH 7.4, 600 mM NaCl, 10 mM Imidazole, 5

mM TCEP). His tag proteins were eluted from the column with an elution buffer (25 mM Na_2HPO_4, pH 7.4, 600 mM NaCl, 500 mM Imidazole, and 5 mM TCEP). PTP1B containing fractions were collected, pooled together and concentrated using centrifugal filters (Amicon Ultra-15,10K MWCO, # UFC901008, Millipore) and diluted (or dialyzed) in the running buffer to reduce NaCl concentration to <20 mM so that it can be used for the second ion exchange purification step using the Q-column (GE #17-1153-01). Collected pool from the Ni-NTA column were bound to the Q-column using a binding buffer consisting of 25 mM Tris-HCl, pH 7.5, 1 mM EDTA and 5 mM TCEP. Proteins were eluted with 1M NaCl in the binding buffer. PTP1B-6His eluates from the Q column were pooled together and concentrated using the Amicon centrifugal filters (10K MWCO). Finally purified protein was dialyzed in 25 mM Tris-HCl, pH 7.0, 50 mM NaCl, 5 mM TCEP, 0.1 mM PMSF, 0.02% NaN_3 and 50% Glycerol.

2.13.3 Reversible Oxidation of PTP1B by H_2O_2: Purified PTP1B (1-321) or (1-394) (15 nM) was mixed with increasing concentration of H_2O_2 (0.05 mM to 100 mM) in phosphatase assay buffer (50 mM HEPES, pH 7.0, 100 mM NaCl, 0.1% BSA) at RT for 10 minutes. H_2O_2 was removed by Zeba Desalting Column (# 89882, Thermo Scientific) and the oxidized protein was buffer exchanged in the phosphatase assay buffer without any reducing agent. Phosphatase activity was measured for each protein sample using ^{32}P labeled reduced carboxamidomethylated and maleylated lysozyme (^{32}P-RCML) as the substrate, with or without 5 mM TCEP. Activity of each sample was compared to that of the untreated PTP1B in the presence of 5 mM TCEP.

2.13.4 Screening for Conformation Sensor scFvs: We designed an in-solution phosphatase assay for screening the conformation sensor scFvs using ^{32}P-Labeled phospho-tyrosyl RCML as the substrate. Recombinant PTP1B was reversibly oxidized and transiently inactivated with H_2O_2. The phosphatase activity was completely restored upon the removal of H_2O_2 by a quick buffer exchange and addition of reducing agent (TCEP/DTT). Purified bacterially expressed scFvs (100X molar excess of PTP1B) were incubated with PTP1B after H_2O_2 treatment and its removal and the effect of individual scFv on stabilizing the reversibly oxidized conformation was assessed by

the phosphatase assay under reducing conditions. Purified individual scFvs (750 nM) was incubated with PTP1B (7.5 nM) under reducing conditions (5 mM TCEP) in 50 mM HEPES, pH 7.0, 100 mM NaCl, 0.1% BSA for 30 minutes at RT to assess whether the scFvs bind to the reduced form of PTP1B and have any direct inhibitory role to phosphatase activity. PTP1B activity in this protein mixture was determined by RCML phosphatase assay. To determine the effect of scFv binding on the reactivation of PTP1B-OX, reversibly oxidized PTP1B (7.5 nM) was incubated similarly with individual scFvs (750 nM) for 30 minutes at RT in the same binding condition without any reducing agent. PTP1B activity in each sample was determined by RCML phosphatase assay using 100 nM ^{32}P-RCML as the substrate with or without 5 mM TCEP.

Chapter 3

Characterization of PTP1B-OX Conformation Sensor scFvs *in vitro*

3.1 Introduction

The activity of protein tyrosine phosphatase 1B (PTP1B) is regulated by reversible oxidation of the catalytic-site cysteine. Crystallographic analysis of the oxidized catalytic domain of PTP1B demonstrated that following oxidation, the active site cysteine is modified to a sulphenic acid (S-OH), which no longer acts as a nucleophile and the enzyme is inactivated. H_2O is rapidly eliminated to convert the sulphenic acid to a cyclic sulphenyl-amide, a novel 5-atom ring structure, in which a covalent bond is formed between the Cys sulfur atom and the main chain nitrogen of the adjacent Ser residue (Salmeen et al., 2003 and van Montfort et al., 2003). This oxidative modification induces profound changes in the architecture of the active site. In this oxidized form, residues that are normally buried now adopt solvent-exposed positions. For example, Tyr46 of the phosphotyrosine loop, which defines the depth of the catalytic cleft, becomes solvent exposed following oxidation of the catalytic cysteine and subsequent breakage of the hydrogen bonds that normally hold the catalytic cleft together. Oxidation also induces movement of the catalytic motif towards the surface, so that the oxidized Cys215 can be presented for its subsequent reduction to the thiolate form by reducing agents. This regulatory mechanism not only protects the phosphatase from irreversible modification due to further oxidation to the sulphinic ($S\text{-}O_2H$) and sulphonic acid ($S\text{-}O_3H$) forms, which are permanently inactivated, but it also promotes reduction to permit the enzyme to regain its active status.

We have generated conformation sensor scFvs by the antibody phage display technique and isolated candidate antibodies that stabilize the reversibly oxidized form of PTP1B, thereby inhibiting the reactivation process, with a net result of decreased phosphatase activity. Here, we present *in vitro* approaches to characterize the candidate conformation sensor scFvs. We have investigated whether the inhibition of the reactivation of PTP1B by candidate scFvs is due to direct binding between PTP1B-OX and scFv *in vitro*. We examined the specificity of scFv45 for PTP1B-OX over oxidized TCPTP, which is the closest relative of PTP1B. Finally, we determined the binding constants for the interaction between scFv45 and PTP1B-OX by Surface Plasmon Resonance (SPR).

Results: Chapter 3

3.2 C-terminal End of PTP1B does not affect scFv45 Mediated Inhibition of PTP1B-OX Reactivation

To investigate further two of the candidate conformation sensor antibodies (scFv45 and 57), we tested their potential to inhibit reactivation of a longer form of recombinant PTP1B (1-394) that contained most of the non-catalytic C-terminal segment. Similar reversible oxidation and inactivation conditions were established by incubating a bacterially purified C-terminally 6His tagged PTP1B (1-394) preparation (Figure 3.1 A) with increasing amount of H_2O_2. We observed that like the shorter form (1-321), PTP1B (1-394) (15 nM) can be reversibly oxidized with H_2O_2, at concentrations ranging from 50 nM to 1 mM (Figure 3.1 B). When incubated with PTP1B (1-394) under non-oxidizing conditions scFvs 45 and 57 did not produce significant inhibition of the enzyme activity (3.1 C). However, when incubated with reversibly oxidized form of 1-394, both caused almost complete inhibition of the reactivation process (Figure 3.1 D).

3.3 Candidate scFvs Bind to PTP1B-OX *in vitro*

In the *in vitro* phosphatase screening assay using reversibly oxidized (with H_2O_2) recombinant PTP1B (1-321 or 1-394), we found four different PTP1B-OX specific scFvs (scFv45, scFv57, scFv64 and scFv106) from the initial pool of 12 different scFvs. We tested whether the candidate scFvs bound to PTP1B-OX/CASA *in vitro* using purified proteins (Figure 3.2 A and B). Two of these scFvs (scFv45 and scFv57) were shown to interact with PTP1B-OX or PTP1B-CASA, but not with reduced PTP1B in the *in vitro* Ni-NTA pull down experiment (Figure 3.2 C). Other scFvs (20, 21, 24, 28, 48, and 105), that did not inhibit the reactivation of PTP1B-OX in the initial phosphatase screening assay, did not show any significant binding with PTP1B-OX (Figure 3.4D), indicating further that the inhibition of the reactivation process by scFvs 45 and 57 was due its binding and stabilization of the reversibly oxidizing conformation.

Figure 3.1

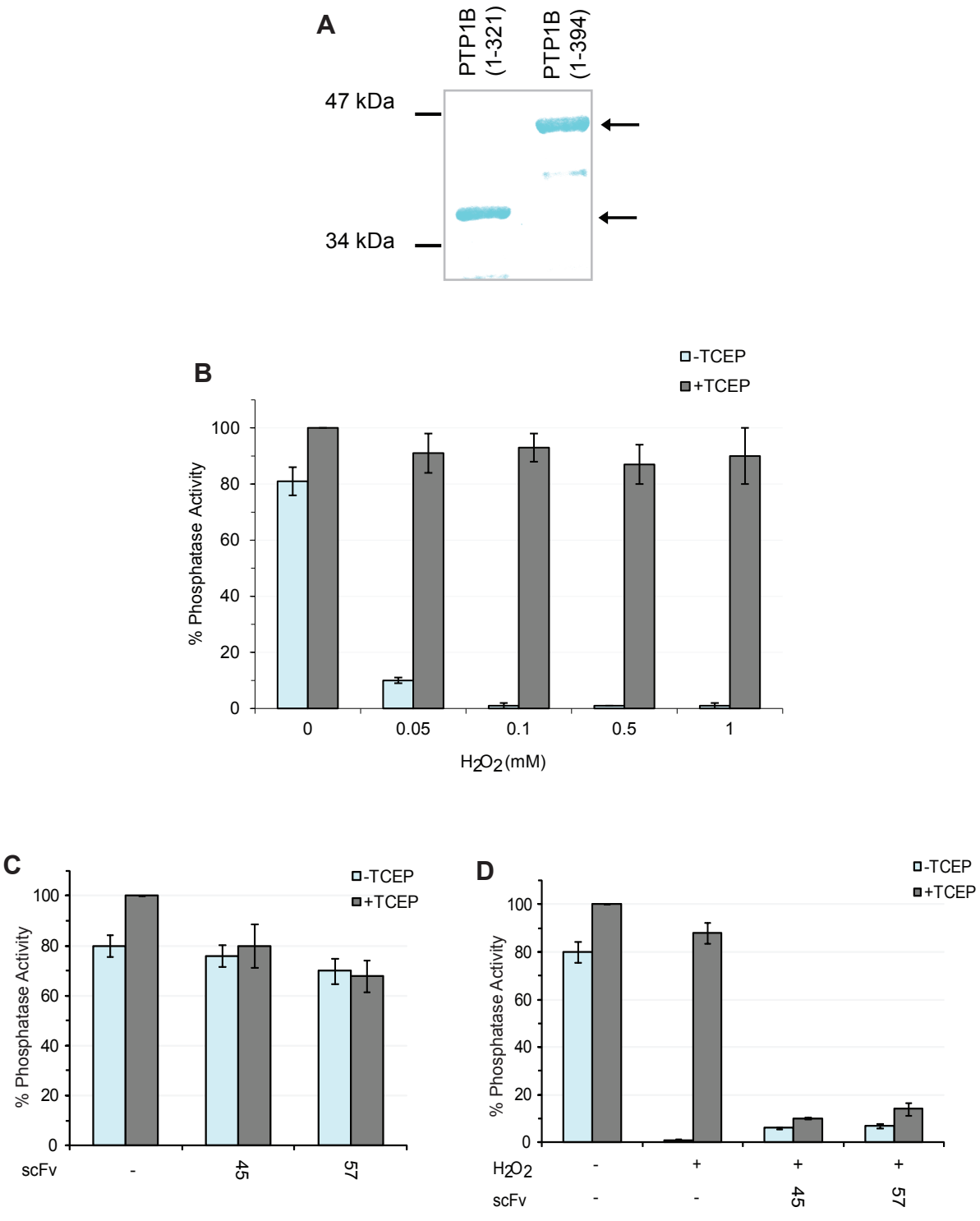
A
PTP1B (1-321)
PTP1B (1-394)
47 kDa
34 kDa
B
-TCEP
+TCEP
% Phosphatase Activity
100
80
60
40
20
0
0
0.05
0.1
0.5
1
H2O2 (mM)
C
-TCEP
+TCEP
% Phosphatase Activity
100
80
60
40
20
0
scFv
-
45
57
D
-TCEP
+TCEP
% Phosphatase Activity
100
80
60
40
20
0
H2O2
-
+
+
+
scFv
-
-
45
57

Figure 3.1. PTP1B-OX-Specific scFvs Inhibit Reactivation of Oxidized PTP1B (1-394)

(A) Recombinant PTP1B (1-321 and 1-394) with C-terminal 6His tag was purified from bacteria in homogeneity as described in the method section.

(B) PTP1B (1-394) (15 nM) was reversibly oxidized by H_2O_2 (50 µM to 1 mM) using the same method as described for oxidation of PTP1B (1-321) in Figure 3.1 and in the method section.

(C) Direct inhibitory effect of scFvs 45 or 57 (750 nM each) were assessed using PTP1B (1-394) (7.5 nM) in similar phosphatase assay under reducing condition.

(D) PTP1B (1-394) (15 nM) was reversibly oxidized with H_2O_2 (75 µM) and reactivation by TCEP with or without scFvs 45 and 57 was observed by phosphatase assay. (Error bar in B, C, and D shows standard deviation from three phosphatase assays).

Figure 3.2

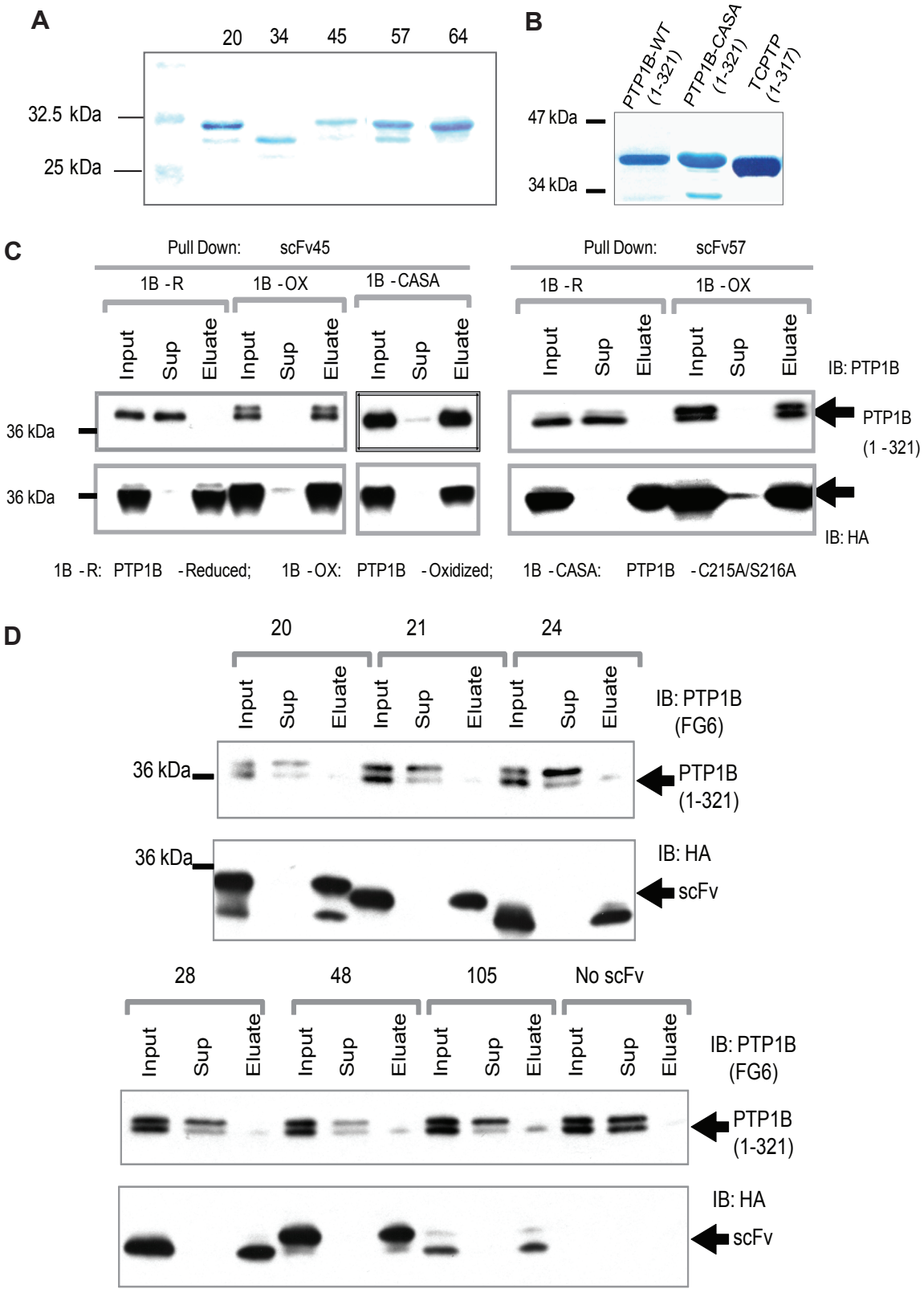
A
20
34
45
57
64
32.5 kDa
25 kDa
B
PTP1B-WT (1-321)
PTP1B-CASA (1-321)
TCPTP (1-317)
47 kDa
34 kDa
C
Pull Down: scFv45
1B -R
1B -OX
1B -CASA
Input
Sup
Eluate
Pull Down: scFv57
IB: PTP1B
PTP1B (1 -321)
36 kDa
IB: HA
1B -R: PTP1B -Reduced;
1B -OX: PTP1B -Oxidized;
1B -CASA: PTP1B -C215A/S216A
D
20
21
24
IB: PTP1B (FG6)
PTP1B (1-321)
IB: HA
scFv
28
48
105
No scFv

Figure 3.2. scFv45 binds Specifically to PTP1B-OX *in vitro*
(A) Panel shows a representation of different purified scFvs from TOP10F´ *E. coli.*
(B) PTP1B-WT (1-321), PTP1B (1-321)-CASA and TCPTP (1-317)-6His were purified in homogeneity from bacteria.
(C) PTP1B (1-321), reversibly oxidized with H_2O_2 (1B-OX) or reduced (1B-R) and PTP1B-CASA were incubated with purified scFvs 45 and 57 and protein complex was pulled down with Ni-NTA bead. Equivalent amount (2.5 ng of PTP1B) of input, supernatant and eluate were subjected to western blot analysis. Presence of PTP1B and scFvs in the complex were detected by anti-PTP1B or anti-HA-HRP antibodies, respectively.
(D) Similar Ni-NTA pull down experiments were done with 6 other purified scFvs, which showed no significant inhibition of PTP1B reactivation in the screening for conformation sensor antibodies as described in Figure 3.1.

3.4 PTP1B-OX-Specific scFv does not bind to TCPTP-OX

It was shown in our lab that TCPTP is reversibly oxidized in mammalian cells, along with PTP1B, following insulin stimulation (Meng et al., 2004). We tested the specificity of scFv45 for PTP1B-OX over TCPTP, which is the closest relative of PTP1B among the classical PTP family of enzymes. TCPTP shows ~75% sequence identity with the catalytic domain of PTP1B (Figure 3.3 A) (Andersen et al., 2001; Iversen et al., 2002). Bacterially purified recombinant TCPTP with a C-terminal 6His tag (Figure 3.2 B) was incubated with increasing concentration of H_2O_2 (75 µM to 200 µM) and reactivated with reducing agent (5 mM TCEP). We observed that TCPTP (15 nM) can be reversibly oxidized with a narrower range of H_2O_2 (75 -100 µM) compared to the reversible oxidation of PTP1B (Figure 2.11 C and 3.3 B). Interestingly, we were also not able to restore the full activity of TCPTP in presence of TCEP (Figure 3.3 B). Incubation of scFv45 with reversibly oxidized TCPTP, however, showed no effect on its reactivation (Figure 3.3 C). This finding was later confirmed when we observed that *in-vitro* oxidized TCPTP did not bind to scFv45 in an HA-agarose pull down experiment (Figure 3.3 D).

3.5 scFv45 Binds to PTP1B-OX with High Affinity

To measure the binding constants for the interaction between scFv45 and PTP1B-OX we used Surface Plasmon Resonance (SPR) on a BIACORE 2000 (Fig 3.4 A). From interaction between increasing concentrations of PTP1B-OX (50 nM to 10 µM) with a fixed amount of scFv45 (500 nM) we found that scFv45 binds with PTP1B-OX with high affinity (K_d = 46 nM) and the interaction has a slow off rate (K_{off} = 2.3 x 10^{-3} s^{-1}) (Figure 3.4 B, and Table 2). PTP1B (1 µM) under reducing condition (2 mM TCEP) did not show any significant detectable binding to the same amount of scFv45 (500 nM), further confirming that scFv45 binds specifically to PTP1B-OX but not to PTP1B in its reduced active conformation (Figure 3.4 C). Interaction between PTP1B-CASA (1 µM) and scFv45 (500 nM) showed binding constants (K_d = 52 nM, K_{off} = 4.6 x 10^{-3} s^{-1}), which are strikingly similar to that between PTP1B-OX (1 µM) and scFv45 (500 nM) (Figure 3.4 D and Table 2). Interaction between PTP1B-CASA and scFv45 was almost identical with or without TCEP (2 mM) (Figure 3.4 E) showing that presence of the reducing

agent is not affecting the PTP1B-scFv45 binding, rather it’s the adopted conformation in either oxidized or reduced environment that is responsible for the specific interaction.

Figure 3.3

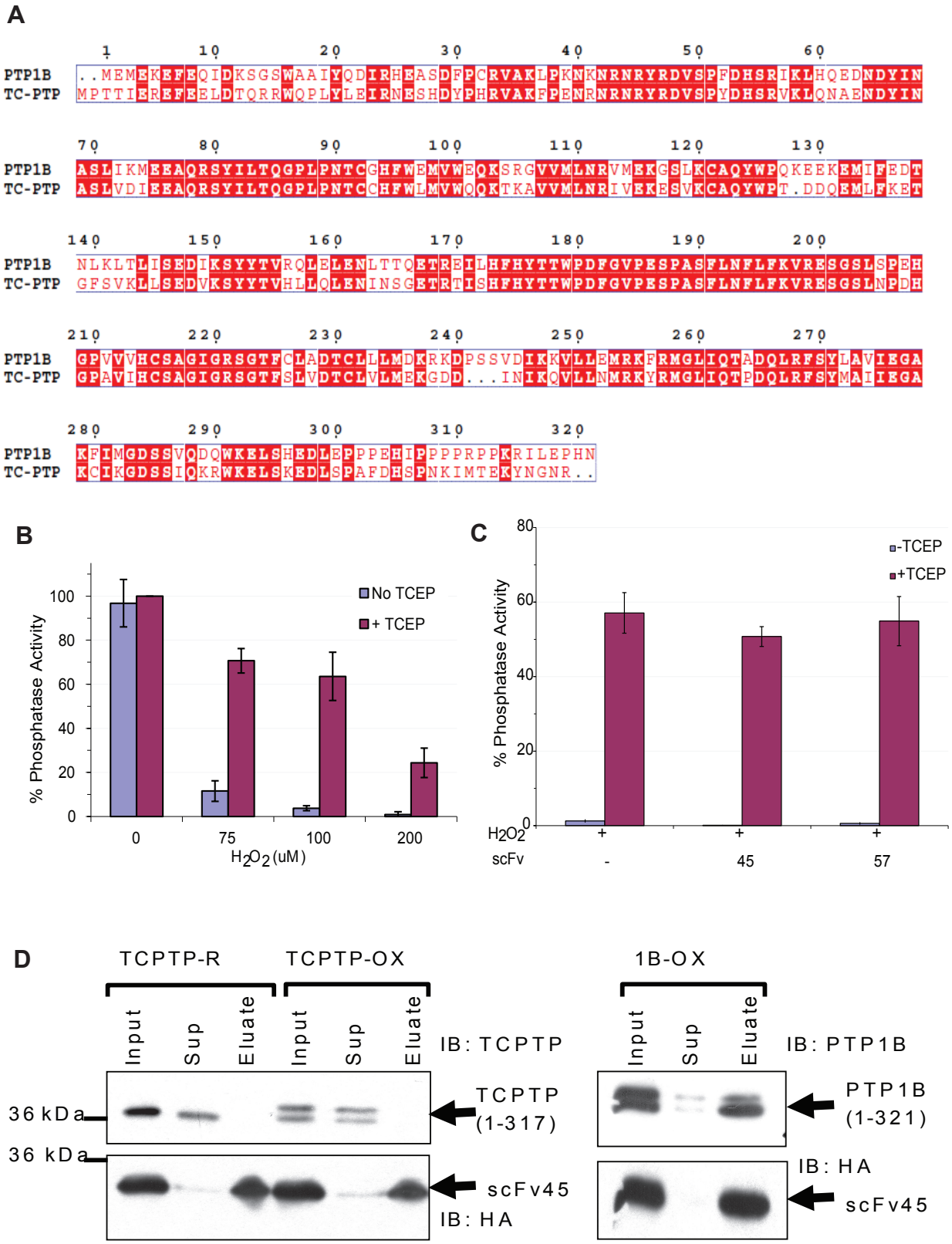
A
PTP1B
TC-PTP
B
% Phosphatase Activity
No TCEP
+ TCEP
H2O2 (uM)
C
% Phosphatase Activity
-TCEP
+TCEP
H2O2
scFv
D
TCPTP-R
TCPTP-OX
1B-OX
Input
Sup
Eluate
IB: TCPTP
IB: PTP1B
36 kDa
TCPTP (1-317)
PTP1B (1-321)
scFv45
IB: HA

Figure 3.3. scFv45 shows Specificity to PTP1B-OX but not to TCPTP-OX
(A) Amino acid sequence alignment of the catalytic domains of PTP1B (1-321) and TCPTP (1-317) showing high degree of identity (~75%). Alignment was done by a web-based multialin software (Corpet, 1988).
(B) Recombinant TCPTP (1-317 with C-terminal 6His tag) was reversibly oxidized by H_2O_2. Increasing amount of H_2O_2 (75 – 200 µM) was added to TCPTP (15 nM) and incubated for 10 min at RT. After removing H_2O_2 by buffer exchange, oxidized samples were reactivated by TCEP (5 mM). Phosphatase assay was determined using 100 nM ^{32}P-RCML and 5 nM of enzyme from each sample. The activity of each sample was compared to that of the non-treated reduced enzyme, which was set as 100%.
(C) Effect of scFvs (45 or 57) that showed inhibition of PTP1B reactivation was assessed for TCPTP-OX reactivation. Purified scFvs (750 nM) were incubated with oxidized TCPTP (7.5 nM) and phosphatase assay was determined in presence of TCEP (5 mM). [Error bar in B and C shows standard deviation from three to six phosphatase assays].
(D) TCPTP (50 nM) was oxidized with H_2O_2 (250 µM) and binding with scFv45 was assessed by HA-Agarose pull down. Equivalent amount (4 ng of TCPTP) of input, supernatant and precipitate were analyzed by western blot. As a control a parallel pull down was performed with reversibly oxidized PTP1B (by H_2O_2) and scFv45. TCPTP was detected with a catalytic domain specific anti-TCPTP rabbit polyclonal antibody (Lorenzen et al., 1995).

Figure 3.4

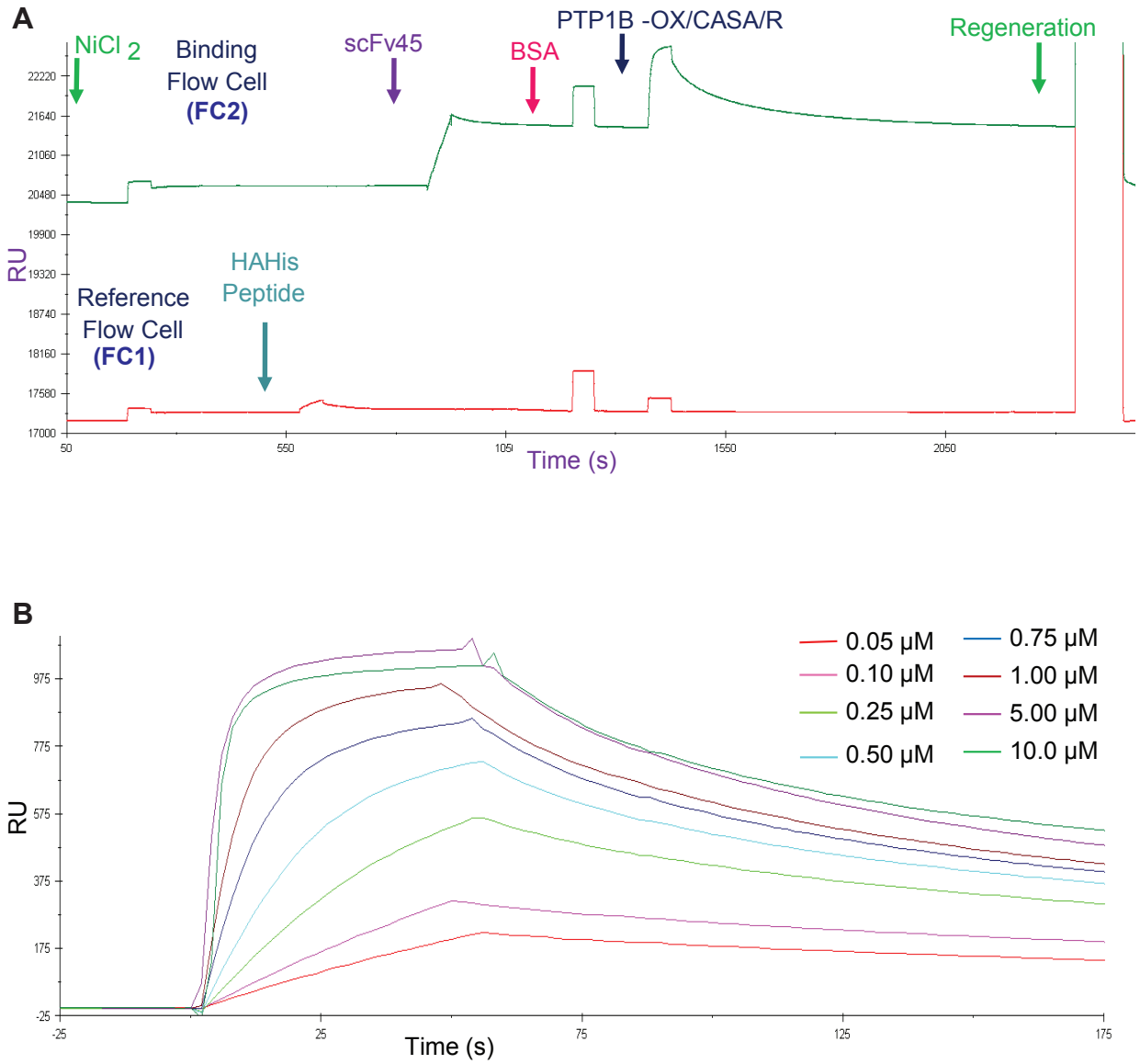
A
NiCl 2
Binding
Flow Cell
(FC2)
scFv45
BSA
PTP1B -OX/CASA/R
Regeneration
HAHis
Peptide
Reference
Flow Cell
(FC1)
RU
Time (s)
B
0.05 µM
0.10 µM
0.25 µM
0.50 µM
0.75 µM
1.00 µM
5.00 µM
10.0 µM
RU
Time (s)

Figure 3.4

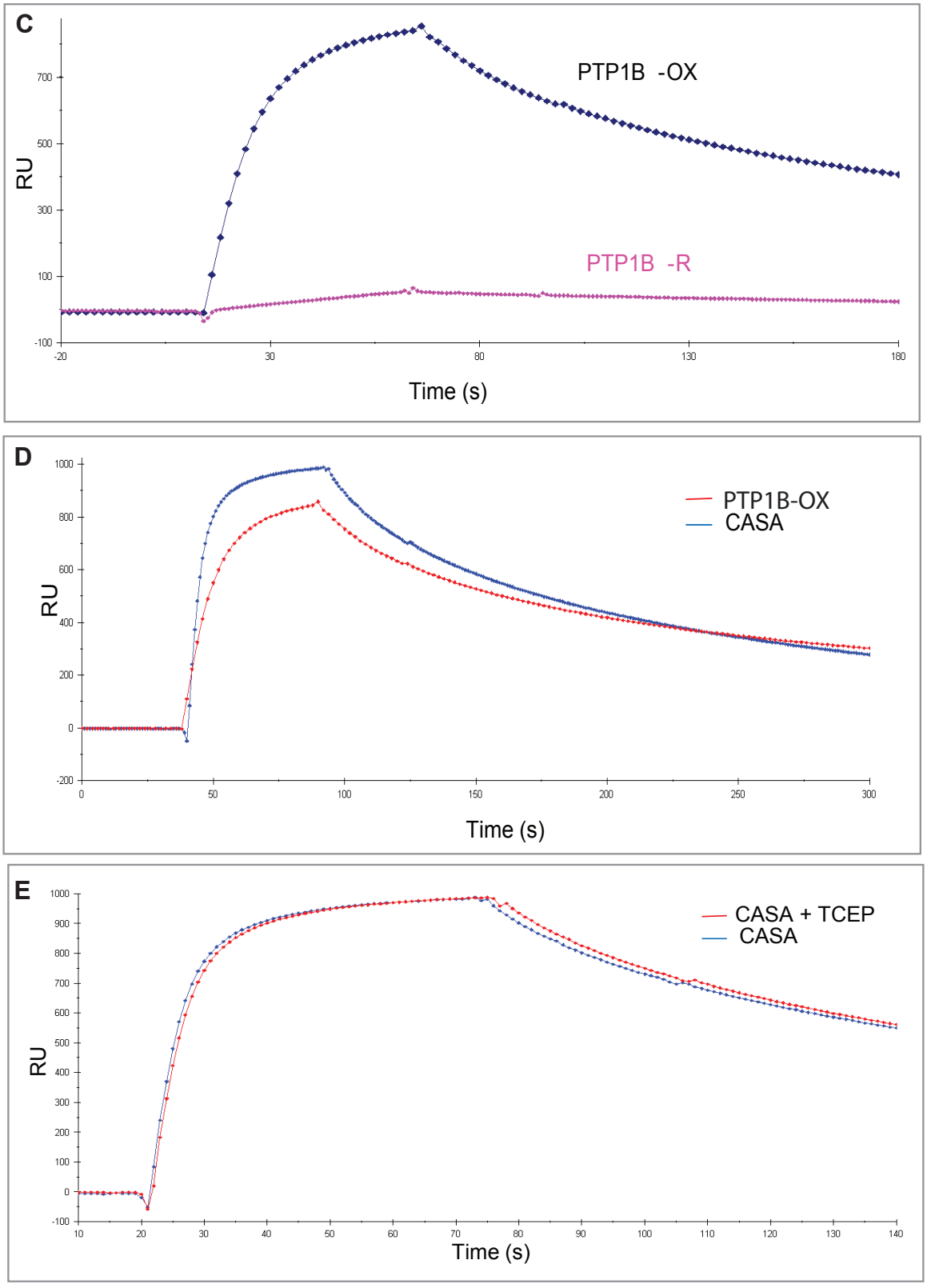
C
PTP1B -OX
PTP1B -R
RU
Time (s)
D
PTP1B-OX
CASA
RU
Time (s)
E
CASA + TCEP
CASA
RU
Time (s)

Table 2

	K_{on} ($M^{-1}s^{-1}$)	K_{off} (s^{-1})	K_d (nM)
PTP1B-OX	5.1×10^{4}	2.3×10^{-3}	46
PTP1B-CASA	8.9×10^{4}	4.6×10^{-3}	52

Figure 3.4. Binding Analysis between PTP1B-OX and scFv45 by Surface Plasmon Resonance

(A) This panel shows the overall scheme for the binding analysis by SPR using BIACORE 2000. We used a dual flow cell system in all the binding assays. Flow Cell 1 (FC1) was used as the reference flow cell to subtract the background non-specific surface binding from the specific binding between the analytes on Flow Cell 2 (FC2). NTA-Ni surface was used for directed immobilization of the C-terminal scFv45 in a uniform orientation so that the antigen binding end is freely accessible in the solution. Purified scFv45 (500 nM) was immobilized on FC2. Equal amount of the HAHis (500 nM) peptide was immobilized on FC1. Both flow cells were then blocked with 0.1% purified BSA. Finally different PTP1B preparations (PTP1B-OX, PTP1B-CASA or PTP1B-R) were injected onto FC2 at 20 µl/min. After each round of binding the NTA surface was regenerated by sequential stripping (0.35 M EDTA) and coating (0.5 mM $NiCl_2$) for another fresh round of binding interaction.

(B) PTP1B was reversibly oxidized with H_2O_2 and different concentration of the PTP1B-OX as indicated were injected on immobilized scFv45 (500 nM). The interaction was allowed to dissociate for 10 minutes for each concentration. The kinetic constants for the binding were calculated with the BIAevaluation 3.1 software (GE Healthcare).

(C) Comparative sensogram shows the interaction between PTP1B-OX (1µM) and PTP1B (1µM) under reducing condition (2 mM TCEP) (PTP1B-R) and scFv45 (500 nM).

(D) PTP1B-CASA (1 µM) and PTP1B-OX (1 µM) were injected separately on scFv45 (500 nM) and the binding sensograms were compared.

(E) PTP1B-CASA (1 µM) with or without 2 mM TCEP was injected on immobilized scFv45 (500 nM) and binding sensograms were compared.

Table 2. Binding Constants of the Interaction between scFv45 and PTP1B-OX.

The binding sensograms were analyzed and the binding constants for interaction between scFv45 and PTP1B-OX or PTP1B-CASA were determined by the BIAevaluation 3.2 software.

Material and Methods: Chapter 3

3.6 Ni-NTA and HA-agarose pull-down Experiments: In order to demonstrate direct interaction between PTP1B-OX and candidate scFvs, we have performed an *in vitro* binding assay using purified recombinant PTP1B (37 kDa, WT or CASA) and purified scFvs under both oxidizing and reducing conditions. Purified PTP1B (50 nM) was reversibly oxidized with 250 μM H_2O_2 followed by a quick buffer exchange to remove H_2O_2. Purified scFv was incubated in molar excess (100 X) with PTP1B-OX or PTP1B-CASA or with PTP1B under reducing condition (with 2 mM TCEP) in binding buffer (20 mM HEPES, pH 7.4, 300 mM NaCl, 0.05% BSA, 0.05% Tween-20 and 10 mM imidazole) for 2 hours at 4ºC. Ni-NTA agarose (50 μl as 50% slurry equilibrated in the binding buffer, # 30210, Qiagen) was added and incubated for one hour at 4ºC. Protein complex bound to Ni-NTA agarose beads was pulled down and washed (three times, 5 minutes each, at 4ºC) with binding buffer containing 20 mM imidazole. The protein complex was eluted from the Ni-NTA agarose beads with 500 mM imidazole (in binding buffer) for 15 minutes at 4ºC with gentle shaking. The complex was separated by SDS-PAGE and PTP1B was detected with anti-PTP1B (FG6) antibody and scFv was detected with anti-HA antibody [anti-HA (3F10)-HRP] by immunoblotting. Eight different scFvs (scFvs 20, 21, 24, 28, 45, 48, 57, and 105), expressed and purified from bacterial cultures were tested by this *in vitro* binding experiment.

In similar experiment recombinant TCPTP (1-317) was reversibly oxidized by H_2O_2 using identical buffer composition and experimental conditions as for PTP1B. Increasing amount of H_2O_2 (75 – 200 μM) was added to TCPTP (15 nM) and incubated for 10 min at RT. After removing H_2O_2 by buffer exchange, oxidized samples were reactivated by TCEP (5 mM). Phosphatase assay was determined using 100 nM ^{32}P-RCML and 5 nM of enzyme from each sample. The activity of each sample was compared to that of the non-treated reduced enzyme, which was set as 100%. To see the effect of scFvs that showed inhibition of PTP1B reactivation purified scFvs (750 nM) were incubated with oxidized TCPTP and phosphatase assay was determined in presence of TCEP (5 mM). To determine whether scFv45 binds to TCPTP either under

reducing condition or when it is oxidized an HA-agarose pull down experiment was performed. Purified TCPTP was C-terminally 6His tagged and we could not do the Ni-NTA pull down for TCPTP because scFv45 also has a C-terminal 6His tag. So for this pull down, we used Anti-HA antibody conjugated to Agarose beads. TCPTP (50 nM) was oxidized with H_2O_2 (250 µM), which was removed immediately with buffer exchange. An aliquot of oxidized TCPTP (5 nM) was incubated with 500 nM of purified scFv45 in binding buffer (20 mM HEPES, pH 7.4, 300 mM NaCl, 0.05% BSA, 0.05% Tween-20) for 2 hours at 4ºC. Anti-HA monoclonal antibody (Clone 3F10, #11815016001, Roche) conjugated to Agarose beads (50 µl 50% slurry in binding buffer) was added and incubated for additional 1 hour at 4ºC. Agarose beads were washed 3X with binding buffer and samples were prepared in SDS-sample buffer. Equivalent amounts (4ng of TCPTP) of input, supernatant and precipitate were analyzed by western blot. A parallel pull down was performed with oxidized PTP1B and scFv45 using anti-HA-agarose beads as a control. TCPTP was detected with a catalytic domain specific anti-TCPTP rabbit polyclonal antibody (1910H) (Lorenzen et al., 1995).

3.7 Surface Plasmon Resonance (SPR): We used the Surface Plasmon Resonance (SPR) technique for affinity measurements and determination of the kinetic constant for the binding interaction between scFv45 and PTP1B (oxidized, reduced or CASA mutant). Binding interactions in real time were analyzed by BIAcore 2000 system (GE Health Science) using NTA sensor chip (#BR-1004-07, GE Health Science). All the binding interactions were performed in 0.01 M HEPES, 0.3 M NaCl, 50 µM EDTA, 10 mM Imidazole, 0.05% Tween-20, pH 7.4 as the running buffer. We used two flow path mode (FC2, FC1) and selected FC1 (Flow Cell 1) for reference flow cell for determining the background binding and FC2 (Flow Cell 2) as the binding flow cell on which the scFv-PTP1B interaction took place. Both flow cells of the chip were coated with 0.5 mM $NiCl_2$ and washed. A His-HA peptide (HHHHHHGAYPYDVPDYAS, 500 nM) was injected on the reference flow cell (FC1) and 500 nM of purified scFv45 was injected on the binding flow cell (FC2). Following a quick wash, 0.1% (w/v) purified BSA was injected on both flow cells as a blocking buffer to minimize background binding of the proteins to the chip and in the integrated fluid system (IFC). Just before the experiment

purified PTP1B was reversibly oxidized with H_2O_2, as described previously and H_2O_2 was removed by buffer exchange. Increasing concentrations (0.05 μM to 10 μM) of PTP1B-OX were injected on the binding flow cell and allowed to dissociate for 10 minutes. All the reagents and protein samples were prepared in the running buffer, unless stated otherwise, and 20 μl of solute, at 20 μl/min, was used for each injection. After each round of PTP1B-OX binding, the chip was regenerated by first stripping with 350 mM EDTA, pH 8.3 in running buffer and then by coating with $NiCl_2$. For different PTP1B-OX concentrations or different redox conditions, each sample was injected every time after stripping and regeneration of the chip followed by freshly immobilizing the scFv on the chip. The binding sensograms were analyzed with the BIAevaluation 3.2 software.

Chapter 4

Use of PTP1B-OX Conformation Sensor scFv as Intrabody: Implication in PTP1B Redox Regulation and Insulin Signaling

4.1 Introduction

Redox regulation of PTPs in response to various physiological stimuli is emerging as a potential regulatory mechanism for controlling PTP-mediated signaling responses. Work in our lab and in others has demonstrated that PTPs are an important target of ROS in the induction of an optimal tyrosine phosphorylation response to various physiological stimuli, such as insulin, EGF, and PDGF (Bae et al., 1997; Boivin et al., 2008; Mahadev et al., 2001; Meng et al., 2004; Meng et al., 2002). It has been demonstrated that stimulation of cells with insulin causes rapid and transient oxidation and reversible inactivation of PTP1B and that this facilitates increased phosphorylation of insulin receptors (Mahadev et al., 2001; Meng et al., 2004). These studies provided an initial link connecting reversible oxidation and inactivation of PTP1B by insulin-induced ROS and the role of this delicate oxidative regulation of PTP1B in the modulation of insulin signal transduction. Understanding the redox regulation of PTP1B in a cellular context, however, has been hampered by the absence of sensitive and robust methods for detecting the oxidized pool and separating it from the reduced background. An antibody specific to the oxidized form of a PTP1B would be very useful tool for this purpose. We have generated conformation-sensor scFvs to the reversibly oxidized form of PTP1B and characterized their interaction with PTP1B-OX *in vitro* as described in the previous chapters.

We have used the shortest possible functional antigen-binding fragments in the form of scFvs to generate the PTP1B-OX conformation-specific antibodies. One of the major advantages of using this approach is that the candidate antibodies can be expressed inside mammalian cells as functional intracellular antibodies or intrabodies. Now that we have identified and characterized scFvs that stabilize PTP1B-OX *in vitro* we wanted to express them in mammalian cells as intrabodies to test their effect on endogenously oxidized PTP1B. In this chapter we investigated interaction of scFv45, expressed as an intrabody, with endogenous PTP1B-OX and examined the effect of this conformation sensor antibody on PTP1B mediated insulin signaling.

Results: Chapter 4

4.2 scFv45 binds to PTP1B-OX in mammalian cells in response to insulin and H_2O_2

Selected scFv sequences were inserted into a mammalian expression vector (pCDNA3.2/V5-GWD-TOPO) by directed cloning (Figure 4.1 A). We developed the mammalian expression construct in such a way that any of the scFvs selected from the *in vitro* screening could be cloned in this vector quickly and efficiently without the need of repeated PCR amplification and cloning.

First we cloned scFv45 into this expression system and transiently expressed it in HEK293T cells. We observed robust and stable expression of the PTP1B-OX conformation-sensor scFv45 in 293T cells, which was detected by the C-terminal HA tag (Figure 4.1 B). Using this initial construct we generated a "mini" mammalian expression library by cloning 28 additional individual scFvs from their corresponding phagemid constructs. Using an Ni-NTA pull down assay with equivalent amounts of transfected (with different intrabodies), H_2O_2 (1 mM)-treated mammalian cell lysates, we identified four additional intrabodies (scFv57, scFv67, scFv102, scFv106) that bound to endogenous PTP1B-OX strongly; five others (scFv 136, scFv 61, scFv62, scFv64, scFv34 and scFv118) bound weakly to PTP1B-OX. None of the 28 intrabodies, however, displayed any binding to endogenous PTP1B under reducing conditions (Figure 4.2). Interestingly, all of the candidate scFvs selected in the *in vitro* PTP1B-OX reactivation screen were also found to bind PTP1B-OX when expressed in 293T cells as intrabodies. This indicates that PTP1B undergoes similar oxidative modification in mammalian cells when treated with H_2O_2 and scFvs that bind PTP1B-OX *in vitro* were also functional when expressed in 293T cells.

We further characterized the interaction of scFv45 and endogenous PTP1B in 293T cells. We demonstrated that scFv45 efficiently immunoprecipitated PTP1B-OX from cells treated with H_2O_2 (1mM) but showed little or no interaction with PTP1B when cells were not treated with H_2O_2, or treated under reducing conditions (Figure 4.3 A).

Figure 4.1

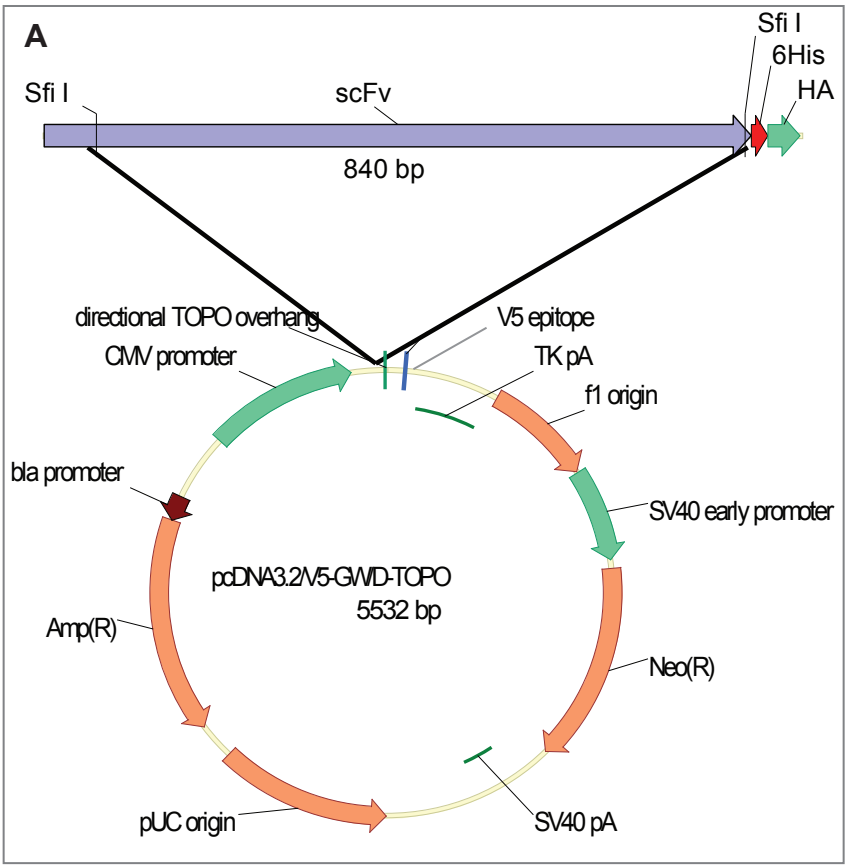
A
Sfi I
6His
HA
Sfi I
scFv
840 bp
directional TOPO overhang
V5 epitope
CMV promoter
TK pA
f1 origin
bla promoter
SV40 early promoter
pcDNA3.2/V5-GW/D-TOPO
5532 bp
Amp(R)
Neo(R)
pUC origin
SV40 pA
B
NT
24 h
36 h
48 h
IB: HA
35 kDa
IB: α - Tubulin

Figure 4.1. Expression of scFvs as Intracellular Antibody or Intrabody in 293T Cells

(A) Selected scFvs from the *in vitro* screening experiments were cloned in mammalian expression vector pCDA3.2/V5-GWD-TOPO. Initially scFv45 was cloned in this vector with the Sfi I site intact. This allows us to clone any of the scFvs in this vector by simple subcloning after restriction digestion of the pCDA3.2/V5-GWD-TOPO-scFv45 (TOPO-45) and other scFvs from their corresponding phagemid construct (pComb3XSS-scFv) with Sfi I, without the need of repeated PCR amplification and cloning.

(B) TOPO-45 was transfected in 293T cells as indicated. Expression of scFv45 was detected by the C-terminal HA tag using anti-HA-HRP antibody after collecting the cell lysate at different post transfection time points.

Figure 4.2

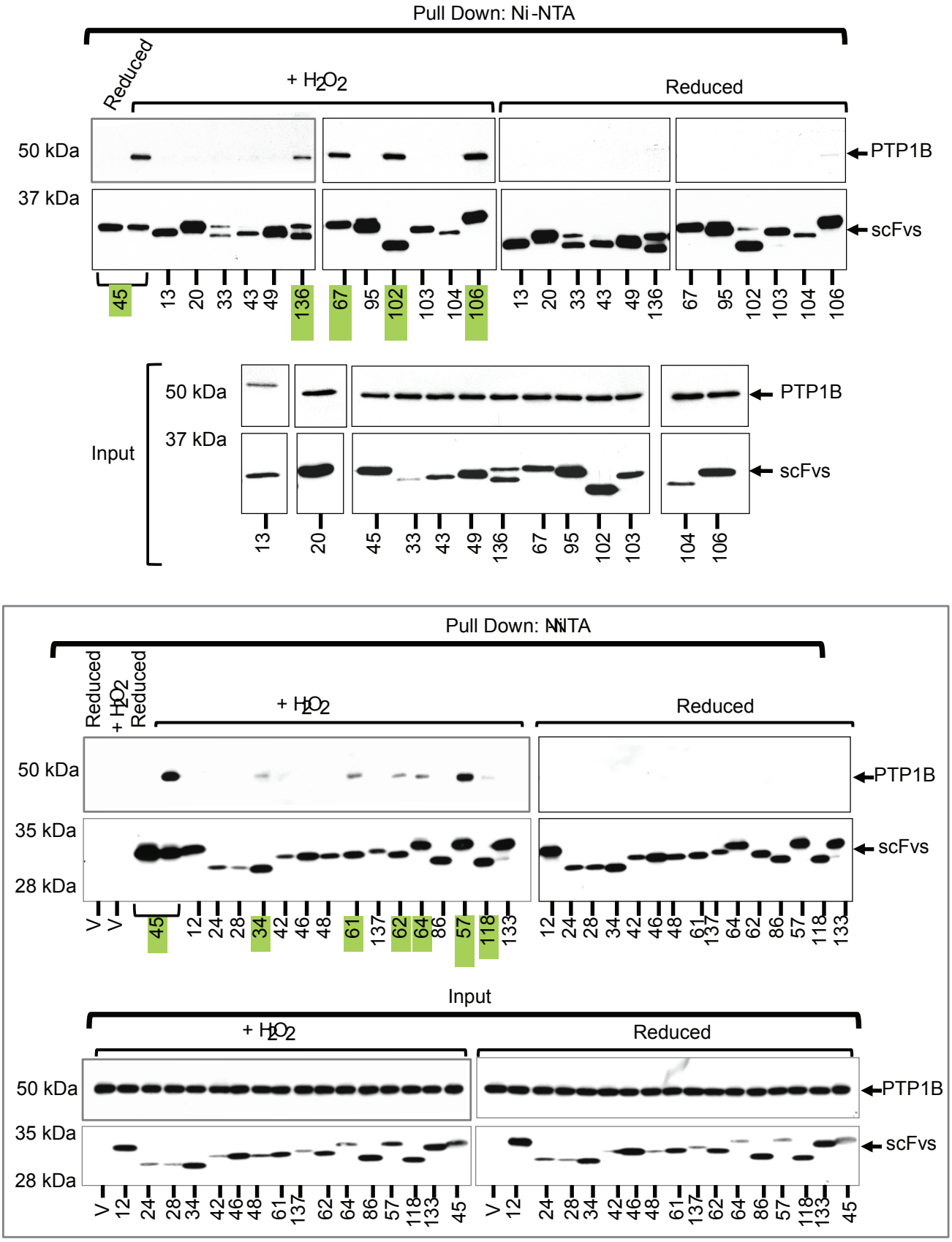
Pull Down: Ni-NTA
Reduced
+ H2O2
Reduced
50 kDa
37 kDa
PTP1B
scFvs
45 13 20 33 43 49 136 67 95 102 103 104 106
13 20 33 43 49 136 67 95 102 103 104 106
Input
50 kDa
37 kDa
PTP1B
scFvs
13 20 45 33 43 49 136 67 95 102 103 104 106
Pull Down: Ni-NTA
Reduced
+ H2O2
Reduced
+ H2O2
Reduced
50 kDa
35 kDa
28 kDa
PTP1B
scFvs
V V 45 12 24 28 34 42 46 48 61 137 62 64 86 57 118 133
12 24 28 34 42 46 48 61 137 64 62 86 57 118 133
Input
+ H2O2
Reduced
50 kDa
35 kDa
28 kDa
PTP1B
scFvs
V 12 24 28 34 42 46 48 61 137 62 64 86 57 118 133 45
V 12 24 28 34 42 46 48 61 137 62 64 86 57 118 133 45

Figure 4.2. Screening for PTP1B-OX specific Intrabodies
Additional 28 different scFvs were transiently expressed in 293T cells as intrabodies to screen and identify new candidate scFvs that can bind to endogenous PTP1B-OX. Transfected cells were treated with H_2O_2 (1 mM) for oxidation of cellular proteins. "Reduced" samples were prepared by treating cells with NAC (20 mM) and preparing the lysates with 2 mM TCEP in the lysis buffer. Oxidized and reduced cell lysates (1 mg) were used for Ni-NTA pull down as indicated. Associated protein complex from the bead was eluted and analyzed by western blot to detect PTP1B and scFvs as described earlier. For all the samples input lysates (50% of the precipitates) were loaded and endogenous PTP1B and overexpressed intrabody were detected. [V in the lower panel indicates cells transfected only with the vector without any scFv insert].

Similar interaction between scFv45 and PTP1B-OX was observed when the intrabody was immunoprecipitated using anti-HA-agarose beads or, in the reciprocal experiment, when PTP1B was immunoprecipitated with anti-PTP1B antibody from transfected cells that were treated with H_2O_2 (Figure 4.3 B). In all these different examples no interaction between PTP1B and scFv45 was observed when the transfected cells were treated under reducing conditions.

4.3 PTP1B and TCPTP are Reversibly Oxidized in 293T Cell

Meng et al. reported that PTP1B and TCPTP are reversibly oxidized in Rat 1 cells under insulin stimulation (Meng et al., 2004). PTP1B oxidation by insulin stimulation of Murine 3T3-L1 preadipocytes (Mahadev et al, JBC 2001) was also reported. To test further whether PTP1B and TCPTP were reversibly oxidized under conditions in which we have seen the scFv45-PTP1B interaction in mammalian cells we performed a cysteinyl labeling assay (Boivin and Tonks, 2010). This assay showed that both PTP1B and TCPTP are reversibly oxidized in 293T cells when treated with ether insulin or H_2O_2 (Figure 4.4 A and B).

4.4 scFv45 binds Specifically to PTP1B-OX in Mammalian Cells

Work in our lab (Meng et al., 2004) and other labs (Mahadev et al., 2001) demonstrated that stimulation of cells with insulin causes rapid and transient oxidation and inhibition of PTP1B, which facilitates increased phosphorylation of the insulin receptor-β subunit. We tested whether scFv45 could bind to endogenous PTP1B upon insulin treatment. We observed that scFv45 immunoprecipitated PTP1B from lysates of transfected 293T cells that were treated with insulin (Figure 4.3 C and D). In cells that were untreated or were kept and processed under reducing conditions, such interaction was absent whereas scFv45 interacted with PTP1B-OX in H_2O_2-treated cell samples performed in parallel. We demonstrated that scFv45 bound specifically to PTP1B-OX but not to TCPTP-OX in our *in vitro* binding experiments. In mammalian cells, scFv45 displayed similar specificity towards endogenous PTP1B-OX, as it did not show any interaction with endogenous TCPTP under insulin induction or H_2O_2 treatment (Figure 4.3 C). Reversible oxidation of the catalytic cysteine residue of other PTPs, including

Figure 4.3

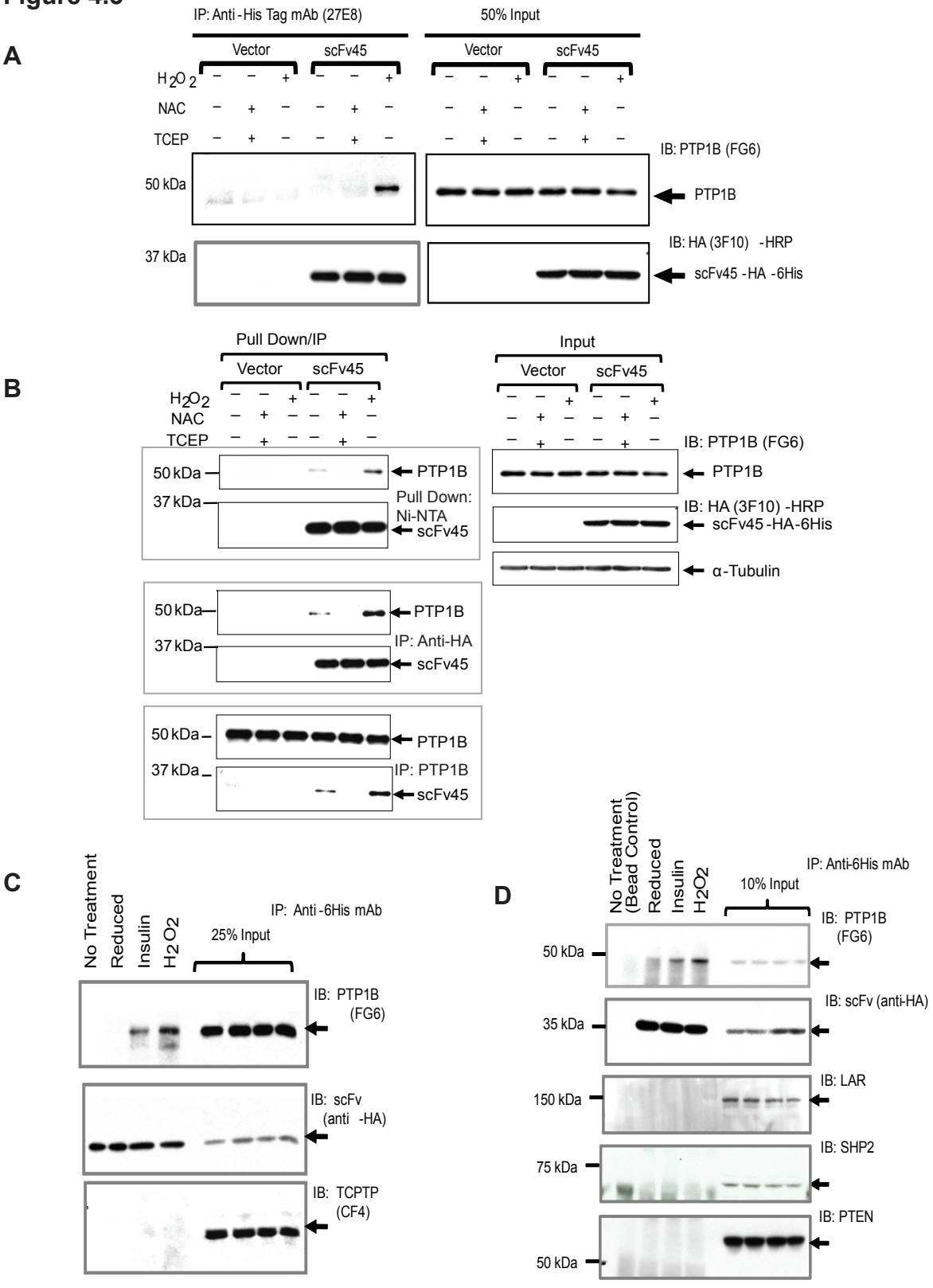
A
IP: Anti-His Tag mAb (27E8)
50% Input
Vector
scFv45
H2O2
NAC
TCEP
IB: PTP1B (FG6)
50 kDa
PTP1B
37 kDa
IB: HA (3F10) -HRP
scFv45 -HA -6His
B
Pull Down/IP
Input
Pull Down: Ni-NTA
IP: Anti-HA
IP: PTP1B
α-Tubulin
C
No Treatment
Reduced
Insulin
IP: Anti-6His mAb
25% Input
IB: PTP1B (FG6)
IB: scFv (anti-HA)
IB: TCPTP (CF4)
D
10% Input
35 kDa
150 kDa
75 kDa
IB: LAR
IB: SHP2
IB: PTEN

Figure 4.3. Intrabody45 Binds to PTP1B-OX in H_2O_2 and Insulin Treated 293T Cells
(A) Intrabody45 expressing 293T cells were treated with H_2O_2 (1 mM) or NAC (20 mM) and cell lysates were prepared with or without TCEP (2 mM). From 1 mg total cell lysate intrabody45 was immunoprecipitated with anti-His tag mouse monoclonal antibody and binding of PTP1B under oxidized or reduced conditions were detected by western blot. Input cell lysates from each sample were loaded to detect the level of endogenous PTP1B and overexpressed intrabody45.
(B) Similar immunoprecipitation experiments were done using anti-HA (to IP intrabody45) or anti-PTP1B antibody (lower two panels). Same cell lysates were also used for Ni-NTA pull down (upper panel).
(C) In similar experiment 293T cells expressing intrabody45 were treated with insulin (25 nM) or H_2O_2 (1 mM) or NAC (20 mM) and lysates were prepared as described previously. Total cell proteins (1 mg) were used for IP with anti-6His mAb and PTP1B was detected from the immunoprecipitated complex by western blot. From each cell lysates inputs (25% of the precipitate) were loaded to detect the endogenous PTP1B and expressed intrabody45. The membrane was stripped and re-probed with anti-TCPTP mouse monoclonal antibody (CF4).
(D) Lysates from insulin (25 nM) or H_2O_2 (1mM) treated cells or from cells grown and lysed under reducing condition (20 mM NAC,1 hour and 2 mM TCEP in lysis buffer) were used for IP with anti-6His mAb. Association of other phosphatases (LAR, SHP2 and PTEN) was investigated by stripping and re-probing with phosphatase specific antibodies as indicated.

Figure 4.4

A

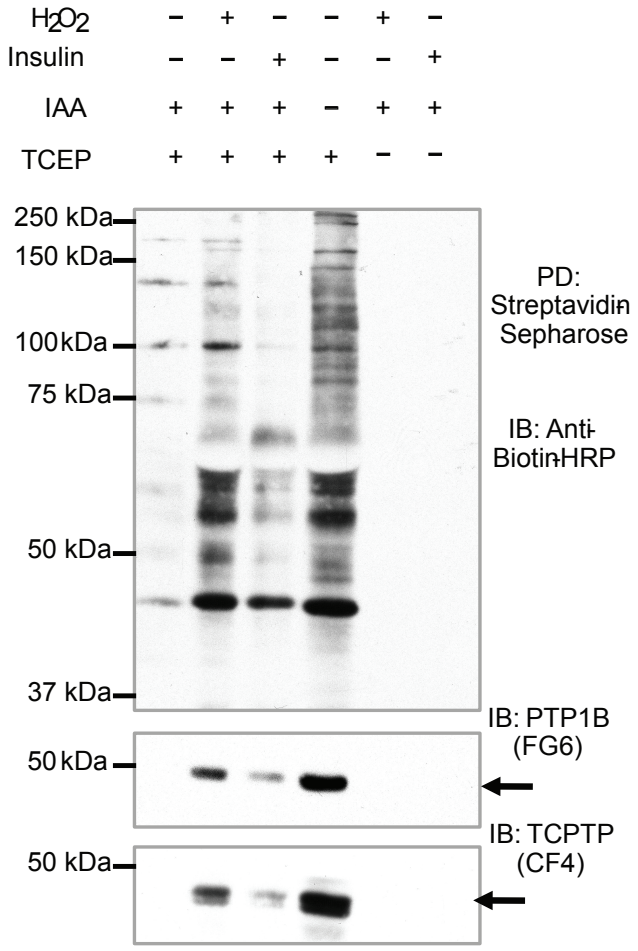
H2O2 − + − − + −
Insulin − − + − − +
IAA + + + − + +
TCEP + + + + − −
250 kDa
150 kDa
100 kDa
75 kDa
50 kDa
37 kDa
PD: Streptavidin Sepharose
IB: Anti-Biotin-HRP
50 kDa
IB: PTP1B (FG6)
50 kDa
IB: TCPTP (CF4)

B

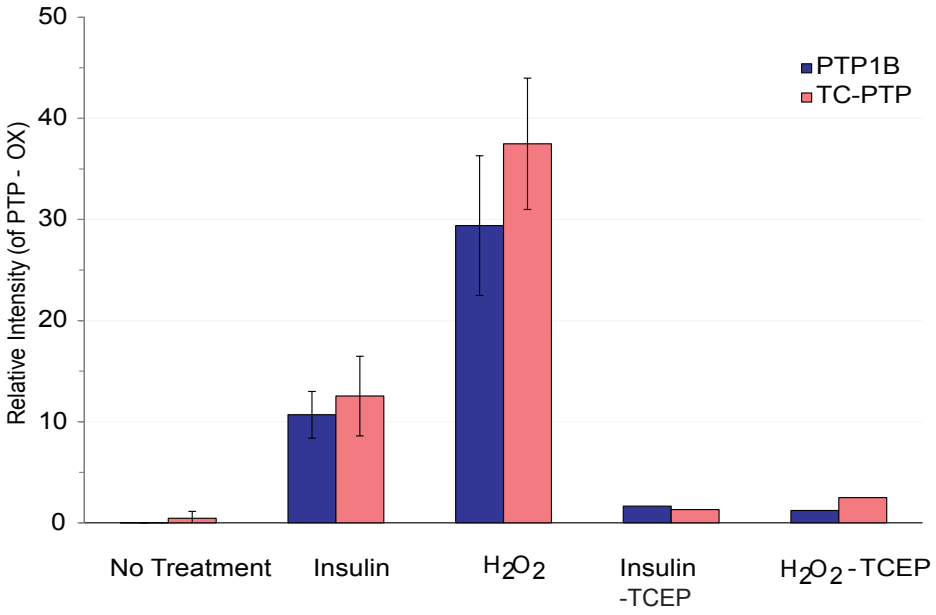
Relative Intensity (of PTP - OX)
50
40
30
20
10
0
PTP1B
TC-PTP
No Treatment
Insulin
H2O2
Insulin -TCEP
H2O2 - TCEP

Figure 4.4 PTP1B and TCPTP are reversibly Oxidized in 293T Cells
293T cells were serum starved and then stimulated with H_2O_2 (1 mM) or insulin (25 nM). Cells were lysed under anaerobic condition and oxidized PTPs were labeled with the sulfhydryl reactive IAP probes (EZ-link iodoacetyl-PEO). Biotinylated proteins from cell lysates were enriched by streptavidin-Sepharose pull downs and processed for immunoblot analysis. Biotinylated proteins were detected with anti-Biotin-HRP and membrane was stripped and re-probed for PTP1B and TCPTP. Band intensity for PTP1B and TCPTP from three separate experiments were measured using ImajeJ Software (Rasband, 1997-2009) and expressed as a percent of total biotinylation in the absence of IAA.

SHP2 (Meng et al., 2002), LAR (Boivin et al., 2008) and PTEN (Kwon et al., 2004; Lee et al., 2002) has been reported. We investigated whether scFv45 interacted with any of the above phosphatases under conditions in which it interacts with PTP1B-OX (insulin induction and H_2O_2 treatment of cells). LAR, SHP2 and PTEN displayed no interaction with scFv45 when it was immunoprecipitated from cells treated with insulin or H_2O_2 (Figure 4.3 D), illustrating again that the intrabody maintains its specificity to PTP1B not only over its closest relative TC-PTP but also over other phosphatases that have been reported to be oxidized under similar conditions to PTP1B oxidation.

4.5 PTP1B-OX Conformation Sensor Intrabody Colocalized with PTP1B in Insulin or H_2O_2-treated Mammalian Cells

In order to visualize the interaction between PTP1B-OX and scFv45 in mammalian cells, we used immunofluorescence to examine whether there was co-localization of PTP1B and scFv45 in Cos1 cells following insulin stimulation or H_2O_2 treatment. Significant co-localization between PTP1B and scFv45 was observed in cells transiently transfected with the intrabody and then stimulated with insulin or H_2O_2 (Figure 4.5 A, 4.5 C. However, such co-localization was absent between the negative control scFv20 and PTP1B (Figure 4.5 B and 4.5 C). No signal for intrabody was detected when identical antibody combinations were used to stain untransfected cos1 cells indicating that there was no cross reactivity between the antibodies used for this immunofluorescence experiment and cellular components (Figure 4.5 D).

4.6 Location Dependent Oxidation of PTP1B in Mammalian Cells

4.6.1 Localized interaction of PTP1B-OX and scFv45: We generated different mammalian expression constructs with or without the ER-targeting sequence (401-435) of PTP1B for differential cellular localization. PTP1B (FL) is expressed with the C-terminal tail anchored in the ER membrane, whereas PTP1B (1-321), devoid of the ER targeting sequences, was generated for cytoplasmic expression of the enzyme. The ER

Figure 4.5
A

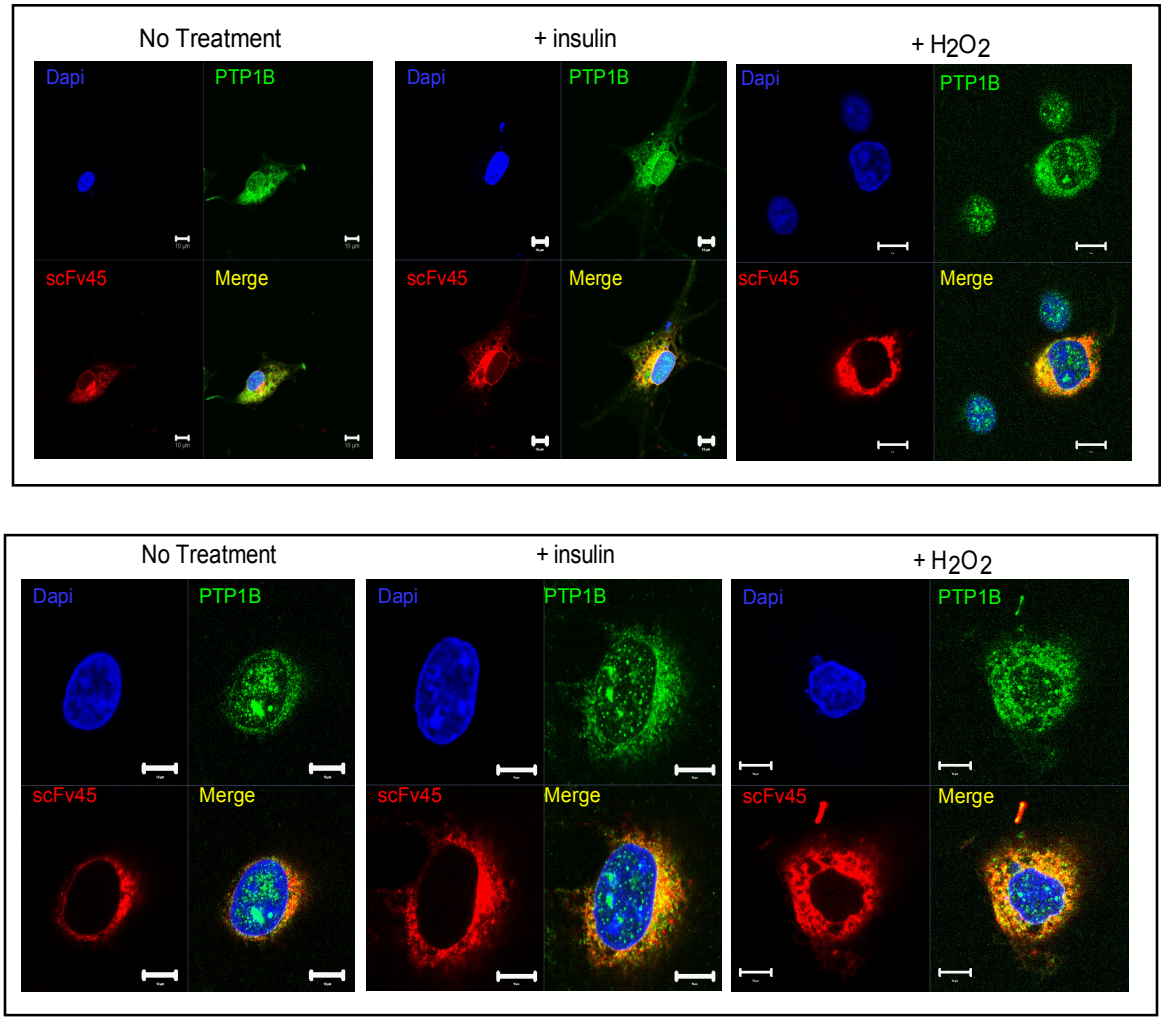
No Treatment
+ insulin
+ H_2O_2
Dapi
PTP1B
scFv45
Merge
Dapi
PTP1B
scFv45
Merge
Dapi
PTP1B
scFv45
Merge
No Treatment
+ insulin
+ H_2O_2
Dapi
PTP1B
scFv45
Merge
Dapi
PTP1B
scFv45
Merge
Dapi
PTP1B
scFv45
Merge

Figure 4.5
B

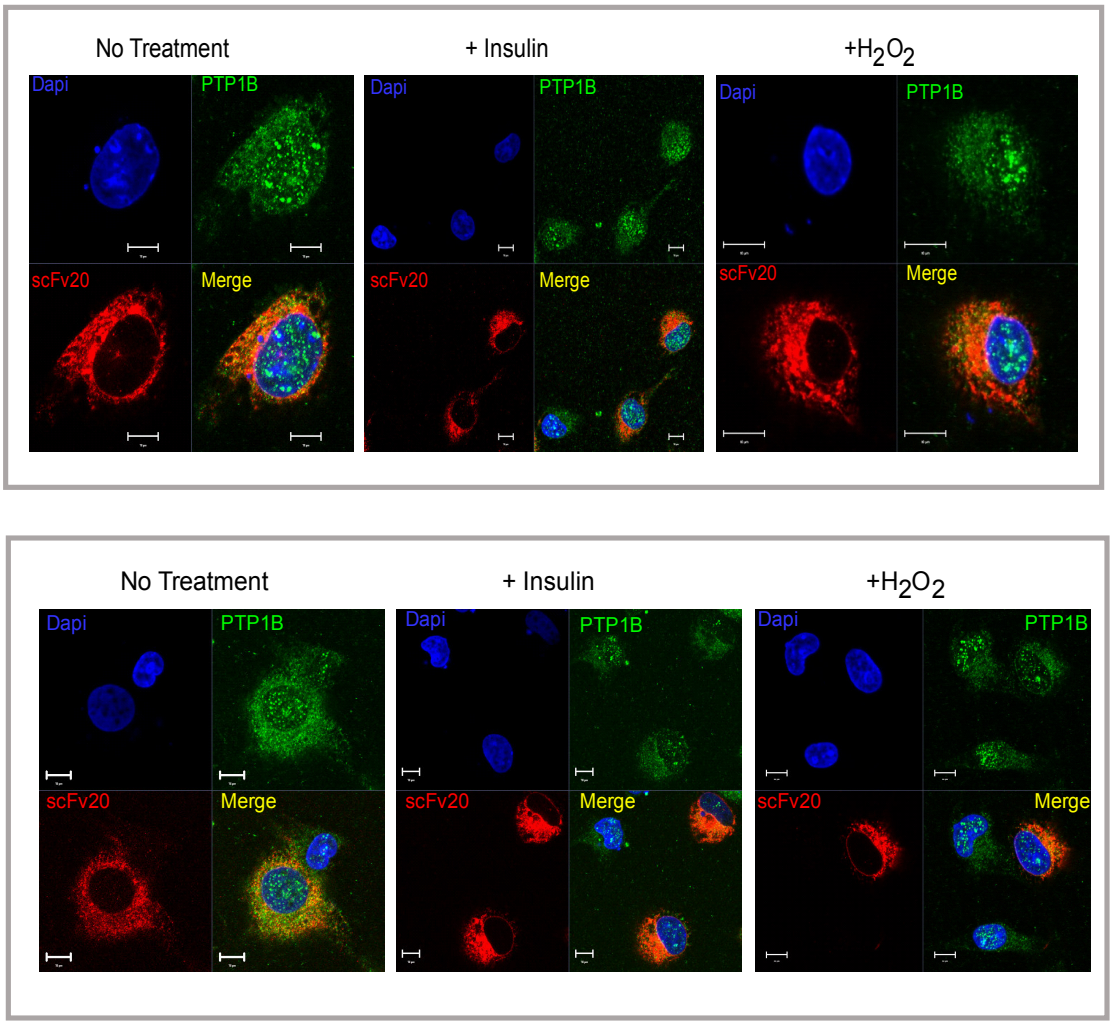
No Treatment
+ Insulin
+H2O2
Dapi
PTP1B
scFv20
Merge
Dapi
PTP1B
scFv20
Merge
Dapi
PTP1B
scFv20
Merge
No Treatment
+ Insulin
+H2O2
Dapi
PTP1B
scFv20
Merge
Dapi
PTP1B
scFv20
Merge
Dapi
PTP1B
scFv20
Merge

Figure 4.5

C

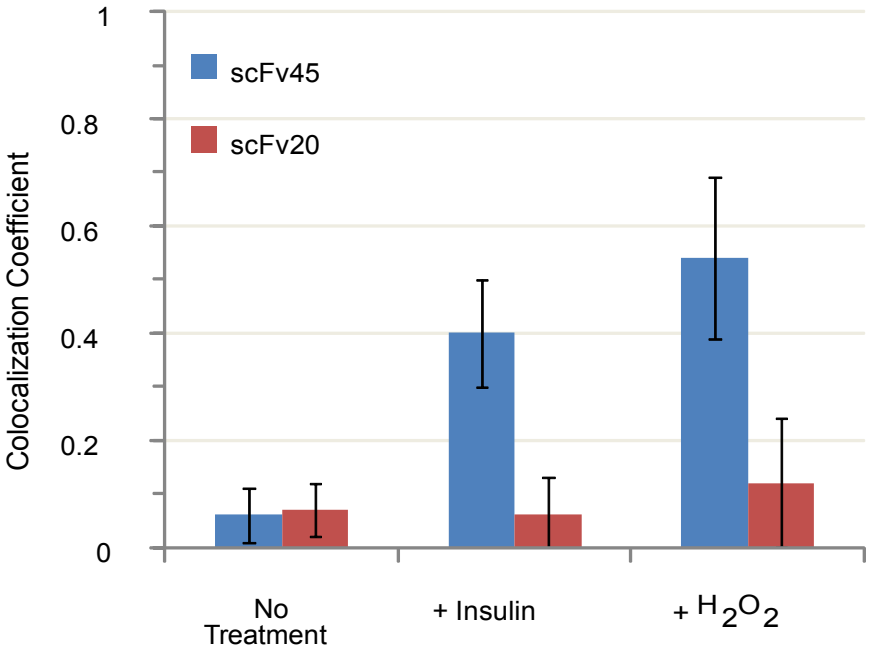
1
0.8
0.6
0.4
0.2
0
Colocalization Coefficient
scFv45
scFv20
No Treatment
+ Insulin
+ H_2O_2

D

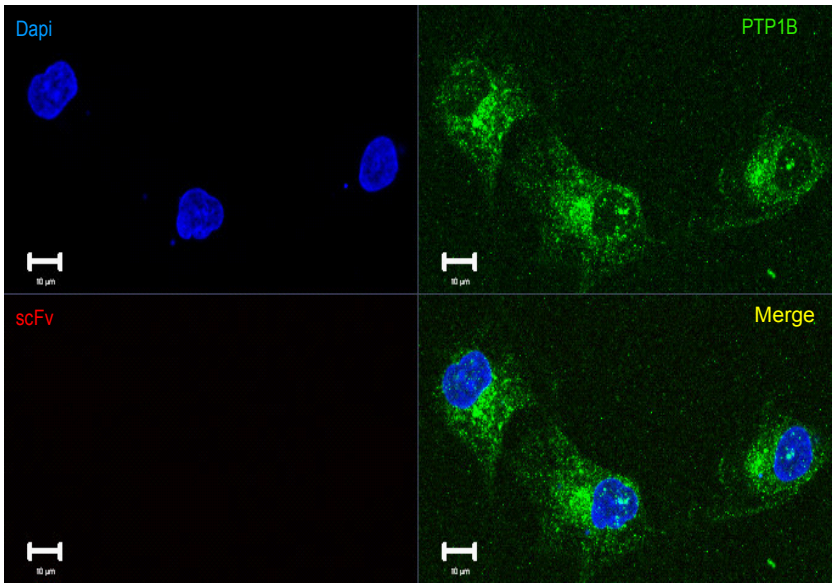
Dapi
PTP1B
scFv
Merge

Figure 4.5 Intrabody 45 Co-localizes with PTP1B in Insulin and H_2O_2 Treated Cos1 cells

(A) Cos1 cells transfected with intrabody45 were treated with insulin (25 nM) or H_2O_2 (1mM) or left untreated. Fixed cells were processed for immunofluorescence as indicated and visualized using confocal microscope (LSM 710 Zeiss) with oil immersion (63X). Panels are showing representative images from three separate experiments. Rabbit polyclonal anti-PTP1B (H-135, Santa Cruz) and anti-HA mouse monoclonal antibody (clone HA.11, Covance) were used for PTP1B and intrabody45, respectively. Alexa-488 and -594 conjugated secondary antibodies were used as described in the method section.

(B) Similarly intrabody 20 was transfected in Cos1 cells and untreated or insulin (25 nM) or H_2O_2 (1 mM) treated cells were visualized using same antibody combination as (A).

(C) Colocalization of PTP1B and intrabody45 was analyzed by Zeiss (LSM 710) Colocalization Viewer Software. The degree of colocalization was expressed as colocalization coefficient that measures relative number of colocalizing pixels for the respective fluorophores for PTP1B and intrabody45, as compared to the total number of pixels. The numeric range for this colocalization method is set as 0 – 1, where “0” indicates no colocalization and “1” indicates colocalization of all pixels in a cell. Error bars indicate standard deviation from colocalization analysis of 25 individual cells for each condition.

(D). Non-transfected Cos 1 cells were visualized using same antibody combination to verify if there is any antibody cross binding.

targeting sequence was also fused back to PTP1B (1-321) to re-establish the ER-anchored localization of this truncated form of the enzyme (4.6 A and B). Interaction between flag tagged PTP1B (full length) and scFv45 was observed when co-transfected 293T cells were treated with either insulin (25 nM) or H_2O_2 (1 mM). When scFv45 was co-expressed with flag-tagged PTP1B (1-321) in which there is not an ER targeting sequence, there was not an interaction between scFv45 and PTP1B after insulin stimulation. Very little interaction was observed between this cytoplasmic PTP1B and scFv45 even after treating cells with 1 mM H_2O_2. When the ER sequence was put back on this 1-321 truncation for its ER-anchored expression, the interaction with scFv45 was restored in cells treated with insulin or H_2O_2 (Figure 4.7 A and B). As a control experiment, when scFv20 was immunoprecipitated after being co-expressed with all these PTP1B constructs, it did not bind to any of the PTP1B constructs when the co-transfected 293T cells were treated with insulin (25 nM) (Figure 4.8 A). This experiment also showed that the protein A/G Agarose beads under these immunoprecipitation conditions did not precipitate the overexpressed PTP1Bs non-specifically in any of the differentially treated cell lysates.

4.6.2 Different Subcellular Expression of PTP1B Mediated by ER Targeting Sequence: We have further confirmed that the Flag-tagged PTP1B constructs were expressed in different cellular compartments by fractionation of the transfected cells into cytoplasmic and membrane pools. As expected, Flag-PTP1B without the ER targeting sequence (1-321/1-298) was detected in cytoplasmic fractions, whereas Flag-PTP1B constructs with the ER-target motif (full length/1-321-ER/1-298-ER) were detected only in the membrane fractions (Figure 4.8 B).

4.6.3 PTP1B Constructs Expressed in Different Subcellular Locations are Enzymatically Active: We then demonstrated that these PTP1B constructs are enzymatically active when overexpressed in 293T cells, by performing a substrate trapping experiment by co-expressing the DA mutant (Flint et al., 1997) of the corresponding constructs along with insulin receptor. This result confirmed that the location-dependent oxidation of PTP1B in response to both insulin and H_2O_2 is not due to any mis-folding of the overexpressed proteins. Interestingly both the ER localized

Figure 4.6

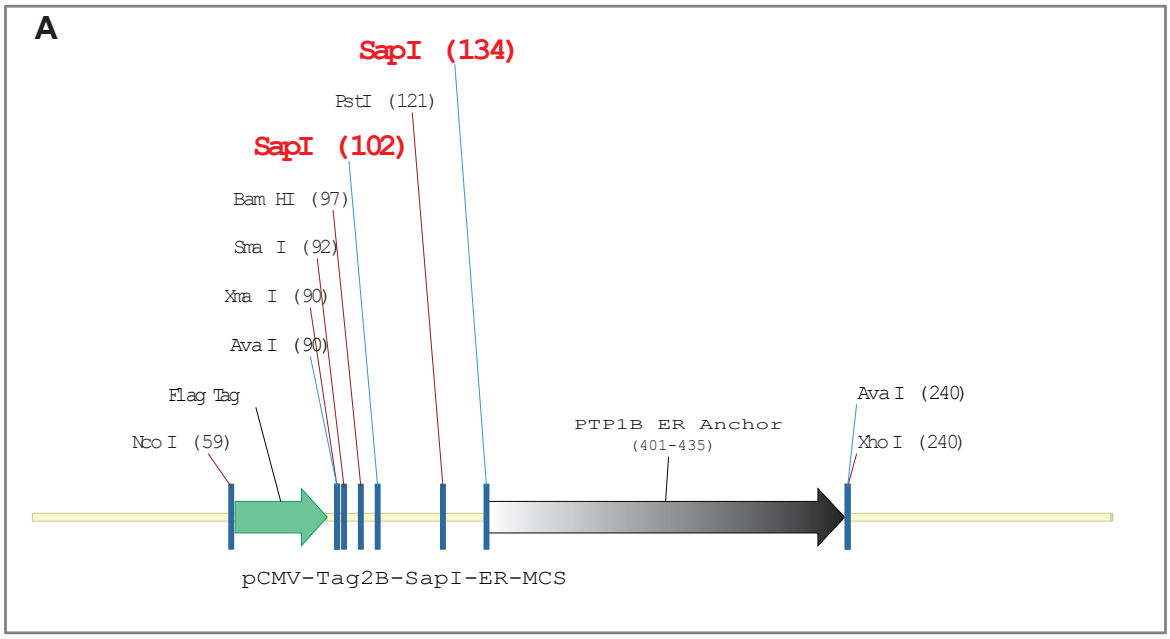
A
SapI (134)
PstI (121)
SapI (102)
Bam HI (97)
Sma I (92)
Xma I (90)
Ava I (90)
Flag Tag
Nco I (59)
PTP1B ER Anchor
(401-435)
Ava I (240)
Xho I (240)
pCMV-Tag2B-SapI-ER-MCS

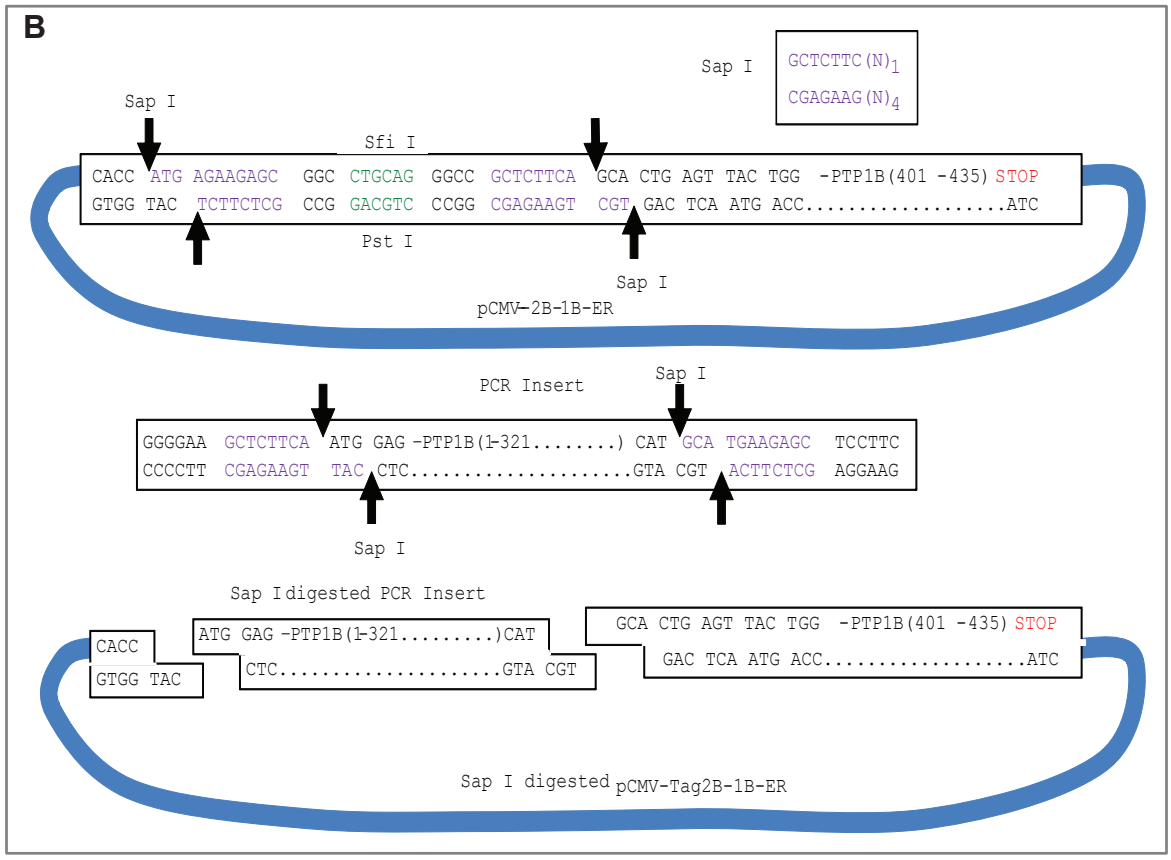
B
Sap I
GCTCTTC(N)1
CGAGAAG(N)4
Sap I
Sfi I
CACC ATG AGAAGAGC GGC CTGCAG GGCC GCTCTTCA GCA CTG AGT TAC TGG -PTP1B(401 -435) STOP
GTGG TAC TCTTCTCG CCG GACGTC CCGG CGAGAAGT CGT GAC TCA ATG ACC.....ATC
Pst I
Sap I
pCMV-2B-1B-ER
PCR Insert
Sap I
GGGGAA GCTCTTCA ATG GAG -PTP1B(1-321.....) CAT GCA TGAAGAGC TCCTTC
CCCCTT CGAGAAGT TAC CTC.....GTA CGT ACTTCTCG AGGAAG
Sap I
Sap I digested PCR Insert
CACC
GTGG TAC
ATG GAG -PTP1B(1-321.....)CAT
CTC.....GTA CGT
GCA CTG AGT TAC TGG -PTP1B(401 -435) STOP
GAC TCA ATG ACC.....ATC
Sap I digested pCMV-Tag2B-1B-ER

Figure 4.6 Generation of PTP1B Constructs for Different Sub-cellular Localization
(A) The ER localization sequence (401-435) of PTP1B was ligated to the pCMV-Tag2B vector (Invitrogen) with two asymmetric Sap I sites (shown in red) at the N-terminus of the ER anchor sequence for directional cloning of any PTP1B fragment fused to the ER-sequence without addition of a linker or deletion of native sequence.

(B) Sap I digested PTP1B insert and pCMV-Tag2B-1B-ER vector were ligated to produce Flag-PTP1B (1-n)-ER expression construct where n is any expression-capable length of PTP1B sequence. To attach with the ER sequence in a “click-fit” manner, two asymmetric Sap I restriction sites were included at both 5´ and 3´ ends of the amplified insert. PTP1B constructs without the ER sequence were generated using the same vector backbone by standard PCR amplification and cloning.

Figure 4.7

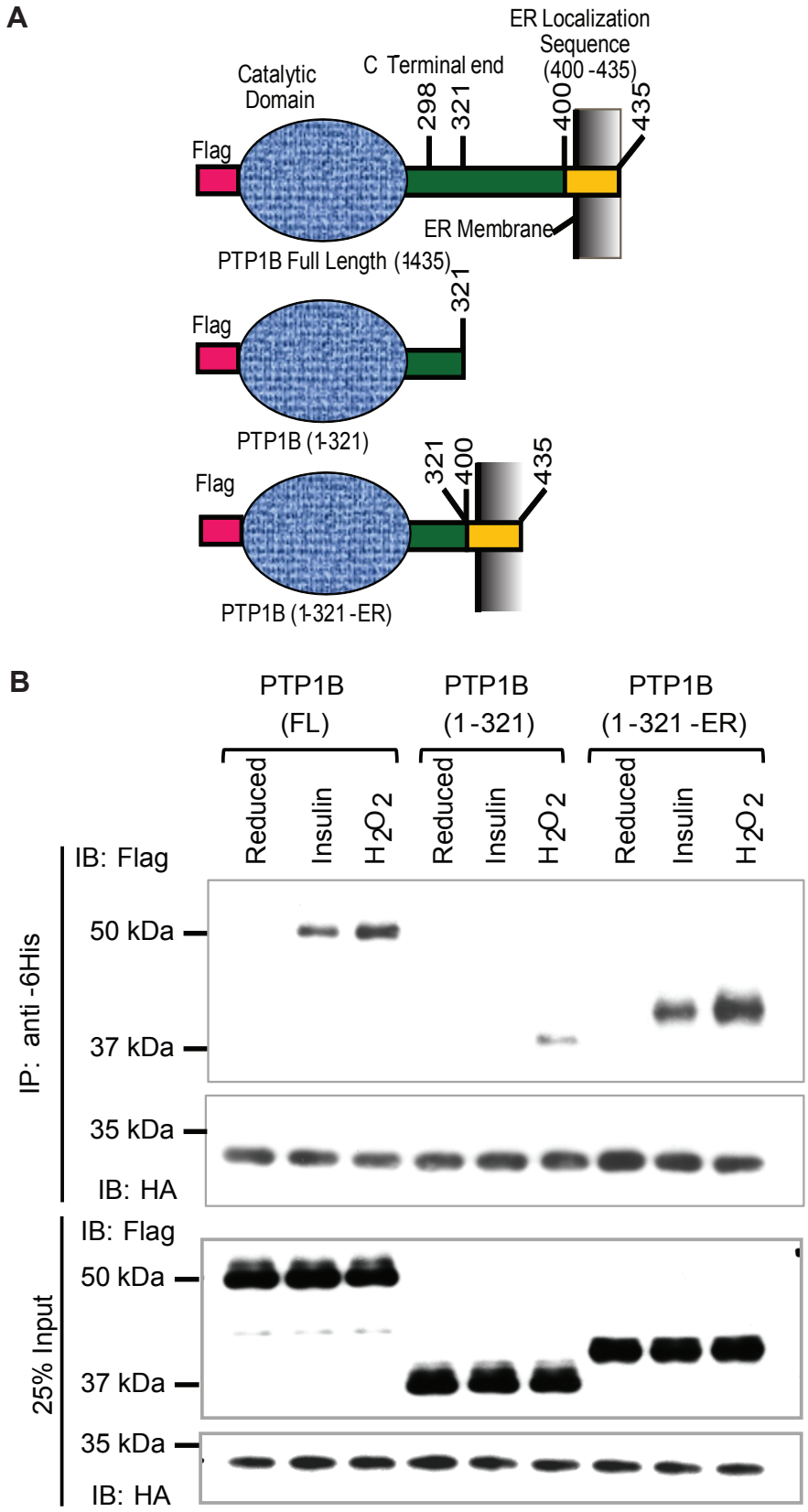
A
ER Localization
Sequence
(400 -435)
Catalytic
Domain
C Terminal end
298
321
400
435
Flag
ER Membrane
PTP1B Full Length (1-435)
321
Flag
PTP1B (1-321)
321
400
435
Flag
PTP1B (1-321 -ER)
B
PTP1B
(FL)
PTP1B
(1 -321)
PTP1B
(1 -321 -ER)
Reduced
Insulin
H2O2
Reduced
Insulin
H2O2
Reduced
Insulin
H2O2
IP: anti -6His
IB: Flag
50 kDa
37 kDa
35 kDa
IB: HA
25% Input
IB: Flag
50 kDa
37 kDa
35 kDa
IB: HA

Figure 4.7 Intrabody45 binding to PTP1B-OX in Mammalian Cell is Mediated by a location Dependent Redox Status of PTP1B

(A) Schematic shows the different N-terminally Flag tagged PTP1B constructs generated for ER-membrane anchored and cytoplasmic expression.

(B) Flag tagged PTP1B [full length (FL)], (1-321) or (1-321)-ER were co-expressed in 293T cells with intrabody45 and cells were treated with insulin (25 nM) or H_2O_2 (1 mM) or treated with NAC (20 mM) for the reduced sample. Total protein (350 µg) from the lysate were immunoprecipitated by anti 6His mAb and equivalent amount of proteins from each sample were processed for western blot analysis of PTP1B (anti-Flag) and intrabody45 (anti-HA-HRP). Input lysates (25% of the precipitates) were subjected to western blot to detect the level of PTP1B expression and intrabody45 expression in all the separate samples.

PTP1Bs (full length and 1-321-ER) showed similar amount of substrate trapping (pY-IR-β) ability, whereas the cytoplasmic version (1-321) showed markedly more efficient substrate trapping (Figure 4.8 C).

We observed similar location-dependent PTP1B oxidation and binding with scFv45 when a set of different PTP1B mammalian expression constructs (in pCDNA 3.2/V5-GWD-TOPO) were used without any N-terminal Flag tag (Figure 4.9 A and B). We used a C-terminally V5-tagged construct (1-321-V5) for cytoplasmic expression. The full-length and PTP1B (1-321-ER) were immunoprecipitated by scFv45 but not by scFv20 when co-transfected cells were treated with insulin. The cytoplasmic version of PTP1B (1-321-V5) did not show any interaction with scFv45 under these conditions. A C-terminal V5 tag (a 39 amino acid extension after the native 1-321 PTP1B sequence) in this cytoplasmic expression construct also ensures that the presence of a random C-terminal sequence (with equivalent length of the ER target sequence, which is 35 amino acid long) does not influence the interaction between PTP1B and scFv45. All these observations suggest that PTP1B oxidation is strongly regulated by cellular localization and the interaction between the ER-targeted PTP1B and scFv45 depends on oxidation of PTP1B in a localized manner. However, the subcellular distribution of intrabody needs to be verified carefully to confirm the location dependent interaction between scFv45 and PTP1B-OX.

4.7 scFv45 Enhanced and Prolonged Tyrosine Phosphorylation in 293T Cells in Response to Insulin in ROS-dependent Manner

Intrabody constructs for scFv45 or scFv20 were transfected in 293T cells, which were subsequently serum starved and then insulin stimulated, to test whether intrabody expression exerted an effect on PTP1B-mediated regulation of inulin signaling in mammalian cells. When cells in which scFv45 was overexpressed were stimulated with insulin, insulin receptor β (IRβ) and insulin receptor substrate-1 (IRS-1) displayed enhanced and prolonged tyrosine phosphorylation in comparison to cells without any intrabody or expressing the negative control scFv20. Interestingly when catalase was overexpressed together with scFv45, the stimulatory effects of the intrabody on insulin

Figure 4.8

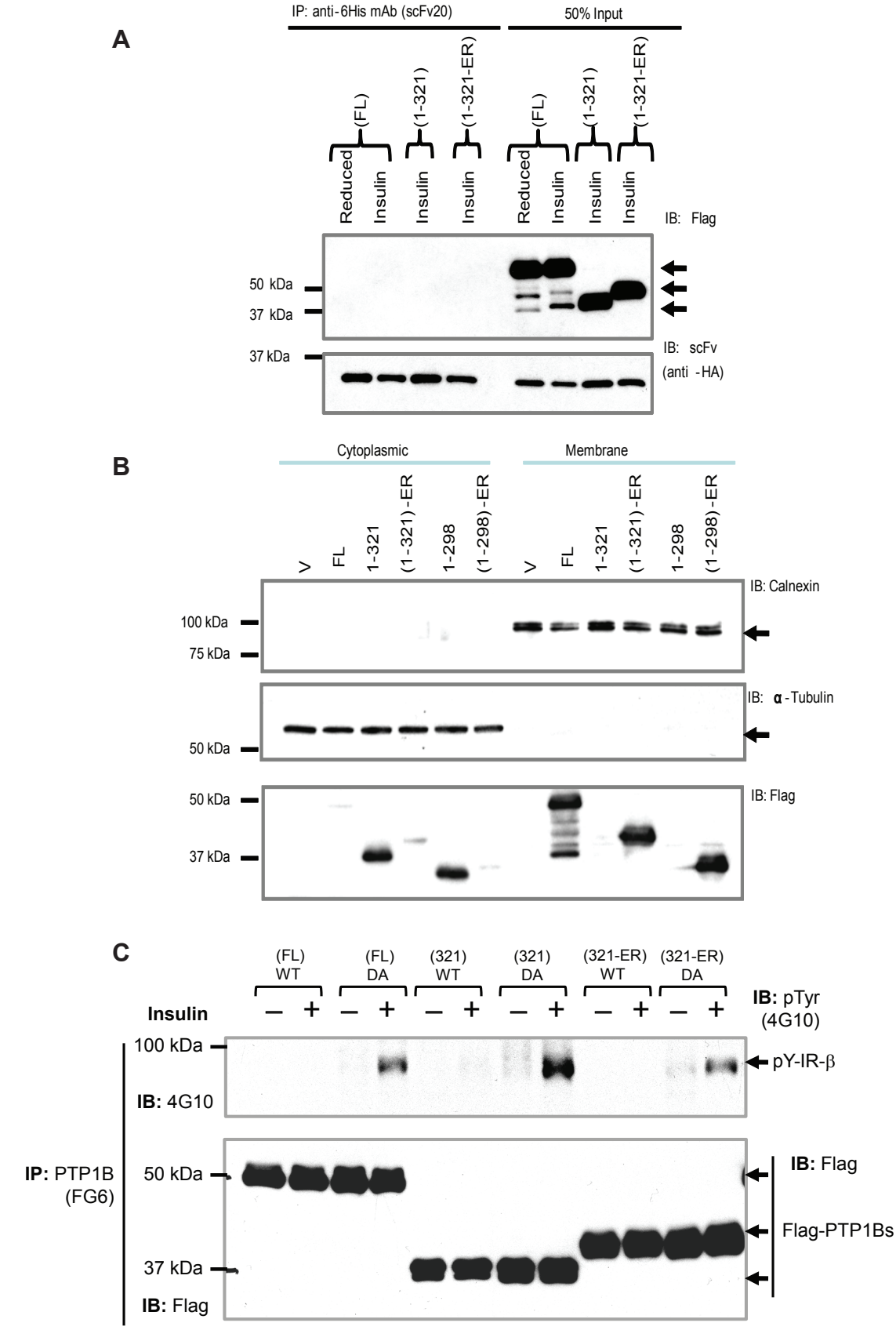
A
IP: anti-6His mAb (scFv20)
50% Input
Reduced
Insulin
Insulin
Insulin
Reduced
Insulin
Insulin
Insulin
(FL)
(1-321)
(1-321-ER)
(FL)
(1-321)
(1-321-ER)
IB: Flag
50 kDa
37 kDa
37 kDa
IB: scFv
(anti -HA)
B
Cytoplasmic
Membrane
V
FL
1-321
(1-321)-ER
1-298
(1-298)-ER
V
FL
1-321
(1-321)-ER
1-298
(1-298)-ER
IB: Calnexin
100 kDa
75 kDa
IB: α-Tubulin
50 kDa
50 kDa
IB: Flag
37 kDa
C
(FL) WT
(FL) DA
(321) WT
(321) DA
(321-ER) WT
(321-ER) DA
Insulin
– + – + – + – + – + – +
IB: pTyr (4G10)
100 kDa
pY-IR-β
IB: 4G10
IP: PTP1B (FG6)
50 kDa
IB: Flag
Flag-PTP1Bs
37 kDa
IB: Flag

Figure 4.8 PTP1B constructs in Different Sub-cellular Compartments are Enzymatically Active and Show Specificity to only scFv45

(A) Intrabody20 was co-expressed with Flag tagged PTP1B (1-FL), (1-321) or (1-321)-ER in 293T cells. Intrabody20 was immunoprecipitated with anti-His mAb to observe its interaction with PTP1B under insulin (25 nM) treatment.

(B) Different Flag-PTP1B constructs as indicated were expressed in 293T cells, cell lysates were fractionated to generate separate cytoplasmic and membrane associated protein pools. Equal amount (10 µg) of total cytoplasmic and membrane pools were subjected to western blot to detect the presence of overexpressed PTP1B by anti-Flag antibody. Membrane was stripped and probed for α-tubulin and calnexin as cytoplasmic and ER-membrane associated loading control, respectively.

(C) Substrate trapping DA mutant of differentially localized Flag-PTP1B constructs and their WT counterparts were co-expressed in 293T cells with insulin receptor (pRK-IR). Cells were serum starved and treated with insulin (25 nM, 10 min) and PTP1B was immunoprecipitated from the cell lysates with anti-PTP1B mAb (FG6). Presence of trapped tyrosine phosphorylated IR-β was detected by anti-phosphotyrosine antibody (4G10).

Figure 4.9

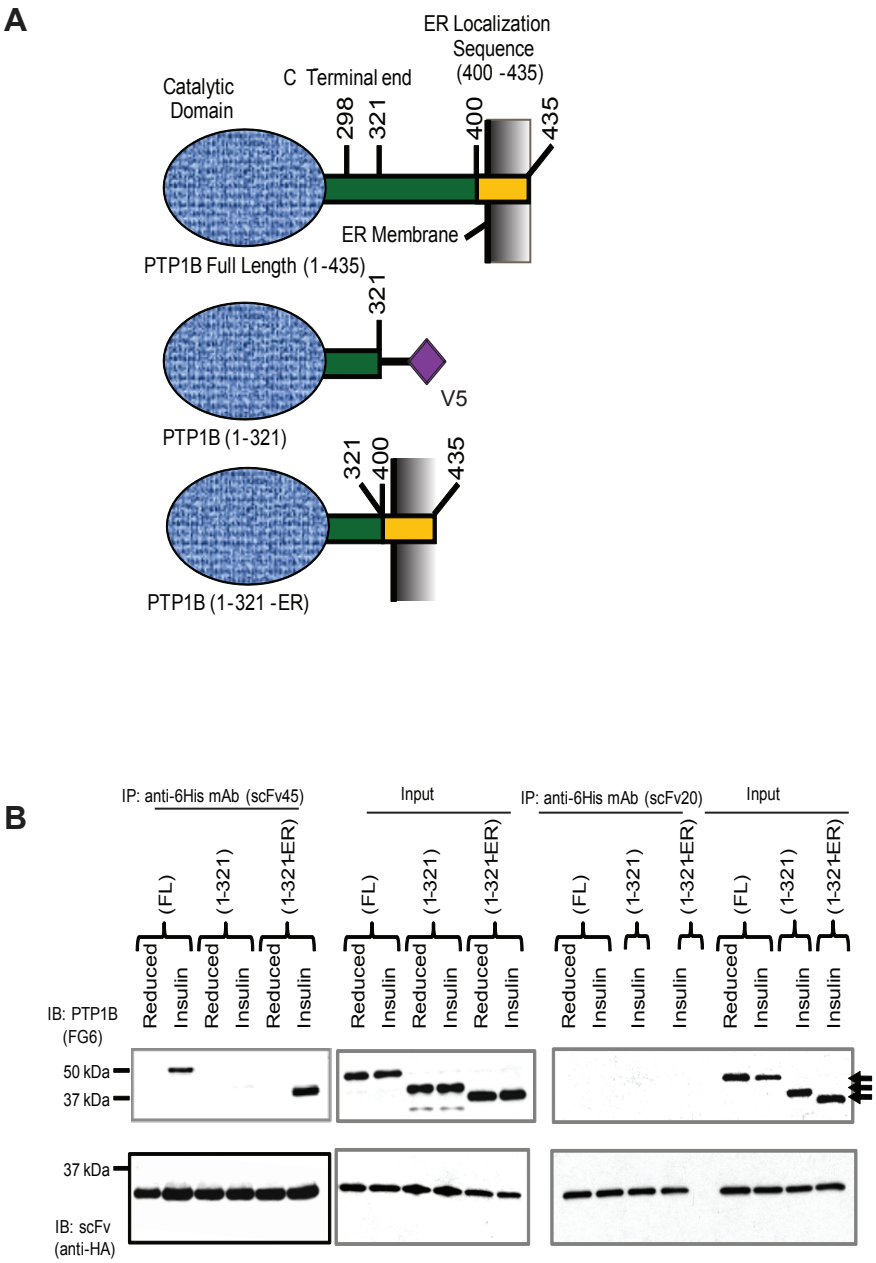
A
ER Localization
Sequence
(400 -435)
Catalytic
Domain
C Terminal end
298
321
400
435
ER Membrane
PTP1B Full Length (1-435)
321
V5
PTP1B (1-321)
321
400
435
PTP1B (1-321 -ER)
B
IP: anti-6His mAb (scFv45)
Input
IP: anti-6His mAb (scFv20)
Input
(FL)
(1-321)
(1-321-ER)
Reduced
Insulin
IB: PTP1B
(FG6)
50 kDa
37 kDa
37 kDa
IB: scFv
(anti-HA)

Figure 4.9 PTP1B Constructs without N-terminal Flag Tag also undergo Localized Oxidation and demonstrate Redox-dependent interaction with scFv45
(H and I) PTP1B constructs without N-terminal flag tag (FL, 1-321-V5, and 1-321) were co-expressed with intrabody45 or 20 in 293T cells and reduced or insulin (25 nM) treated cell lysates (350 µg) were subjected to immunoprecipitation as before and PTP1B and intrabodies were detected in the immunoprecipitated complex.

signaling were ablated. (Figure 4.10 A and B). This result supports the hypothesis that the intrabody stabilizes the reversibly oxidized conformation of PTP1B (induced by ROS produced in response to insulin stimulation) *in vivo* and inhibits reactivation of oxidized PTP1B by cellular reducing machinery.

4.8 scFv45 Caused Increased AKT Phosphorylation in response to Insulin

Insulin induces activation of the insulin-receptor kinase (IRK) through autophosphorylation (Saltiel and Pessin, 2002). Recruitment of insulin-receptor substrate (IRS) proteins induces activation of phosphatidylinositol 3-kinases (PI3K). PI3K activation triggers downstream effectors, such as phosphatidylinositol-dependent kinase 1 (PDK1) and protein kinase B (PKB) or AKT, leading to translocation of glucose transporter 4 (GLUT4) and glucose uptake in muscle, and inactivation of glycogen-synthase kinase 3 (GSK3) (Bryant et al., 2002). PTP1B dephosphorylates membrane-bound or endocytosed insulin receptors, causing their deactivation, and plays a negative, inhibitory role in the signaling events downstream of insulin receptor (Haj et al., 2002). PTP1B negatively regulates insulin signaling by dephosphorylating the tandem tyrosine residues ($pYpY^{1162/1163}$) of activated insulin receptor β subunit (Salmeen et al., 2000). When 293T cells expressing scFv45 was stimulated with insulin we observed enhanced tyrosine phosphorylation of the tandem residues ($YY^{1162/1163}$) of the activation loop of IR-β and this enhancement was attenuated when catalase was ectopically overexpressed with scFv45 (Figure 4.11 A and 4.11 B).

Cells overexpressing scFv45 displayed enhanced and sustained AKT phosphorylation at residue Threonine 308 (T308) when treated with insulin (Figure 4.10, 4.11 and 4.12). We stimulated cells expressing scFv45 with insulin for prolonged time periods and observed that the downstream read-out of insulin signaling in terms of AKT activation was enhanced and sustained over this time course. This effect again was diminished in presence of catalase (Figure 4.12 A and B). We also checked the level of endogenous PTP1B in all those insulin-treated and intrabody-expressing cells and found no difference in PTP1B expression level in any of those conditions as compared with the untreated 293T cells without the expression of any intrabody. This observation

illustrates that change in PTP1B expression or stability does not underlie the effects. Overall, our data are consistent with a model in which scFv45 binds and stabilizes endogenous PTP1B-OX, thereby effectively attenuating PTP1B activity and causing an enhanced phosphorylation of insulin receptor β subunit (IRβ) and insulin receptor substrate 1 (IRS-1), which is transmitted downstream to cause an enhanced and prolonged activation of AKT.

Figure 4.10

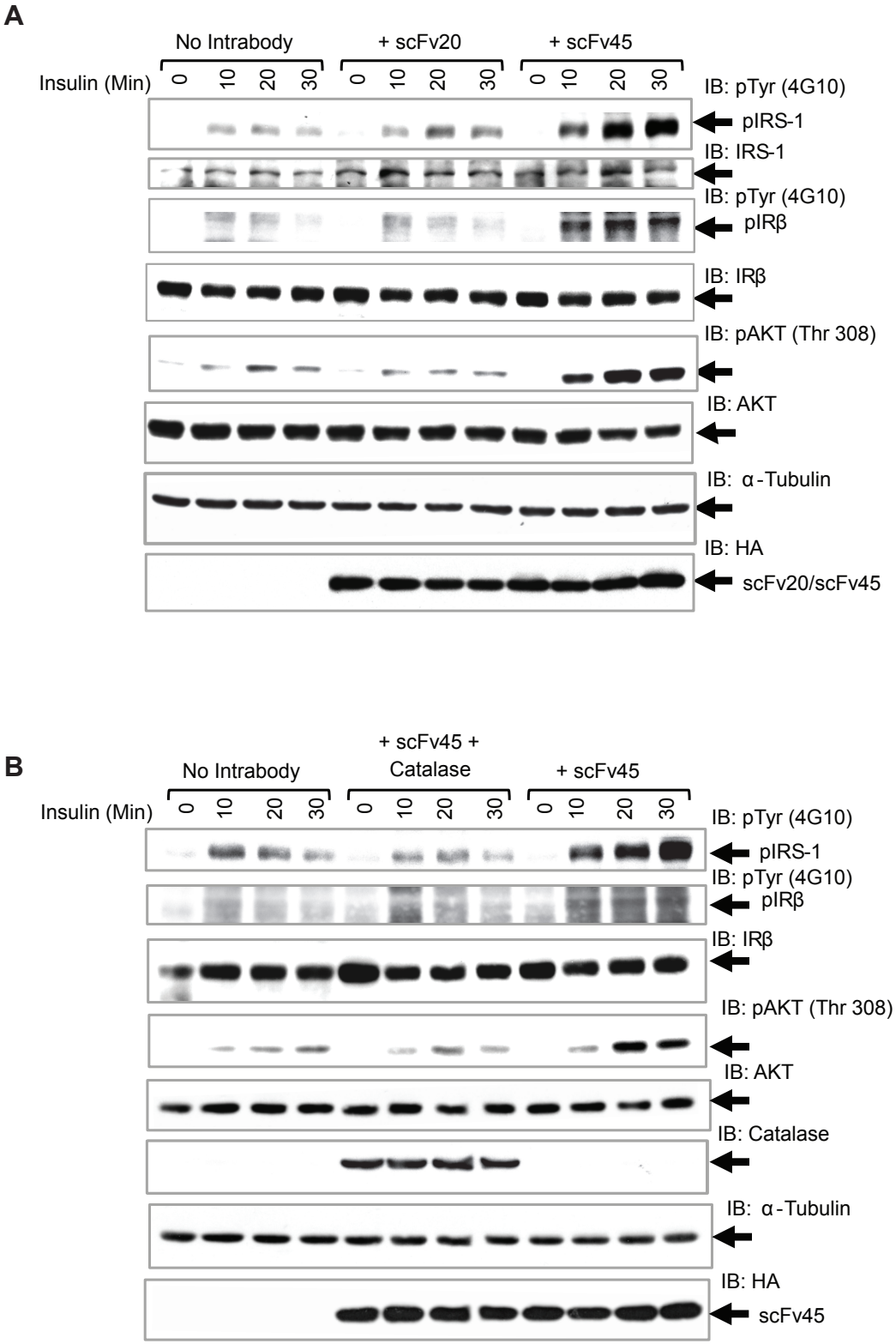
A
No Intrabody
+ scFv20
+ scFv45
Insulin (Min)
0
10
20
30
IB: pTyr (4G10)
pIRS-1
IB: IRS-1
IB: pTyr (4G10)
pIRβ
IB: IRβ
IB: pAKT (Thr 308)
IB: AKT
IB: α-Tubulin
IB: HA
scFv20/scFv45
B
No Intrabody
+ scFv45 + Catalase
+ scFv45
Insulin (Min)
IB: pTyr (4G10)
pIRS-1
IB: pTyr (4G10)
pIRβ
IB: IRβ
IB: pAKT (Thr 308)
IB: AKT
IB: Catalase
IB: α-Tubulin
IB: HA
scFv45

Figure 4.10. Intrabody45 Enhances Insulin Signaling in 293T cells in a Redox-dependent Manner

(A) Cells (293T) transiently expressing intrabody45 or intrabody20 or non-transfected cells were treated with insulin (25 nM) for indicated time points and total cell lysates (60 µg) were subjected to western blot analysis. Tyrosine phosphorylation of IR-β and IRS-1 were detected with anti-phospho-tyrosine antibody (4G10). Akt activation was detected by probing for phospho-AKT (Thr308).

(B) Inrabody45 was co-expressed with ectopic catalase in 293T cells, which were serum starved, treated with insulin (25 nM) and cell lysates (60 µg) were processed for western blot to detect the level of tyrosine phosphorylation of IR-β and IRS-1. Akt activation in the same samples was also detected with anti-phoshpo AKT (Thr308) antibody. Extent of catalase overexpression in the cotransfected samples was observed by anti-catalase antibody.

Figure 4.11

A

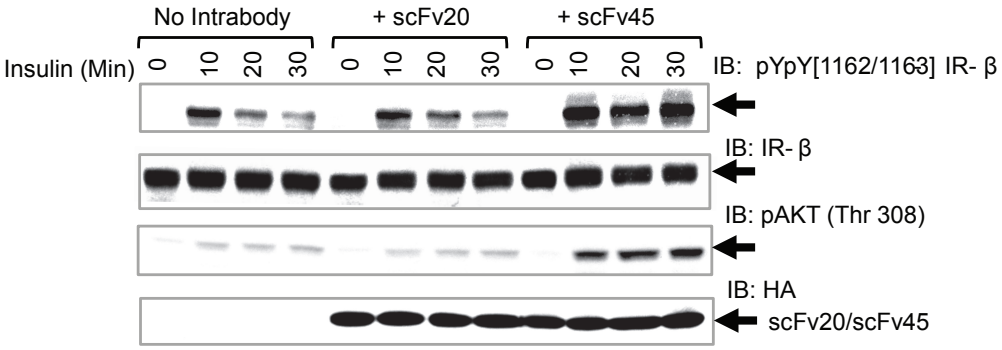

B

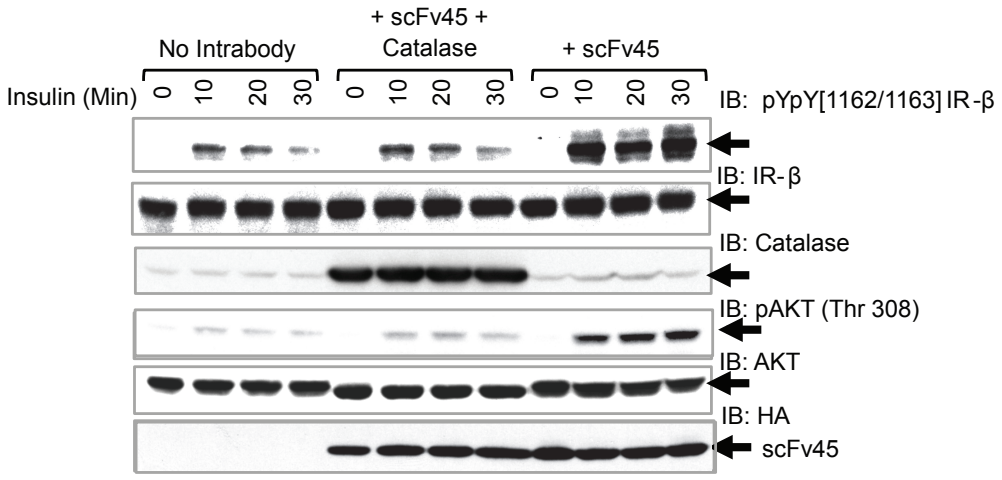

Figure 4.11. Intrabody45 Enhances Insulin Receptor Autophosphorylation
(A) Cell lysates (80 µg) from 293T cells expressing intrabodies 45 or 20 or no intrabody and treated with insulin (25 nM) for different times as indicated were subjected to western blot analysis. Phosphorylation of the activation loop of IR-β subunit was detected by rabbit polyclonal site specific anti-phosphotyrosine antibody pYpY [1162/1163]-IR-β. AKT activation was observed in the same samples with anti-pAKT (Thr308) antibody.
(B) Similar experiment was done with co-expressing intrabody45 with ectopic expression of catalase and autophosphorylation of activated insulin receptor was detected by western blot from 80 µg of total cell lysates.

Figure 4.12

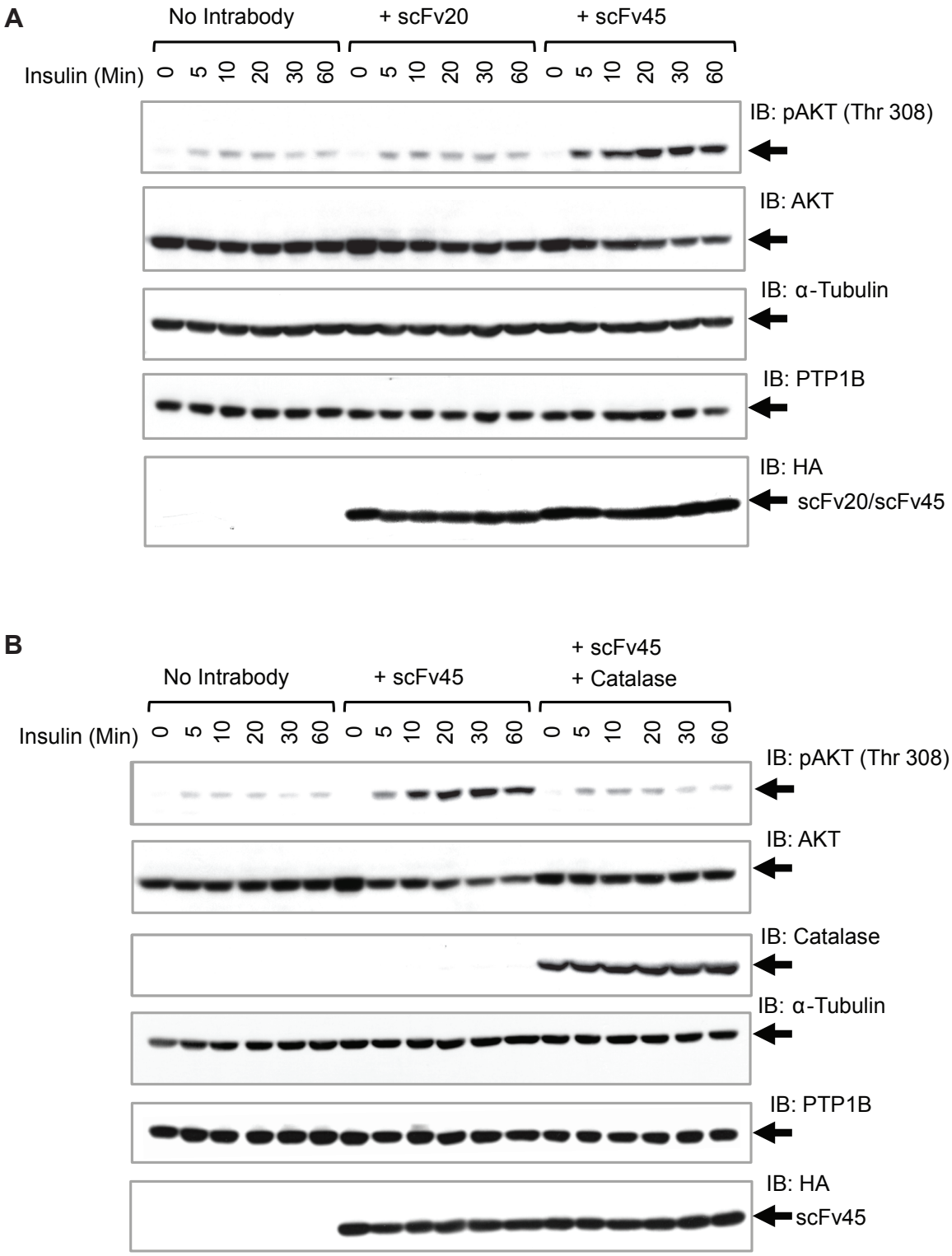
A
No Intrabody
+ scFv20
+ scFv45
Insulin (Min)
0 5 10 20 30 60 0 5 10 20 30 60 0 5 10 20 30 60
IB: pAKT (Thr 308)
IB: AKT
IB: α-Tubulin
IB: PTP1B
IB: HA
scFv20/scFv45
B
No Intrabody
+ scFv45
+ scFv45
+ Catalase
Insulin (Min)
0 5 10 20 30 60 0 5 10 20 30 60 0 5 10 20 30 60
IB: pAKT (Thr 308)
IB: AKT
IB: Catalase
IB: α-Tubulin
IB: PTP1B
IB: HA
scFv45

Figure 4.12. Intrabody45 Causes Prolonged Enhancement of Insulin Signaling Downstream of the Insulin Receptor

(A) Cells (293T) overexpressing intrabodies 45 or 20 or no intrabody were treated with insulin (25 nM) for different time points as indicated and cell lysates (60 µg) were subjected to western blot analysis. AKT phosphorylation at the activation loop Thr308 was detected by anti-pAKT (Thr308) antibody.

(B) In Similar experiment catalase was co-expressed with intrabody45 and AKT activation was followed for 60 minutes post insulin treatment. In both A and B, endogenous PTP1B protein level was also detected to verify if there was any effect of intrabody expression or prolonged insulin treatment on PTP1B expression or stability.

Materials and Methods: Chapter 4

4.9 Expression of Intrabody in Mammalian Cells

We wanted to express scFvs as intrabodies in mammalian cells to observe interaction between PTP1B-OX that was generated either by exogenous H_2O_2 treatment or insulin induction and conformation sensor intrabodies. In order to expand the scopes of our cell-based screening of intrabodies we included 36 individual scFvs to express in 293T cells.

At first scFv45 was cloned in pCDNA3.2/V5-GW/D-TOPO expression vector for transient expression of this single chain antibody fragment in mammalian cells as intrabody to PTP1B-OX. The scFv45 sequence from the pCom3XSS phagemid construct was PCR amplified and cloned directionally in the pCDNA3.2/V5-GW/D-TOPO vector in such a way that the 5´ and 3´ Sfi I restriction sites were retained in the mammalian construct. This particular intrabody was transiently transfected in 293T cells using Fugene 6 transfection reagent. Transfected cells were harvested 24, 36 and 48 hours post transfection and lysed in RIPA buffer [25 mM HEPES, pH 7.5, 150 mM NaCl, 0.25% Deoxychloate, 10% Glycerol, 25 mM NaF, 10 mM $MgCl_2$, 1 mM EDTA, 1% TritonX-100, 0.5 mM PMSF, 10 mM Benzamidine, Complete protease inhibitor cocktail (#11873580001, Roche). Soluble fractions from the samples were blotted with HRP conjugated anti-HA antibody to detect the expressed scFv. Stable expression of scFv 45 was shown at 24-48 hours post transfection.

4.10 Cysteinyl-Labeling Assay

We have expressed PTP1B-OX-specific intrabodies in 293T cells to examine binding with PTP1B in insulin stimulated or H2O2-treated conditions. To assess whether PTP1B, or its closest relative TCPTP, is reversibly oxidized in these cells under those conditions we used the cysteinyl labeling assay as described by Boivin et al., (Boivin and Tonks, 2010). Cells (293T) were grown in DMEM supplemented with 10% FBS. Confluent cultures were serum-starved for 16 hours in growth medium without serum. Cells were then treated with insulin (100 nM) for 10 minutes or H_2O_2 (1 mM) for 5

minutes at 37ºC or kept untreated. Cell plates were moved inside an anaerobic work station (COY Laboratory Products), washed rapidly with ice-cold degassed PBS and lysis was performed in freshly prepared degassed lysis buffer [50 mM sodium acetate (pH 5.5), 150 mM NaCl, 1% Surfact-Amps Nonidet P-40 (#28324, Thermo Scientific), 10% (v/v) glycerol, 25 µg/ml aprotinin, 25 µg/ml leupeptin, 100 µg/ml catalase, and superoxide dismutase (219261 and 574593; Calbiochem) with or without 10 mM iodoacetic acid (IAA).

Complete alkylation of free thiols by IAA in cell lysates was performed on a shaker for 1 h at room temperature. To remove the free IAA, 1 mg of cell lysate was buffer exchanged quickly with Zeba desalting columns, equilibrated with IAA-free lysis buffer. Reactivation of the oxidized proteins (PTPs) was performed by incubating the lysate with 1 mM TCEP for 30 min on a shaker at room temperature. Two control samples – one insulin treated and one H_2O_2 treated, were incubated without TCEP to assess the degree of cysteine biotinylation of reversibly oxidized samples. The lysates were finally incubated with 5 mM of IAP probes (EZ-link iodoacetyl-PEO, #21334, Thermo Scientific) for 1 h on a shaker at room temperature. Proteins, specifically biotinylated at the redox sensitive cysteine residue(s), were enriched by using streptavidin–Sepharose beads (17-5113-01, GE Healthcare) for 16 h at 4°C. Sepharose beads were washed initially with the lysis buffer (1X) and then with two additional washes of PBS at 4ºC. Protein complex associated with the beads were separated by SDS-PAGE and detected by western blot using anti-biotin-HRP antibody (#7075, Cell Signaling Technology) and anti-PTP1B (FG6) and anti-TCPTP (CF4) antibodies.

4.11 Interaction between PTP1B-OX and scFvs in Mammalian Cells

To detect PTP1B-OX and scFv45 interaction in mammalian cells, scFv45 was overexpressed in 293T cells as described before and 48 hours post transfection the cells were serum-starved for 16 hours in growth medium (DMEM, without serum). Cells were then treated with 25 nM insulin (human insulin, Calbiochem) for 10 minutes, with 1 mM H_2O_2 (in growth medium without serum) for 5 minutes at 37ºC or with 20 mM NAC

(in growth medium without serum) for 1 hour at 37ºC. Cells treated with insulin and H_2O_2 were washed twice with cold (4ºC) PBS and lysed in lysis buffer (25 mM HEPES, pH 7.4, 150 mM NaCl, 0.25% Deoxychloate, 1% TritonX-100, 25 mM NaF, 10 mM $MgCl_2$, 1 mM EDTA, 10% Glycerol, 0.5 mM PMSF, 10 mM Benzamidine, Complete protease inhibitor cocktail). Cells treated with NAC were lysed with lysis buffer containing 2 mM TCEP to ensure a post-lysis reducing environment. Interaction between PTP1B and scFv45 were tested by pulling down the protein complex from 1 mg of total cell lysate with Ni-NTA agarose or by immunoprecipitating scFvs either with anti-His mouse monoclonal antibody or with anti-HA agarose conjugate or by immunoprecipitating PTP1B with anti-PTP1B (FG6). For the pull down experiment, Ni-NTA agarose beads (50 µl of 50% slurry in lysis buffer) were incubated with the lysates (both oxidized and reduced) at 4ºC for 2 hours. Protein complex bound to the Ni-NTA agarose beads was pulled down and washed three times; first with lysis buffer containing 20 mM imidazole followed by two more washes with wash buffer (PBS, pH 7.4, 20 mM imidazole, 0.05% BSA, 0.05% Tween-20 and protease inhibitors). We used 20 mM imidazole in the wash buffer to reduce the non-specific binding of proteins with the Ni-NTA agarose beads. The complex was eluted with wash buffer containing 500 mM imidazole with gentle shaking at 4ºC for 15 minutes and the eluate was prepared for SDS-PAGE.

For the immunoprecipitation experiments, 1 mg of total cell lysate (both oxidized and reduced) was incubated with anti-His mouse monoclonal antibody, or anti-HA agarose conjugate or with anti-PTP1B antibody (FG6) at 4ºC. The interacting protein complex was immunoprecipitated after incubating the lysate-antibody mixture with protein A/G Sepharose at 4ºC. After immunoprecipitation, Sepharose beads were washed three times (5 minutes each) at 4ºC; first with lysis buffer followed by two more washes with wash buffer (PBS, pH 7.4, 0.05% BSA, 0.05% Tween-20 and protease inhibitors). The Sepharose beads were then heated at 90ºC in 2X SDS sample buffer with DTT. Proteins from the pulled down or immunoprecipitated complex were separated by SDS-PAGE. PTP1B was detected with anti-PTP1B antibody (FG6) and

the intrabodies were detected with anti-HA (3F10)-HRP antibody [anti-HA (3F10)-HRP, Roche] by immunoblotting.

Further assessment was carried out to identify additional PTP1B-OX-specific intrabodies. Additional scFvs have been subcloned in pCDNA3.2/V5-GW/D-TOPO mammalian expression vector from their respective phagemid constructs. After transient overexpression of these scFvs as intrabodies in 293T cells, the interaction between endogenous PTP1B and these intrabodies in both H_2O_2-treated cells and cells under reducing condition (treated with NAC and lysed with lysis buffer containing TCEP) was investigated.

4.12 Colocalization of Intrabody 45 and PTP1B-OX under Oxidizing Conditions: In order to verify the interaction between PTP1B-OX and scFv45 in mammalian cells, we determined whether PTP1B and scFv45 colocalized after insulin stimulation, using immunofluorescence. Cos1 cells were grown on cover slips and transfected with intrabody constructs of scFv45 or scFv20 as a negative control, using Fugene6 as the transfection reagent according to manufacturer's instructions. The cells were serum-starved 24 hours post transfection, for 16 hours at 37ºC and then stimulated with 25 nM insulin (in growth medium without serum) or treated with 1 mM H_2O_2 (in growth medium without serum) or left untreated. Following insulin treatment the cells were washed 2X with PBS and fixed with 5% formalin (in PBS) for 15 minutes at room temperature. The cells were washed with PBS three times at room temperature. The fixed cells were permeabilized with 0.5% Triton-X100 (in PBS) for 5 minutes at room temperature. Cells were rinsed with Wash Buffer [PBS, pH 7.4 with 0.1% BSA, 0.2% TritonX-100, 0.05% Tween-20 and 0.05% sodium azide] at room temperature. The coverslips were blocked with 5% normal goat serum in Wash Buffer for 1 hour at room temperature to reduce the non-specific binding of the secondary antibodies. To detect endogenous PTP1B and overexpressed intrabody the coverslips were incubated with a cocktail of anti-PTP1B antibody [rabbit polyclonal anti-PTP1B (H-135), # sc-14021, Santa Cruz Biotechnology] and anti-HA mouse monoclonal antibody, clone HA.11 (MMS-101R, Covance) at RT for 1 hour. The cells were washed with the wash

buffer at room temperature to remove excess antibodies. A cocktail of secondary antibodies- Alexa 594 conjugated goat anti-mouse IgG (A-11005, Invitrogen) and Alexa 488 conjugated goat anti-rabbit IgG (Invitrogen, A-11034) in the blocking buffer (5% normal goat serum) was added to the coverslip and incubated in the dark at RT for 1 hour. The coverslips were washed 3X with IF wash buffer and incubated with DAPI (0.3 µg/ml in PBS, #D9542, Sigma) for 10 minutes at room temperature to stain the nucleus and washed again with IF wash buffer to remove excess unbound DAPI. The cover slip was mounted on glass slide with Vectashield Mounting Medium (H-1000, Vector Laboratories) and observed using confocal microscope (LSM 710, Zeiss) with 63X objective lens and immersion oil. To quantify colocalization of PTP1B and scFv45, individual images were analyzed by Zeiss (LSM 710) Colocalization Viewer Software. The degree of colocalization of PTP1B and scFv45 in each cell was expressed as colocalization coefficients that measure relative number of colocalizing pixels for the respective fluorophores for PTP1B and scFv45, as compared to the total number of pixels. The numeric range for this colocalization method is set as 0 – 1, where “0” indicates no colocalization and “1” indicates colocalization of all pixels in a cell.

4.13 Cellular Localization of PTP1B Redox Regulation

4.13.1 Generation of PTP1B Mammalian Expression Constructs for differential cellular localization: The ER localization sequence of PTP1B (400-435) was amplified with Phusion DNA polymerase (NEB) using a forward primer that consists of two SapI restriction sites in opposite orientation at the 5□ end of the ER localization sequence and a reverse primer with a stop codon, which is complimentary to the C-terminal end of PTP1B. The Sap I restriction sites allowed uniform directional cloning by utilizing the unique asymmetry and position of the two sites. This amplified DNA also has additional appropriate restriction sites at the 5□ for cloning in the pCMV-Tag2B vector (Stratagene). It was ligated to the pCMV-Tag2B vector (Invitrogen) to generate N-terminally Flag-tagged PTP1B constructs of different C-terminal truncations fused directly with the ER sequence. Vector containing the ER sequence in the right orientation was selected by sequencing. We call this the pCMV-Tag2B-1B-ER vector. The SapI restriction sites in this ER sequence harboring vector were placed in opposite

orientation in such a way that any fragment PTP1B segment can be directly cloned in the vector and fused to the ER localization sequence in frame without any addition or deletion of a single amino acid. This allowed us to construct PTP1B fragments with different C-terminal truncations and fuse them directly with the ER sequence. After digesting both the amplified PTP1B insert and the pCMV-Tag2B-1B-ER vector with Sap I restriction enzyme, the insert was ligated in the vector using T4 DNA ligase. For generating PTP1B truncations without the ER localization sequence amplified PCR inserts were cloned directly in the original pCMV-Tag2B vector. The only difference between a PTP1B (1-n) and PTP1B (1-n)-ER constructs is the presence of the last 35 amino acid sequence in the later.

Similarly another vector harboring the ER sequence was created in the TOPO expression vector (pcDNA3.2/V5-GW/D-TOPO, Invitrogen) to generate PTP1B constructs with or without the ER sequence at the C-terminus, but without any N-terminal tag. We have generated the 1-321 segment of PTP1B in the TOPO vector with a V5 epitope at the C-terminal end that has an additional 39 amino acid including the V5 tag and linker. This construct, therefore, serves as a control to observe whether any amino acid sequence with the similar length of the ER targeting sequence at the C-terminus has any effect on localization and redox regulation of PTP1B.

4.13.2 Subcellular Protein Fractionation: Protein extracts from different subcellular locations were prepared by Subcellular Protein Fractionation kit (#78840, Thermo Scientific). PTP1B expression constructs were expressed in 293T cells as before in 10-cm dish. Cytoplasmic and membrane associated protein pools were prepared according to the manufacture's protocol and total protein concentration was determined by Bradford method. Total cytoplasmic and membrane proteins were separated by SDS-PAGE and PTP1B was detected with anti-Flag antibody (M2, # F3165, Sigma). Alpha-Tubulin was detected with anti-α-tubulin mouse monoclonal antibody (clone B-5-1-2, #T5168, Sigma) and calnexin was detected with mouse monoclonal anti calnexin antibody (#MA3-027, Thermo Scientific) as loading control for separate cytoplasmic and membrane pools, respectively.

4.13.3 Immunoprecipitation and Western Blots: PTP1B constructs were co-transfected in 293T cells together with constructs encoding scFv45 or scFv20 with Fugene6 as the transfection reagent following the manufacturer's protocol. Transfected cells were serum starved 48 hours post transfection in DMEM for 16 hours. Serum starved cells were treated with 100 nM insulin or 1 mM H_2O_2 in DMEM without serum for 10 minutes or 5 minutes, respectively at 37 °C. Another co-transfected cell sample was treated with 20 mM NAC (in growth medium without serum) for 1 hour at 37ºC to maintain a reduced environment prior to cell lysis. Cells treated with insulin or H_2O_2 were washed twice with cold (4ºC) PBS and lysed in lysis buffer (25 mM HEPES, pH 7.4, 150 mM NaCl, 0.25% Deoxychloate, 1% TritonX-100, 25 mM NaF, 10 mM $MgCl_2$, 1 mM EDTA, 10% Glycerol, 0.5 mM PMSF, 10 mM Benzamidine, Complete protease inhibitor cocktail from Roche). Cells treated with NAC were lysed with the same lysis buffer with 2 mM TCEP to ensure a post-lysis reducing environment. Interaction between PTP1B and scFv45 were tested by immunoprecipitating intrabody with anti-6His mouse monoclonal antibody (1.5 µg) using 350 µg total protein in 750 µl lysis buffer.

4.13.4 Substrate Trapping Experiments: Different PTP1B constructs (1 µg/60-cm plate) were co-transfected in 293T cells with pRK-IR (1 µg/60-cm plate) with Fugene6 as the transfection reagent following the manufacturer's protocol. Transfected cells were serum starved 48 hours post transfection in DMEM for 16 hours. Serum starved cells were treated with 100 nM insulin in DMEM without serum for 10 minutes at 37 °C or kept untreated. Cells were washed twice with cold (4ºC) PBS and lysed in substrate trapping lysis buffer (25 mM HEPES, pH 7.4, 150 mM NaCl, 0.25% Deoxychloate, 1% TritonX-100, 25 mM NaF, 10 mM $MgCl_2$, 1 mM EDTA, 10% Glycerol, 0.5 mM PMSF, 10 mM Benzamidine, protease inhibitor cocktail from Roche with 10 mM iodoacetic acid). PTP1B was immunoprecipitated from 1 mg of total cell lysate in 1 ml of lysis buffer using anti-PTP1B (FG6) mouse monoclonal antibody (5 µl/IP). Immunoprecipitated complex was isolated with protein A/G-Sepharose (40 µl of a 50% slurry/IP, at 4ºC for 1 hour) and washed 3 times (15 minutes each) with lysis buffer at 4ºC. Protein complexes were boiled in SDS Sample buffer with DTT and separated with

10% polyacrylamide gel. Tyrosine phosphorylated IR-β subunit was detected with anti-phosphotyrosine mouse monoclonal antibody 4G10 (#05-321, Millipore) and PTP1B was detected with anti-Flag monoclonal antibody (M2, # F3165, Sigma).

4.14 Role of Reversible PTP1B Oxidation in the Cellular Signaling Response to Insulin

Intrabody constructs for scFv45 or scFv20 (2 µg/6-cm plate) was transfected in 293T cells using Fugene6 and serum starved 48 hours post transfection. Serum-starved cells were stimulated with insulin for various times to investigate the effects of intrabody expression in mammalian cells in the context of PTP1B mediated regulation of insulin signaling. Insulin stimulated 293T cells with or without the intrabody were harvested in RIPA buffer (25 mM HEPES, pH 7.5, 150 mM NaCl, 0.25% Deoxychloate, 10% Glycerol, 25 mM NaF, 10 mM $MgCl_2$, 1 mM EDTA, 1% TritonX-100, 0.5 mM PMSF, 10 mM Benzamidine, protease inhibitor cocktail, 1mM sodium vanadate) and the total protein concentration in the lysate was determined by Bradford method. Total proteins in the cell lysates were separated by SDS-PAGE and global tyrosyl phosphorylation was detected by anti-phosphotyrosine antibody 4G10 (#05-321, Millipore). To detect specific tyrosyl phosphorylation of IR-β subunit we used rabbit polyclonal anti-insulin receptor [$pYpY^{1162/1163}$] phospho-specific antibody (#44804G, Invitrogen). Intrabodies were immunoblotted with anti-HA-Peroxidase, High Affinity (3F10, #12013819001, Roche). For loading controls for corresponding phosphotyrosine proteins the membrane was stripped by Restore Stripping Buffer (#21059, Thermo Scientific) and re-probed with antibodies against the total protein. We used anti-IR-β rabbit polyclonal antibody (C-19, #sc-711, Santa Cruz) to detect total IR-β subunit and anti-IRS1 rabbit polyclonal antibody (#06-248, Millipore or sc-559, Santa Cruz) to detect total IRS-1. To test the effect of suppressing H_2O_2 levels on intrabody function, catalase was ectopically co-expressed using $p^{S3\text{-}Catalase}$ (a gift from Dr. Toren Finkel's laboratory) along with scFv45 and the effects on insulin induced signaling were observed. The intrabody construct (2 µg/6-cm plate) and the $p^{S3\text{-}Catalase}$ construct (2 µg/6-cm plate) were co-transfected in 293T cells with Fugene6 and the effect of insulin stimulation at different time points was

observed as described earlier. Catalase expression was detected in the cell samples with anti-Catalase rabbit polyclonal antibody (219010, Calbiochem).

4.15 Effect of scFv45 on the Cellular Signaling Response Downstream of Insulin Receptor:

We wanted to assess the effect of PTP1B-OX specific intrabody on the phosphorylation (activation) status of AKT/PKB as a downstream readout of insulin signaling. Cells with or without overexpression of scFv45 or scFv20 were stimulated with insulin for different times and phosphorylation of the AKT activation loop at residue Threonine 308 (T308) was observed with phospho-specific antibody [phospho-Akt (Thr308), #9275, Cell Signaling]. Total endogenous Akt levels were detected by stripping the membrane and re-probing with Anti-Akt rabbit polyclonal antibody (9272, Cell Signaling). To investigate whether Akt phosphorylation in presence of scFv45 in insulin-stimulated cells were ROS mediated, we co-expressed catalase with the intrabody as described above and detected the level of Akt phosphorylation under this condition. Furthermore, to evaluate whether the expression of PTP1B was affected by the presence of intrabody or catalase, we measured endogenous PTP1B levels using mouse monoclonal anti-PTP1B antibody (FG6) in all the experiments.

Chapter 5

Discussion, Summary and Future Perspectives

5.1 Use of Antibody Phage Display to Generate Conformation Sensor scFv

Antibody phage display is a powerful and effective technique for generation and selection of specific antibodies. Single chain Variable Fragments (scFvs) retain the binding specificity of full-length antibodies, but they can be expressed as single polypeptides, which allows efficient *in vitro* selection from a large library displayed on phage. The success in isolating specific antibodies, however, largely depends on the strategy of library enrichment, or panning, and subsequent screening procedure. We used this *in vitro* technique with several empirically optimized modifications to enrich and isolate candidate scFvs systematically. We emphasized the necessity to perform the selections under conditions as close as possible to the screening assays and downstream applications of the candidates. We adopted a solution-based selection and subsequent screening method that was crucial for preserving specific interaction between the candidate scFvs and PTP1B-CASA. By allowing successive rounds of panning under extensively controlled *in vitro* selection conditions in the presence of excess wild-type PTP1B, we were able to enrich the library for PTP1B-OX conformation-specific scFvs. The use of active PTP1B as a soluble competitor during panning minimized the isolation of cross-reacting binders. The affinity of selected scFvs reported in the literature is usually found to be in the nanomolar range. By employing the subtractive panning strategy in the presence of excess wild type enzyme we were also able to isolate scFv45 with similar high affinity.

Use of scFvs as intrabodies has received substantial attention in the last 15 years. Successful applications of scFvs as intrabodies for a number of intracellular targets have been reported by various laboratories (Deshane et al., 1995; Jendreyko et al., 2005; Lynch et al., 2008; Marasco et al., 1993; Nizak et al., 2003; Popkov et al., 2005; Ruberti et al., 2000; Visintin et al., 2004; Yuan and Sierks, 2009). Generation of antibodies that bind specifically to an activated form of RAS in cancer cells has been reported (Carney et al., 1986). A similar approach has been described to follow the GTP-bound conformation of the small guanosine triphosphatase (GTPase) Rab6 by using GFP-tagged recombinant intrabodies expressed in the cytoplasm of cultured cells

(Nizak et al., 2003). Use of intrabodies for studying biological processes and for blocking target proteins inside cells has been reported (Visintin et al., 2004).

Intrabodies operate at the posttranslational level and, therefore, can be designed and generated to recognize precise epitopes on target proteins specifically (Marasco, 1997). Because of its high specificity and low possibility of having “off-target” effects, intrabodies present a powerful complement to gene inactivation methods by antisense techniques or RNA interference (Hannon, 2002). We have demonstrated that when *in vitro* selected PTP1B-OX-specific scFv45 was expressed as an intrabody, it not only recognized a unique post-translational regulatory modification of an important mediator of insulin signaling with high specificity, but it also stabilized that inactive conformation to potentiate signaling effects.

5.2 Redox Regulation of PTPs

Controlled production of reactive oxygen species (ROS), such as superoxide anions and H_2O_2, to serve physiological functions in non-phagocytic cells, has been observed in response to a variety of ligands acting through receptor tyrosine kinases (Bae et al., 1997; Krieger-Brauer and Kather, 1992; Lo and Cruz, 1995; Mahadev et al., 2001; Meng et al., 2004; Meng et al., 2002; Sundaresan et al., 1995). In some of these studies the time course of ROS production was reported to coincide with the time course of the growth factor stimulated tyrosine phosphorylation (Bae et al., 1997; Sundaresan et al., 1995). Addition of exogenous H_2O_2 positively affected growth factor-induced tyrosine phosphorylation, whereas enhanced levels of H_2O_2-quenchers, such as catalase, diminished this effect (Lee et al., 1998; Meng et al., 2004; Sundaresan et al., 1995). These observations paved the way for our understanding that ligand-induced ROS production, in the form of H_2O_2, regulates cellular signaling by mediating tyrosine phosphorylation of receptor tyrosine kinases and downstream effectors.

In phagocytes, molecular oxygen is reduced by a multicomponent nicotinamide adenine dinucleotide phosphate (NADPH) oxidase system generating superoxide ($O_2^{\cdot -}$), which is converted to H_2O_2 spontaneously or by enzymatic processes (May and de Haen, 1979). Non-phagocytic cells also contain similar NADPH oxidase systems,

capable of generating ROS in response to growth factors (De Deken et al., 2000; Lambeth, 2004; Suh et al., 1999). Protein tyrosine phosphatases were later identified as the direct targets of ROS produced in response to ligand binding to the receptor tyrosine kinases. PTP1B, in particular was reported to be susceptible to transient inactivation by reversible oxidation of the active site cysteine residue by H_2O_2 treatment *in vitro* (Salmeen et al., 2003; Van Montfort et al., 2003) and by insulin induced generation of H_2O_2 in mammalian cells (Mahadev et al., 2001; Meng et al., 2004). Under basal conditions when ROS levels are low, PTP1B suppresses the tyrosine phosphorylation and activation of the receptor PTK and acts as negative regulator of signaling. However, under ligand stimulated conditions, PTP1B is reversibly oxidized and inactivated by H_2O_2, triggering a transient hyperactivity of the receptor kinase that subsequently enhances down-stream signaling events. The production and maintenance of ROS is tightly regulated in the cell and when the level of excess ROS is normalized by ROS-scavengers, the activity of PTP1B is restored following its reactivation to the reduced active state by cellular reducing machinery, presumably by glutathione or thioredoxin, which allows the phosphatase to terminate the signal.

5.3 PTP1B Redox Regulation in Mammalian Cells

The PTP1B-OX conformation sensor intrabody allowed us to investigate location-based redox regulation of PTP1B in cell in response to insulin and exogenous H_2O_2. PTP1B is a cytosolic protein that is located on the cytoplasmic face of ER membranes through a C-terminal ER targeting motif (Frangioni et al., 1992). However, it is not known where the redox regulation is taking place in response to ROS generating physiological stimuli such as insulin or EGF. How PTP1B gains access to the activated RTKs is also still a matter of debate. Several possible mechanisms have been reported for PTP1B to dephosphorylate the substrates located at the plasma membrane. Some reports suggest that the activated insulin receptor (IR), epidermal growth factor receptor (EGFR), or platelet-derived growth factor receptor (PDGFR) are dephosphorylated after endocytosis (Boute et al., 2003; Haj et al., 2002; Romsicki et al., 2004). It was reported in HEK293 cells that the interaction between PTP1B and activated IR occurred intracellularly at perinuclear patches, presumably on the endocytic recycling

compartment (ERC) (Romsicki et al., 2004). In another example, using Chinese Hamster Ovary cells with stable expression of insulin receptor (CHO-IR), it was demonstrated that depletion of PTP1B by siRNA enhanced IR phosphorylation in the ERC emphasizing the strict compartmentalization of this regulation (Cromlish et al., 2006). It has also been demonstrated that PTP1B activity is spatially regulated in controlled microenvironments within the cell (Yudushkin et al., 2007).

In all the above cases PTP1B remains ER-bound, supporting the idea that ligand stimulated oxidative regulation of PTP1B probably happens in a membrane-proximal location. We showed that intrabody45, which is specific for PTP1B-OX, binds to PTP1B after insulin stimulation only when PTP1B is anchored to the ER (Figure 3.12). Interestingly oxidation of PTP1B and its subsequent recognition by intrabody45 is also favored for ER-bound PTP1B even in cells exogenously treated with H_2O_2. This suggests that exogenously administered H_2O_2 follow a controlled cellular uptake and distribution for localized oxidation of PTP1B. Interestingly, it has been reported very recently that the water channel Aquaporin-3 (AQP3) and Aquaporin-8 (AQP8) can facilitate controlled uptake of H_2O_2 into mammalian cells (Miller et al., 2010) and yeast (Bienert et al., 2007) and mediate downstream intracellular signaling. Miller et al, used molecular imaging with Peroxy Yellow 1 Methyl-Ester (PY1-ME), a chemo-selective fluorescent indicator for H_2O_2, to demonstrate that aquaporin isoforms AQP3 and AQP8, but not AQP1, can promote uptake of H_2O_2 through membranes in HEK293 cells. They also provided evidence that AQP3 is required for selective and regulated diffusion of NOX-generated extracellular H_2O_2 upon EGF stimulation. This recent finding of controlled uptake of exogenous H_2O_2 and its membrane association supports our observation of selective oxidation of ER-bound PTP1B following insulin or H_2O_2 treatment and its recognition by intrabody45. However, it will be important to check precisely the subcellular distribution of scFv45 and make sure this result is not a surrogate readout of intrabody distribution.

Efficient oxidation of ER-bound PTP1B is probably achieved by localized ROS generation by ER membrane resident Nox4. It has been reported that plasma membrane-proximal PTP1B is maintained in a low-activity state (Yudushkin et al.,

2007). This could be due to the oxidative inactivation of PTP1B following localized production of reactive oxygen species by ER-targeted NADPH oxidase 4 (NOX4) (Chen et al., 2008). Interestingly, Nox4 was reported to be colocalized with PTP1B on the cytoplasmic face of the ER membrane (Chen et al., 2008; Martyn et al., 2006). Chen et al., also reported that PTP1B, when overexpressed exclusively in the cytosol, is not subject to oxidation by Nox4 (Chen et al., 2008). In an oxidative environment around the membrane, the reducing machineries such as thioredoxin or glutaredoxin could themselves be oxidized and inactivated, and probably less capable of reactivating PTP1B. Localized production of H_2O_2 by the NOX complex may be essential to attain an effective concentration for mediating the oxidation of PTP1B. Also specific location-based generation of H_2O_2 could serve as a general mechanism for protection from catalase, GPx or peroxiredoxin. Peroxiredoxins, especially, are present at high concentrations in the cytosol in order to maintain homeostasis by removing H_2O_2 produced by normal cellular metabolism (Rhee et al., 2005).

5.4 Generation of scFv as PTP1B-OX Conformation Stabilizer

We have reported the generation of conformation sensor single chain variable fragment (scFv) antibodies that can recognize and stabilize the reversibly oxidized form of PTP1B (PTP1B-OX). PTP1B can be reversibly oxidized and adopt a novel conformation in the oxidized state. PTP1B-CASA mutant adopts that same conformation in a stable manner and therefore was used as an antigen for generating conformation-specific antibodies.

Using PTP1B-CASA as the antigen, the antibody phage display technique allowed us to select and isolate scFvs, which are specific to PTP1B-OX, from a large library. By adopting the subtractive panning strategy with the addition of up to 50X molar access of the reduced wild-type enzyme, we ensured that antibodies recognizing the common epitopes on both forms of the protein are depleted and those specific to PTP1B-CASA were enriched. For enriching specific scFvs from the phage display library we used biotinylated PTP1B-CASA and streptavidin bead capture. Initially we used a chemical biotinylation approach, which added biotin moieties to free amines non-

specifically. We found that this method caused significant reduction in PTP1B activity. Since we wished to isolate conformation-specific scFvs, we decided not to use this modification to isolate candidate scFvs. Consequently we adopted an *in vivo* biotinylation method in which a specific biotinylation tag was fused to the N-terminus of the target antigen (PTP1B-CASA). This biotinylation method allows specific addition of biotin moiety to a single Lys residue only in the tag leaving the rest of the protein unmodified. When we verified the activity of the wild type enzyme biotinylated by this method we found no change in activity, suggesting that this specific modification did not cause any structural change.

Specific individual scFvs were selected from an in-solution screen using an *in vitro* phosphatase assay to measure reactivation of PTP1B-OX that had been reversibly oxidized by H_2O_2. This screening method allowed us to isolate scFvs that not only bound to PTP1B-OX, but also stabilized the inactive conformation, as measured by decreased net phosphatase activity upon reactivation by reducing agent. Two of these candidate scFvs (scFv45 and scFv57) indeed showed significant inhibition of PTP1B-OX reactivation with an IC_{50} value ≤ 20 nm. We demonstrated that scFv45 bound only to PTP-OX but not to reduced PTP1B in an *in vitro* pull down assay and showed that this is a tight interaction with a K_d value ~ 50 nM and a slow off rate. The binding constants of scFv45 to both PTP1B-CASA and PTP1B-OX were similar, consistent with our initial structural analysis, which showed identical conformation for both of these proteins. The striking similarity of the binding between the CASA mutant and scFv45 in both reducing and non-reducing conditions also validated our *in vitro* approach to perform the subtractive panning under reducing condition for generation and selection of the specific scFvs.

5.5 PTP1B C-Terminal End Does not Interfere scFv Binding to PTP1B-OX

We have generated the antibody library against the CASA mutant of the commonly used catalytic domain of PTP1B (1-321). The full length form of the enzyme, however, exists as a 435-amino acid long protein. We wanted to verify whether the C-terminal segment affected scFv-PTP1B-OX interaction. Interestingly two *in vitro*

characterized scFvs (45 and 57) that inhibit the reactivation of the shorter (1-321) oxidized form, also inhibited the reactivation of a near full length form (1-394) of PTP1B-OX (i.e., ≥ 90% inhibition) (Figure 3.3). This observation indicated that the scFvs generated against the shorter form would recognize and stabilize the full-length form of the enzyme. This also indicates that the C-terminal segment of PTP1B did not interfere with the interaction between scFv and PTP1B-OX *in vitro* and that this specific scFv can be used as functional intrabody against endogenous PTP1B-OX in mammalian cells.

5.6 Selective Stabilization of PTP1B-OX by Conformation Sensor scFv

In generating effective active site-specific inhibitors, selectivity over closely related PTPs has been a challenging issue because of the highly conserved nature of the active site across the PTP family. TCPTP has the highest degree of similarity to PTP1B both in primary and tertiary structures. TCPTP displays ~75% sequence identity to PTP1B in its catalytic domain and the active sites of the two enzymes are even more closely related (Andersen et al., 2001). This sequence identity is reflected also in the tertiary structures of these two enzymes, as overlap between the crystal structures of these two proteins is also very close (Iversen et al., 2002). Because of this structural similarity, most potent catalytic site-directed PTP1B inhibitors show some degree of inhibition of TCPTP activity as well (Johnson et al., 2002; Stuible and Tremblay, 2010). Homozygous $TCPTP^{-/-}$ mice have severe hematopoietic defects and die soon after birth, whereas heterozygous $TCPTP^{+/-}$ mice are normal (You-Ten et al., 1997). It has been reported that both PTP1B and TCPTP regulate insulin signaling in a cooperative manner. So a potent PTP1B inhibitor with low degree of inhibition to TCPTP may not always be undesirable. However, a high degree of selectivity in PTP1B inhibitors is beneficial because of the chronic nature of the target diseases (i.e., diabetes and obesity).

Our approach for generating scFvs that can stabilize PTP1B-OX and inhibit its reactivation has resulted in remarkable selectivity over the reactivation of TCPTP-OX. The conformation sensor scFv45, which showed high selectivity for recognizing PTP1B-OX and inhibiting its reactivation, did not bind to oxidized TCPTP *in vitro* (Figure 3.3) or

in 293T cells treated with exogenous H_2O_2 or insulin (Figure 4.3). This is a noteworthy finding considering the fact that both of these closely related phosphatases were found to be reversibly oxidized upon insulin stimulation (Meng et al., 2004). Even though the crystal structures of PTP1B and TCPTP overlap considerably, thorough comparative analysis revealed that there are some structural differences (Iversen et al., 2002). One of these differences is in a region that is of particular interest as this motif constitutes the phospho-tyrosine loop, which in PTP1B becomes solvent exposed following oxidation. This observation prompted us to think that because of these differences, namely Cys32 (PTP1B)/His34 (TCPTP), Arg39 (PTP1B)/ Asp41 (TCPTP) and Phe52 (PTP1B)/Tyr54 (TCPTP), the phosphotyrosine loop could be presented differently upon oxidation and could provide selection attributes for the scFvs to recognize PTP1B-OX but not to TCPTP-OX. This possibility, however, has yet to be validated by systematic point mutations and binding experiments with the mutated proteins. PTPs are active in the reducing environment of cells under basal conditions. All PTPs share a conserved catalytic motif and even though they show high specificity for their physiological substrates, they all share a general mechanism of catalysis. Finding specific inhibitors directed to the catalytic site of PTPs is, therefore, challenging. This approach of inhibiting PTPs by preventing their reactivation through stabilization of the inactive oxidized conformation may represent a new way of inhibiting other redox sensitive PTPs selectively for pathophysiological intervention.

5.7 Conformation Sensor PTP1B-OX Demonstrates that the Sulphenyl-amide Structure Exists in vivo

In the reversible oxidation of PTP1B by H_2O_2, an unstable sulphenic acid form (Cys–S-OH) is generated initially. This sulphenic acid then undergoes a rapid condensation reaction to produce a unique five-membered cyclic sulphenyl-amide species, in which the sulfur atom of the active site cysteine is covalently linked to the nitrogen of a neighboring serine residue (Salmeen et al., 2003; Van Montfort et al., 2003). We observed that highly selective scFvs to PTP1B-OX *in vitro* can also bind to PTP1B in mammalian cells only following ROS production. The target antigen (PTP1B-

CASA) for antibody generation and selection is structurally identical to PTP1B-OX at the active site. One of the characterized specific scFvs (scFv45) bound to both CASA and PTP-OX with remarkably similar binding constants. More importantly all the *in vitro* selected scFvs when expressed as intrabodies, bound to endogenous PTP1B only when cells were treated with H_2O_2. The conformation sensor intrabody45 also bound to PTP1B in cells that are treated with insulin. All these results indicate that similar reversible redox modification involving a sulphenyl-amide structure formation also occurs in cells following exogenous treatment with H_2O_2 or stimulation with insulin, thereby removing concerns that the structure was an artifact of crystallization.

5.8 Implications of PTP1B-OX Conformation Sensor scFv in Insulin Signaling

We have demonstrated the application of a conformation sensor scFv as an intrabody to stabilize PTP1B-OX in insulin stimulated cells. We demonstrated that intrabody45 binds to PTP1B in insulin-stimulated cells and enhances tyrosine phosphorylation of IRβ and IRS-1. This enhancement was not due to changes in the steady-state amount of protein levels during insulin treatment or overexpression of the intrabody, as total protein levels of IR β subunit and IRS-1 were unchanged. Under reducing conditions (millimolar concentration of NAC), or in untreated cells, scFv45 did not bind to PTP1B implying a strict selectivity for the conformation sensor intrabody for PTP1B-OX. Similarly, scFv45 did not cause any changes in basal tyrosine phosphorylation of the effectors of insulin signaling, a finding that confirms that the conformation sensor intrabody does not affect the constitutive role of reduced active PTP1B in cell. It functions as an insulin-sensitizer rather than as an insulin-mimetic.

ROS produced following Insulin stimulation transiently oxidize the catalytic cysteine of PTP1B leading to its reversible inactivation and concomitant increase in tyrosine phosphorylation of the effectors of insulin signaling. The fact that enhanced tyrosine phosphorylation is coupled to both production of H_2O_2 and oxidative inactivation of PTPs, it is suggestive that redox status of PTPs presents an additional tier of regulation to fine-tune signaling. Our approach has shown a way to exploit this delicate regulatory mechanism by stabilizing PTP1B-OX, which favors the balance towards

tyrosine phosphorylation. Inhibition of PTP1B by preventing or delaying its reactivation by PTP1B-OX specific intrabody shifts the equilibrium toward phosphorylation and thereby enhances and prolongs insulin signaling events.

Our findings indicate that a high affinity intrabody to PTP1B-OX can inhibit the pool of PTP1B by keeping the oxidized enzyme in its inactive form and hindering its reactivation. This provided us the opportunity to dissect the status of both upstream and downstream elements of the signaling mechanism in response to insulin. Insulin-mediated receptor auto-phosphorylation allows the activated β subunit of the receptor to phosphorylate IRS-1 on several tyrosine residues. These phosphorylated tyrosine residues in specific motifs on IRS-1 serve as the docking sites for a number of signaling molecules that carry on the downstream signal transduction (Saltiel and Pessin, 2002). PTP1B dephosphorylates the tandem phospho-tyrosine residues (pYpY1162/1163) in the activation loop of the β-subunit of insulin receptor, which is a physiological substrate of the enzyme. We have reported here that stabilization of PTP1B-OX by intrabody45 in insulin-treated cells enhanced IRβ tyrosine phosphorylation at Y1162 and Y1163. This again directly shows how redox regulation of PTP1B can influence insulin signaling and the ability of a PTP1B-OX conformation specific scFv to manipulate these signaling events.

In our study the role of endogenously produced H_2O_2 following insulin stimulation in reversible regulation of PTP1B activity has been demonstrated. The conformation-sensor scFv45 binds to PTP1B-OX in both insulin and H_2O_2 treated cells but no interaction was observed in non-treated cells or in cells which were treated and processed under reducing conditions. Enhanced insulin signaling effect was demonstrated in presence of intrabody45 and such signal enhancement was attenuated when accumulation of H_2O_2 was blocked by catalase overexpression. Meng et al., showed that ectopic overexpression of catalase in Rat1 cells neutralizes intracellular H_2O_2 generated by insulin treatment and that this removal of H_2O_2 abrogates insulin mediated signaling events (Meng et al., 2004). Similar catalase mediated removal of ROS level was reported by either exogenous administration or adenoviral gene transfer for intracellular catalase to inhibit PDGF-induced tyrosine phosphorylation and MAPK activation (Sundaresan et al., 1995). Overexpression of intracellular catalase has also

been used to scavenge H_2O_2 generated by Nerve Growth Factor (NGF) stimulation of neuronal cells (Suzukawa et al., 2000). We also observed that overexpression of catalase in the cytosol suppressed downstream AKT phosphorylation in presence of scFv45. These observations indicate that the effects of scFv45 on both immediate and late events in insulin-induced signaling are dependent on the level of ROS.

We demonstrated that endogenous PTP1B-OX can be stabilized in mammalian cells to potentiate ligand mediated signaling. This is supported by three observations. First, intrabody45 binds to PTP1B under exogenous H_2O_2 or insulin treatment but shows no binding in cells which are kept untreated or treated under reducing conditions. Secondly, intrabody45 enhances and prolongs tyrosine phosphorylation of both IRβ and IRS-1, which is transduced downstream to yield a sustained increase in AKT activation. Thirdly, this intrabody45 mediated effect was diminished in presence of robust overexpression of catalase. Insulin stimulated rise in intracellular H_2O_2 transiently inactivates PTP1B and distorts the delicate balance between phosphatase and receptor kinase, allowing a peak in increased activation of the receptor and downstream signaling, which in the presence of intrabody45 is stabilized and prolonged.

5.9 Therapeutic Perspectives

PTP1B has been considered a validated target for treating diabetes and obesity for its direct negative regulatory role in insulin and leptin signaling. However generation of pharmaceutically acceptable drugs by targeting the active site of the enzyme has proven extremely challenging due to the biochemical properties of the catalytic site. Reversibly oxidized PTP1B forms a unique sulphenyl-amide structure involving the catalytic cysteine *in vitro*. This modification at the catalytic core causes profound conformational change at the active site. This structural modification was the basis for generating conformation sensor scFvs. The ability of the conformation sensor scFvs to specifically recognize PTP1B-OX both *in vitro* and in cell indicates that similar structural changes around the catalytic site of PTP1B occurs by ROS in a physiological setting, especially after insulin stimulation. Our data show that this oxidized inactive

conformation of PTP1B can be stabilized by specific scFv *in vitro* and in mammalian cells to potentiate insulin signaling. Since this oxidation induced conformation presents new binding sites at the surface of the enzyme, the stabilizing agents do not have to deal with the problematic catalytic site and therefore, may be clinically feasible to be considered as potent inhibitors. We also showed, by using PTP1B-OX-specific intrabody, that oxidation of PTP1B in response to insulin is a local event and possibly only a relevant pool, which is important for regulation of insulin signaling, is inactivated instead of the inactivation of the entire population. Therefore, ligand mediated oxidation of PTP1B probably serves as a tag to specify a particular pool and targeting this pool by specific molecules for selective inhibition will reduce complications of global effects from broad spectrum targeting and inhibition of the entire pool.

Overall, our data show that the *in vitro* subtractive panning approach allowed for the successful selection and isolation of PTP1B-OX conformation specific scFvs, which can be used to stabilize the reversibly oxidized conformation of PTP1B. These conformation sensor scFvs allowed us to dissect and subsequently manipulate the role of PTP1B as a negative regulator of insulin signaling. This approach can be extended to delineate the regulatory mechanism of PTP1B in other ligand-induced signaling cascades that triggers ROS production, where PTP1B is a known mediator or even to systems where the role of PTP1B or its redox regulation is not appreciated. In addition to providing insight into the redox regulation of PTP1B both *in vitro* and under ligand induced conditions in mammalian cells, our observations provide a novel therapeutic approach to inhibit this validated target for treating diabetes and obesity. Most importantly this allows us to generate novel ideas to inhibit important biological mediators for which conventional direct inhibitory approach is challenging.

5.10 Future Direction

5.10.1 Structural Study with Co-Crystal between scFv45 and PTP1B-OX: We have selected PTP1B-OX-specific scFv (i.e., scFv45) that shows high binding affinity and specificity. Using this well characterized scFv we will attempt to generate co-crystals with PTP1B-OX to determine the binding interface. Co-crystals of scFv45 and PTP1B-OX can provide structural coordinates, which are useful for identifying scFv-mimetic that could bind to the altered conformation of the reversibly oxidized PTP1B and inhibit its reactivation by reducing agents. Coordinates obtained from such a crystal structure may guide identification of such mimetic, either by de-novo design in silico or by modification of hits identified by screening a library of small molecules for compounds that disrupt the scFv-PTP1B interaction. After such screening and selection, various assays may be carried out to measure the biological or physiological activity (e.g., tyrosine phosphorylation in insulin signaling).

5.10.2 Use of Transgenic scFv Mouse as Animal Model: We have shown that scFv45 can act as a functional intrabody to recognize PTP1B-OX in mammalian cells. One interesting area to extend this research would be to investigate if the intrabody approach can be replicated in an animal model. Tissue specific expression of the intrabody, driven by Cre-mediated recombination with tissue specific promoter can be useful to investigate the effect of redox regulation of PTP1B in regulating relevant signaling pathways and physiological functions *in vivo*. It is also possible to generate whole-body “knock-in” mouse by expressing the intrabody using a general promoter. Investigating redox regulation in an animal model is extremely challenging because of the complexity of the animal and the lack of available tools and techniques. It will be very exciting to use this highly specific scFv simply as a tool to test whether ROS induced regulation of PTP1B occurs *in vivo*. It is also important to show the effect of the intrabody as a proof of principle to investigate whether the approach of generating inhibitor by stabilizing the oxidized inactive conformation of PTP1B is also possible in an animal model. The general readout from such an animal model would be glucose homeostasis, energy metabolism and weight gain.

5.10.3 Role of Redox Regulation of PTP1B in Cancer: Recent studies established a vital positive regulatory role of PTP1B in ErbB2 signaling, in particular in the context of mammary tumorigenesis and malignancy (Bentires-Alj and Neel, 2007; Julien et al., 2007). These studies have emphasized the potential importance of PTP1B as a therapeutic target in cancer. However, the molecular mechanism of this regulation remains to be understood. Lou et al., showed that the catalytic cysteine residue of PTP1B is oxidized to high stoichiometry in response to intrinsic reactive oxygen species production in human cancer cells (Lou et al., 2008). They demonstrated that oxidative inactivation of PTP1B in HepG2 and A431 cancer cells coincides with decreased tyrosine phosphorylation of cellular proteins and inhibition of anchorage-independent cell growth indicating a role of PTP1B redox regulation in the transformed phenotype of these cells. It will be interesting to understand whether redox regulation of PTP1B is also involved in the intricate mechanism of ErbB2 induced tumorigenesis. Using PTP1B-OX specific intrabody in this context will provide us insights to dissect whether there is role of ROS and PTP1B redox regulation in the mechanism of tumorigenesis and cancer progression.

5.10.4 Use of PTP1B-OX-Specific scFvs as Tools for Understanding the Fine Details of PTP1B Redox Regulation in Mammalian Cells: Our results indicate that PTP1B-mediated regulation of insulin receptor phosphorylation is regulated by the site of oxidation of specific PTP1B pool. Our finding suggests the idea that redox regulation of PTP1B is regulated in a localized manner in response to insulin stimulated receptor activation and concomitant production of ROS. Using the PTP1B-OX specific intrabody and sophisticated imaging techniques it may be possible to pinpoint these sites of PTP1B-RTK contact within cells upon ligand-mediated activation of the corresponding receptors.

Specific scFvs that have already been characterized to be sensors for PTP1B-OX, can be used as intrabodies to investigate the dynamics of PTP1B oxidation *in vivo*. By subcloning selected scFv from the phagemid vector into a mammalian expression vector with in-built EGFP or its spectral variants CFP or YFP we can observe and track

in real time, and in living cells, the dynamics of oxidative regulation of PTP1B upon stimulation of the cells with H_2O_2, insulin or ROS inducing ligands such as EGF or PDGF. A similar approach has been reported recently to follow the GTP-bound conformation of the small guanosine triphosphatase (GTPase) Rab6 by using GFP-tagged recombinant intrabodies expressed in the cytoplasm of cultured cells. We can use time-lapse microscopy to follow the dynamics of fluorescent scFvs bound to PTP1B-OX in live cells and compare it to the dynamics in non-stimulated cells. Nox4, a member of the family of NADPH oxidases, has recently been reported to mediate ROS production and subsequent regulation of the oxidation of PTP1B in response to insulin (Mahadev et al., 2004; Martyn et al., 2006). By using the PTP1B-OX specific intrabody, the role of Nox4 or other ROS generating system(s) in the regulation of PTP1B upon insulin stimulation can be investigated further.

Reference List

Amersham Biosciences Product Overview: Recombinant Phage Antibody System. (279400PL Rev-A). 2000.

Ahmad, F., Considine, R.V., Bauer, T.L., Ohannesian, J.P., Marco, C.C., and Goldstein, B.J. (1997). Improved sensitivity to insulin in obese subjects following weight loss is accompanied by reduced protein-tyrosine phosphatases in adipose tissue. Metabolism *46*, 1140-1145.

Ahmad, F., Li, P.M., Meyerovitch, J., and Goldstein, B.J. (1995). Osmotic loading of neutralizing antibodies demonstrates a role for protein-tyrosine phosphatase 1B in negative regulation of the insulin action pathway. JBiolChem *270*, 20503-20508.

Andersen, J.N., Mortensen, O.H., Peters, G.H., Drake, P.G., Iversen, L.F., Olsen, O.H., Jansen, P.G., Andersen, H.S., Tonks, N.K., and Moller, N.P. (2001). Structural and evolutionary relationships among protein tyrosine phosphatase domains. Mol Cell Biol *21*, 7117-7136.

Andris-Widhopf, J., Rader, C., Steinberger, P., Fuller, R., and Barbas, C.F. (2000). Methods for the generation of chicken monoclonal antibody fragments by phage display. Journal of Immunological Methods *242*, 159-181.

Aoki, N., and Matsuda, T. (2000). A cytosolic protein-tyrosine phosphatase PTP1B specifically dephosphorylates and deactivates prolactin-activated STAT5a and STAT5b. JBiolChem *275*, 39718-39726.

Arregui, C.O., Balsamo, J., and Lilien, J. (1998). Impaired integrin-mediated adhesion and signaling in fibroblasts expressing a dominant-negative mutant PTP1B. JCell Biol *143*, 861-873.

Bae, Y.S., Kang, S.W., Seo, M.S., Baines, I.C., Tekle, E., Chock, P.B., and Rhee, S.G. (1997). Epidermal growth factor (EGF)-induced generation of hydrogen peroxide - Role in EGF receptor-mediated tyrosine phosphorylation. Journal of Biological Chemistry *272*, 217-221.

Barford, D., Flint, A.J., and Tonks, N.K. (1994). Crystal structure of human protein tyrosine phosphatase 1B. Science *263*, 1397-1404.

Barford, D., Jia, Z., and Tonks, N.K. (1995). Protein tyrosine phosphatases take off. NatStructBiol *2*, 1043-1053.

Bentires-Alj, M., and Neel, B.G. (2007). Protein-tyrosine phosphatase 1B is required for HER2/Neu-induced breast cancer. Cancer Res *67*, 2420-2424.

Bienert, G.P., Moller, A.L., Kristiansen, K.A., Schulz, A., Moller, I.M., Schjoerring, J.K., and Jahn, T.P. (2007). Specific aquaporins facilitate the diffusion of hydrogen peroxide across membranes. J Biol Chem *282*, 1183-1192.

Bird, R.E., Hardman, K.D., Jacobson, J.W., Johnson, S., Kaufman, B.M., Lee, S.M., Lee, T., Pope, S.H., Riordan, G.S., and Whitlow, M. (1988). Single-chain antigen-binding proteins. Science *242*, 423-426.

Bjørbæk, C., Elmquist, J.K., Frantz, J.D., Shoelson, S.E., and Flier, J.S. (1998). Identification of SOCS-3 as a potential mediator of central leptin resistance. Molecular Cell *1*, 619-625.

Bjorge, J.D., Pang, A., and Fujita, D.J. (2000). Identification of protein-tyrosine phosphatase 1B as the major tyrosine phosphatase activity capable of dephosphorylating and activating c-Src in several human breast cancer cell lines. JBiolChem *275*, 41439-41446.

Boivin, B., and Tonks, N.K. (2010). Analysis of the redox regulation of protein tyrosine phosphatase superfamily members utilizing a cysteinyl-labeling assay. Methods Enzymol *474*, 35-50.

Boivin, B., Zhang, S., Arbiser, J.L., Zhang, Z.Y., and Tonks, N.K. (2008). A modified cysteinyl-labeling assay reveals reversible oxidation of protein tyrosine phosphatases in angiomyolipoma cells. Proc Natl Acad Sci U S A *105*, 9959-9964.

Boute, N., Boubekeur, S., Lacasa, D., and Issad, T. (2003). Dynamics of the interaction between the insulin receptor and protein tyrosine-phosphatase 1B in living cells. EMBO Rep *4*, 313-319.

Boyle, J.P., Thompson, T.J., Gregg, E.W., Barker, L.E., and Williamson, D.F. (2010). Projection of the year 2050 burden of diabetes in the US adult population: dynamic modeling of incidence, mortality, and prediabetes prevalence. Popul Health Metr *8*, 29.

Brown-Shimer, S., Johnson, K.A., Lawrence, J.B., Johnson, C., Bruskin, A., Green, N.R., and Hill, D.E. (1990). Molecular cloning and chromosome mapping of the human gene encoding protein phosphotyrosyl phosphatase 1B. ProcNatlAcadSciUSA *87*, 5148-5152.

Bryant, N.J., Govers, R., and James, D.E. (2002). Regulated transport of the glucose transporter GLUT4. Nat Rev Mol Cell Biol *3*, 267-277.

Buckley, D.A., Cheng, A., Kiely, P.A., Tremblay, M.L., and O'Connor, R. (2002). Regulation of insulin-like growth factor type I (IGF-I) receptor kinase activity by protein tyrosine phosphatase 1B (PTP-1B) and enhanced IGF-I-mediated suppression of apoptosis and motility in PTP-1B-deficient fibroblasts. MolCell Biol *22*, 1998-2010.

Burton, D.R., Barbas, C.F., 3rd, Persson, M.A., Koenig, S., Chanock, R.M., and Lerner, R.A. (1991). A large array of human monoclonal antibodies to type 1 human

immunodeficiency virus from combinatorial libraries of asymptomatic seropositive individuals. Proc Natl Acad Sci U S A *88*, 10134-10137.

Carney, W.P., Petit, D., Hamer, P., Der, C.J., Finkel, T., Cooper, G.M., Lefebvre, M., Mobtaker, H., Delellis, R., Tischler, A.S.*, et al.* (1986). Monoclonal antibody specific for an activated RAS protein. Proc Natl Acad Sci U S A *83*, 7485-7489.

Chen, H., Wertheimer, S.J., Lin, C.H., Katz, S.L., Amrein, K.E., Burn, P., and Quon, M.J. (1997). Protein-tyrosine phosphatases PTP1B and syp are modulators of insulin-stimulated translocation of GLUT4 in transfected rat adipose cells. J Biol Chem *272*, 8026-8031.

Chen, K., Kirber, M.T., Xiao, H., Yang, Y., and Keaney, J.F., Jr. (2008). Regulation of ROS signal transduction by NADPH oxidase 4 localization. J Cell Biol *181*, 1129-1139.

Cheng, A., Uetani, N., Simoncic, P.D., Chaubey, V.P., Lee-Loy, A., McGlade, C.J., Kennedy, B.P., and Tremblay, M.L. (2002). Attenuation of leptin action and regulation of obesity by protein tyrosine phosphatase 1B. DevCell *2*, 497-503.

Chernoff, J., Schievella, A.R., Jost, C.A., Erikson, R.L., and Neel, B.G. (1990). Cloning of a cDNA for a major human protein-tyrosine-phosphatase. ProcNatlAcadSciUSA *87*, 2735-2739.

Chiarugi, P., and Cirri, P. (2003). Redox regulation of protein tyrosine phosphatases during receptor tyrosine kinase signal transduction. Trends in Biochemical Sciences *28*, 509-514.

Clackson, T., Hoogenboom, H.R., Griffiths, A.D., and Winter, G. (1991). Making antibody fragments using phage display libraries. Nature *352*, 624-628.

Combs, A.P. (2010). Recent advances in the discovery of competitive protein tyrosine phosphatase 1B inhibitors for the treatment of diabetes, obesity, and cancer. J Med Chem *53*, 2333-2344.

Corpet, F. (1988). Multiple sequence alignment with hierarchical clustering. Nucleic Acids Res *16*, 10881-10890.

Cromlish, W.A., Tang, M., Kyskan, R., Tran, L., and Kennedy, B.P. (2006). PTP1B-dependent insulin receptor phosphorylation/residency in the endocytic recycling compartment of CHO-IR cells. Biochem Pharmacol *72*, 1279-1292.

Davies, E.L., Smith, J.S., Birkett, C.R., Manser, J.M., Andersondear, D.V., and Young, J.R. (1995). Selection of Specific Phage-Display Antibodies Using Libraries Derived from Chicken Immunoglobulin Genes. Journal of Immunological Methods *186*, 125-135.

De Deken, X., Wang, D., Many, M.C., Costagliola, S., Libert, F., Vassart, G., Dumont, J.E., and Miot, F. (2000). Cloning of two human thyroid cDNAs encoding new members of the NADPH oxidase family. J Biol Chem *275*, 23227-23233.

Deshane, J., Siegal, G.P., Alvarez, R.D., Wang, M.H., Feng, M., Cabrera, G., Liu, T., Kay, M., and Curiel, D.T. (1995). Targeted tumor killing via an intracellular antibody against erbB-2. J Clin Invest *96*, 2980-2989.

Drake, P.G., and Posner, B.I. (1998). Insulin receptor-associated protein tyrosine phosphatase(s): Role in insulin action. Molecular and Cellular Biochemistry *182*, 79-89.

Elchebly, M., Payette, P., Michaliszyn, E., Cromlish, W., Collins, S., Loy, A.L., Normandin, D., Cheng, A., Himms-Hagen, J., Chan, C.C.*, et al.* (1999). Increased insulin sensitivity and obesity resistance in mice lacking the protein tyrosine phosphatase-1B gene. Science *283*, 1544-1548.

Fischer, E.H., and Krebs, E.G. (1955). Conversion of phosphorylase b to phosphorylase a in muscle extracts. J Biol Chem *216*, 121-132.

Flint, A.J., Tiganis, T., Barford, D., and Tonks, N.K. (1997). Development of "substrate-trapping" mutants to identify physiological substrates of protein tyrosine phosphatases. ProcNatlAcadSciUSA *94*, 1680-1685.

Frangioni, J.V., Beahm, P.H., Shifrin, V., Jost, C.A., and Neel, B.G. (1992). The Nontransmembrane Tyrosine Phosphatase Ptp-1B Localizes to the Endoplasmic-Reticulum Via Its 35 Amino-Acid C-Terminal Sequence. Cell *68*, 545-560.

Frangioni, J.V., Oda, A., Smith, M., Salzman, E.W., and Neel, B.G. (1993). Calpain-Catalyzed Cleavage and Subcellular Relocation of Protein Phosphotyrosine Phosphatase-1B (Ptp-1B) in Human Platelets. Embo Journal *12*, 4843-4856.

Gagnon, E., Duclos, S., Rondeau, C., Chevet, E., Cameron, P.H., Steele-Mortimer, O., Paiement, J., Bergeron, J.J., and Desjardins, M. (2002). Endoplasmic reticulum-mediated phagocytosis is a mechanism of entry into macrophages. Cell *110*, 119-131.

Givol, D. (1991). The minimal antigen-binding fragment of antibodies--Fv fragment. Mol Immunol *28*, 1379-1386.

Goldstein, B.J., Bittner-Kowalczyk, A., White, M.F., and Harbeck, M. (2000). Tyrosine dephosphorylation and deactivation of insulin receptor substrate-1 by protein-tyrosine phosphatase 1B. Possible facilitation by the formation of a ternary complex with the Grb2 adaptor protein. JBiolChem *275*, 4283-4289.

Greenwood, J., Hunter, G.J., and Perham, R.N. (1991). Regulation of filamentous bacteriophage length by modification of electrostatic interactions between coat protein and DNA. J Mol Biol *217*, 223-227.

Griffiths, A.D., Williams, S.C., Hartley, O., Tomlinson, I.M., Waterhouse, P., Crosby, W.L., Kontermann, R.E., Jones, P.T., Low, N.M., Allison, T.J.*, et al.* (1994). Isolation of high affinity human antibodies directly from large synthetic repertoires. EMBO J *13*, 3245-3260.

Gross, S., Knebel, A., Tenev, T., Neininger, A., Gaestel, M., Herrlich, P., and Bohmer, F.D. (1999). Inactivation of protein-tyrosine phosphatases as mechanism of UV-induced signal transduction. Journal of Biological Chemistry *274*, 26378-26386.

Gu, F., Dube, N., Kim, J.W., Cheng, A., Ibarra-Sanchez, M.J., Tremblay, M.L., and Boisclair, Y.R. (2003). Protein tyrosine phosphatase 1B attenuates growth hormone-mediated JAK2-STAT signaling. MolCell Biol *23*, 3753-3762.

Guan, K.L., Haun, R.S., Watson, S.J., Geahlen, R.L., and Dixon, J.E. (1990). Cloning and Expression of A Protein-Tyrosine-Phosphatase. Proceedings of the National Academy of Sciences of the United States of America *87*, 1501-1505.

Haj, F.G., Markova, B., Klaman, L.D., Bohmer, F.D., and Neel, B.G. (2003). Regulation of receptor tyrosine kinase signaling by protein tyrosine phosphatase-1B. JBiolChem *278*, 739-744.

Haj, F.G., Verveer, P.J., Squire, A., Neel, B.G., and Bastiaens, P.I. (2002). Imaging sites of receptor dephosphorylation by PTP1B on the surface of the endoplasmic reticulum. Science *295*, 1708-1711.

Hannon, G.J. (2002). RNA interference. Nature *418*, 244-251.

Hao, L., Tiganis, T., Tonks, N.K., and Charbonneau, H. (1997). The noncatalytic C-terminal segment of the T cell protein tyrosine phosphatase regulates activity via an intramolecular mechanism. J Biol Chem *272*, 29322-29329.

Hoogenboom, H.R., Griffiths, A.D., Johnson, K.S., Chiswell, D.J., Hudson, P., and Winter, G. (1991). Multi-subunit proteins on the surface of filamentous phage: methodologies for displaying antibody (Fab) heavy and light chains. Nucleic Acids Res *19*, 4133-4137.

Hoogenboom, H.R., and Winter, G. (1992). By-passing immunisation. Human antibodies from synthetic repertoires of germline VH gene segments rearranged in vitro. J Mol Biol *227*, 381-388.

Huston, J.S., and Haber, E. (1996). An overview of the 1996 Keystone meeting. Exploring and exploiting antibody and Ig superfamily combining sites. Immunotechnology *2*, 253-260.

Huston, J.S., Levinson, D., Mudgett-Hunter, M., Tai, M.S., Novotny, J., Margolies, M.N., Ridge, R.J., Bruccoleri, R.E., Haber, E., Crea, R.*, et al.* (1988). Protein engineering of antibody binding sites: recovery of specific activity in an anti-digoxin single-chain Fv analogue produced in Escherichia coli. Proc Natl Acad Sci U S A *85*, 5879-5883.

Iversen, L.F., Moller, K.B., Pedersen, A.K., Peters, G.H., Petersen, A.S., Andersen, H.S., Branner, S., Mortensen, S.B., and Moller, N.P. (2002). Structure determination of T cell protein-tyrosine phosphatase. J Biol Chem *277*, 19982-19990.

Jendreyko, N., Popkov, M., Rader, C., and Barbas, C.F. (2005). Phenotypic knockout of VEGF-R2 and Tie-2 with an intradiabody reduces tumor growth and angiogenesis in vivo (vol 102, pg 8293, 2005). Proceedings of the National Academy of Sciences of the United States of America *102*, 12997-12997.

Jia, Z., Barford, D., Flint, A.J., and Tonks, N.K. (1995). Structural basis for phosphotyrosine peptide recognition by protein tyrosine phosphatase 1B. Science *268*, 1754-1758.

Johnson, T.O., Ermolieff, J., and Jirousek, M.R. (2002). Protein tyrosine phosphatase 1B inhibitors for diabetes. Nat Rev Drug Discov *1*, 696-709.

Julien, S.G., Dube, N., Read, M., Penney, J., Paquet, M., Han, Y., Kennedy, B.P., Muller, W.J., and Tremblay, M.L. (2007). Protein tyrosine phosphatase 1B deficiency or inhibition delays ErbB2-induced mammary tumorigenesis and protects from lung metastasis. Nat Genet *39*, 338-346.

Kenner, K.A., Anyanwu, E., Olefsky, J.M., and Kusari, J. (1996). Protein-tyrosine phosphatase 1B is a negative regulator of insulin- and insulin-like growth factor-I-stimulated signaling. JBiolChem *271*, 19810-19816.

Klaman, L.D., Boss, O., Peroni, O.D., Kim, J.K., Martino, J.L., Zabolotny, J.M., Moghal, N., Lubkin, M., Kim, Y.B., Sharpe, A.H.*, et al.* (2000). Increased energy expenditure, decreased adiposity, and tissue-specific insulin sensitivity in protein-tyrosine phosphatase 1B-deficient mice. MolCell Biol *20*, 5479-5489.

Krebs, E.G., and Fischer, E.H. (1956). The phosphorylase b to a converting enzyme of rabbit skeletal muscle. Biochim Biophys Acta *20*, 150-157.

Krieger-Brauer, H.I., and Kather, H. (1992). Human fat cells possess a plasma membrane-bound H2O2-generating system that is activated by insulin via a mechanism bypassing the receptor kinase. J Clin Invest *89*, 1006-1013.

Kwon, J., Lee, S.R., Yang, K.S., Ahn, Y., Kim, Y.J., Stadtman, E.R., and Rhee, S.G. (2004). Reversible oxidation and inactivation of the tumor suppressor PTEN in cells stimulated with peptide growth factors. Proc Natl Acad Sci U S A *101*, 16419-16424.

Lambeth, J.D. (2004). Nox enzymes and the biology of reactive oxygen. Nature Reviews Immunology *4*, 181-189.

LaMontagne, K.R., Jr., Flint, A.J., Franza, B.R., Jr., Pandergast, A.M., and Tonks, N.K. (1998). Protein tyrosine phosphatase 1B antagonizes signalling by oncoprotein tyrosine kinase p210 bcr-abl in vivo. MolCell Biol *18*, 2965-2975.

Lee, S.R., Kwon, K.S., Kim, S.R., and Rhee, S.G. (1998). Reversible inactivation of protein-tyrosine phosphatase 1B in A431 cells stimulated with epidermal growth factor. Journal of Biological Chemistry *273*, 15366-15372.

Lee, S.R., Yang, K.S., Kwon, J., Lee, C., Jeong, W., and Rhee, S.G. (2002). Reversible inactivation of the tumor suppressor PTEN by H2O2. Journal of Biological Chemistry *277*, 20336-20342.

Liang, F., Lee, S.Y., Liang, J., Lawrence, D.S., and Zhang, Z.Y. (2005). The role of protein-tyrosine phosphatase 1B in integrin signaling. JBiolChem *280*, 24857-24863.

Liu, F., Sells, M.A., and Chernoff, J. (1998). Protein tyrosine phosphatase 1B negatively regulates integrin signaling. CurrBiol *8*, 173-176.

Lo, Y.Y., and Cruz, T.F. (1995). Involvement of reactive oxygen species in cytokine and growth factor induction of c-fos expression in chondrocytes. J Biol Chem *270*, 11727-11730.

Lorenzen, J.A., Dadabay, C.Y., and Fischer, E.H. (1995). COOH-terminal sequence motifs target the T cell protein tyrosine phosphatase to the ER and nucleus. J Cell Biol *131*, 631-643.

Lou, Y.W., Chen, Y.Y., Hsu, S.F., Chen, R.K., Lee, C.L., Khoo, K.H., Tonks, N.K., and Meng, T.C. (2008). Redox regulation of the protein tyrosine phosphatase PTP1B in cancer cells. FEBS J *275*, 69-88.

Lowman, H.B., Bass, S.H., Simpson, N., and Wells, J.A. (1991). Selecting high-affinity binding proteins by monovalent phage display. Biochemistry *30*, 10832-10838.

Lynch, S.M., Zhou, C., and Messer, A. (2008). An scFv intrabody against the nonamyloid component of alpha-synuclein reduces intracellular aggregation and toxicity. J Mol Biol *377*, 136-147.

Mahadev, K., Zilbering, A., Zhu, L., and Goldstein, B.J. (2001). Insulin-stimulated hydrogen peroxide reversibly inhibits protein-tyrosine phosphatase 1B in vivo and enhances the early insulin action cascade. Journal of Biological Chemistry *276*, 21938-21942.

Marasco, W.A. (1997). Intrabodies: turning the humoral immune system outside in for intracellular immunization. Gene Ther *4*, 11-15.

Marasco, W.A., Haseltine, W.A., and Chen, S.Y. (1993). Design, intracellular expression, and activity of a human anti-human immunodeficiency virus type 1 gp120 single-chain antibody. Proc Natl Acad Sci U S A *90*, 7889-7893.

Martyn, K.D., Frederick, L.M., von Loehneysen, K., Dinauer, M.C., and Knaus, U.G. (2006). Functional analysis of Nox4 reveals unique characteristics compared to other NADPH oxidases. Cellular Signalling *18*, 69-82.

Mauro, L.J., and Dixon, J.E. (1994). 'Zip codes' direct intracellular protein tyrosine phosphatases to the correct cellular 'address'. Trends Biochem Sci *19*, 151-155.

May, J.M., and de Haen, C. (1979). Insulin-stimulated intracellular hydrogen peroxide production in rat epididymal fat cells. J Biol Chem *254*, 2214-2220.

McCafferty, J., Griffiths, A.D., Winter, G., and Chiswell, D.J. (1990). Phage antibodies: filamentous phage displaying antibody variable domains. Nature *348*, 552-554.

Meng, T.C., Buckley, D.A., Galic, S., Tiganis, T., and Tonks, N.K. (2004). Regulation of insulin signaling through reversible oxidation of the protein-tyrosine phosphatases TC45 and PTP1B. Journal of Biological Chemistry *279*, 37716-37725.

Meng, T.C., Fukada, T., and Tonks, N.K. (2002). Reversible oxidation and inactivation of protein tyrosine phosphatases in vivo. Molecular Cell *9*, 387-399.

Meng, T.C., Hsu, S.F., and Tonks, N.K. (2005). Development of a modified in-gel assay to identify protein tyrosine phosphatases that are oxidized and inactivated in vivo. Methods *35*, 28-36.

Miller, E.W., Dickinson, B.C., and Chang, C.J. (2010). Aquaporin-3 mediates hydrogen peroxide uptake to regulate downstream intracellular signaling. Proc Natl Acad Sci U S A *107*, 15681-15686.

Myers, M.P., Andersen, J.N., Cheng, A., Tremblay, M.L., Horvath, C.M., Parisien, J.P., Salmeen, A., Barford, D., and Tonks, N.K. (2001). TYK2 and JAK2 are substrates of protein-tyrosine phosphatase 1B. JBiolChem *276*, 47771-47774.

Nizak, C., Monier, S., del Nery, E., Moutel, S., Goud, B., and Perez, F. (2003). Recombinant antibodies to the small GTPase Rab6 as conformation sensors. Science *300*, 984-987.

Nizak, C., Sandrine, M., Goud, B., and Perez, F. (2005). Selection and Application of Recombinant Antibodies as Sensors of Rab Protein Conformation. Methods in Enzymology *403* 135-153.

Parmley, S.F., and Smith, G.P. (1988). Antibody-selectable filamentous fd phage vectors: affinity purification of target genes. Gene *73*, 305-318.

Perelson, A.S., and Oster, G.F. (1979). Theoretical studies of clonal selection: minimal antibody repertoire size and reliability of self-non-self discrimination. J Theor Biol *81*, 645-670.

Popkov, M., Jendreyko, N., McGavern, D.B., Rader, C., and Barbas, C.F. (2005). Targeting tumor angiogenesis with adenovirus-delivered anti-Tie-2 intrabody. Cancer Research *65*, 972-981.

Rhee, S.G., Kang, S.W., Jeong, W., Chang, T.S., Yang, K.S., and Woo, H.A. (2005). Intracellular messenger function of hydrogen peroxide and its regulation by peroxiredoxins. Curr Opin Cell Biol *17*, 183-189.

Roitt, I.M., and Delves, P.J. (2006). Roitt's essential immunology, 11th edn (Malden, Mass., Blackwell Pub.).

Romsicki, Y., Reece, M., Gauthier, J.Y., Asante-Appiah, E., and Kennedy, B.P. (2004). Protein tyrosine phosphatase-1B dephosphorylation of the insulin receptor occurs in a perinuclear endosome compartment in human embryonic kidney 293 cells. J Biol Chem *279*, 12868-12875.

Rondinone, C.M., Trevillyan, J.M., Clampit, J., Gum, R.J., Berg, C., Kroeger, P., Frost, L., Zinker, B.A., Reilly, R., Ulrich, R.*, et al.* (2002). Protein tyrosine phosphatase 1B reduction regulates adiposity and expression of genes involved in lipogenesis. Diabetes *51*, 2405-2411.

Ruberti, F., Capsoni, S., Comparini, A., Di Daniel, E., Franzot, J., Gonfloni, S., Rossi, G., Berardi, N., and Cattaneo, A. (2000). Phenotypic knockout of nerve growth factor in adult transgenic mice reveals severe deficits in basal forebrain cholinergic neurons, cell death in the spleen, and skeletal muscle dystrophy. J Neurosci *20*, 2589-2601.

Salmeen, A., Andersen, J.N., Myers, M.P., Meng, T.C., Hinks, J.A., Tonks, N.K., and Barford, D. (2003). Redox regulation of protein tyrosine phosphatase 1B involves a sulphenyl-amide intermediate. Nature *423*, 769-773.

Salmeen, A., Andersen, J.N., Myers, M.P., Tonks, N.K., and Barford, D. (2000). Molecular basis for the dephosphorylation of the activation segment of the insulin receptor by protein tyrosine phosphatase 1B. MolCell *6*, 1401-1412.

Saltiel, A.R. (2001). New Perspectives into the Molecular Pathogenesis and Treatment of Type 2 Diabetes. Cell *104*, 517-529.

Saltiel, A.R., and Pessin, J.E. (2002). Insulin signaling pathways in time and space. Trends Cell Biol *12*, 65-71.

Savitsky, P.A., and Finkel, T. (2002). Redox regulation of Cdc25C. Journal of Biological Chemistry *277*, 20535-20540.

Schatz, P.J. (1993). Use of peptide libraries to map the substrate specificity of a peptide-modifying enzyme: a 13 residue consensus peptide specifies biotinylation in Escherichia coli. Biotechnology (N Y) *11*, 1138-1143.

Schindler, T., Bornmann, W., Pellicena, P., Miller, W.T., Clarkson, B., and Kuriyan, J. (2000). Structural mechanism for STI-571 inhibition of Abelson tyrosine kinase. Science *289*, 1938-1942.

Seely, B.L., Staubs, P.A., Reichart, D.R., Berhanu, P., Milarski, K.L., Saltiel, A.R., Kusari, J., and Olefsky, J.M. (1996). Protein tyrosine phosphatase 1B interacts with the activated insulin receptor. Diabetes *45*, 1379-1385.

Singh, D.K., Kumar, D., Siddiqui, Z., Basu, S.K., Kumar, V., and Rao, K.V.S. (2005). The strength of receptor signaling is centrally controlled through a cooperative loop between Ca2+ and an oxidant signal. Cell *121*, 281-293.

Skerra, A. (1993). Bacterial expression of immunoglobulin fragments. Curr Opin Immunol *5*, 256-262.

Smith, G.P. (1985). Filamentous fusion phage: novel expression vectors that display cloned antigens on the virion surface. Science *228*, 1315-1317.

Sommavilla, R. (2010). Antibody Engineering: Advances in Phage Display Technology and in the Production of Therapeutic Immunocytokines. In Thesis (Zurich, Swiss Federal Institute of Technology - Zurich (ETHZ) and Philochem AG, Switzerland).

Stuible, M., and Tremblay, M.L. (2010). In control at the ER: PTP1B and the down-regulation of RTKs by dephosphorylation and endocytosis. Trends Cell Biol.

Suh, Y.A., Arnold, R.S., Lassegue, B., Shi, J., Xu, X., Sorescu, D., Chung, A.B., Griendling, K.K., and Lambeth, J.D. (1999). Cell transformation by the superoxide-generating oxidase Mox1. Nature *401*, 79-82.

Sundaresan, M., Yu, Z.X., Ferrans, V.J., Irani, K., and Finkel, T. (1995). Requirement for generation of H2O2 for platelet-derived growth factor signal transduction. Science *270*, 296-299.

Suzukawa, K., Miura, K., Mitsushita, J., Resau, J., Hirose, K., Crystal, R., and Kamata, T. (2000). Nerve growth factor-induced neuronal differentiation requires generation of Rac1-regulated reactive oxygen species. J Biol Chem *275*, 13175-13178.

Taghibiglou, C., Rashid-Kolvear, F., Van Iderstine, S.C., Le-Tien, H., Fantus, I.G., Lewis, G.F., and Adeli, K. (2002). Hepatic very low density lipoprotein-ApoB overproduction is associated with attenuated hepatic insulin signaling and overexpression of protein-tyrosine phosphatase 1B in a fructose-fed hamster model of insulin resistance. J Biol Chem *277*, 793-803.

Tiganis, T., Flint, A.J., Adam, S.A., and Tonks, N.K. (1997). Association of the T-cell protein tyrosine phosphatase with nuclear import factor p97. J Biol Chem *272*, 21548-21557.

Tonks, N.K. (2003). PTP1B: from the sidelines to the front lines! FEBS Lett *546*, 140-148.

Tonks, N.K., Diltz, C.D., and Fischer, E.H. (1988a). Characterization of the major protein-tyrosine-phosphatases of human placenta. J Biol Chem *263*, 6731-6737.

Tonks, N.K., Diltz, C.D., and Fischer, E.H. (1988b). Purification of the major protein-tyrosine-phosphatases of human placenta. JBiolChem *263*, 6722-6730.

Tonks, N.K., and Muthuswamy, S.K. (2007). A brake becomes an accelerator: PTP1B--a new therapeutic target for breast cancer. Cancer Cell *11*, 214-216.

Tonks, N.K., and Neel, B.G. (1996). From form to function: signaling by protein tyrosine phosphatases. Cell *87*, 365-368.

Van Montfort, R.L.M., Congreve, M., Tisi, D., Carr, R., and Jhoti, H. (2003). Oxidation state of the active-site cysteine in protein tyrosine phosphatase 1B. Nature *423*, 773-777.

Visintin, M., Quondam, M., and Cattaneo, A. (2004). The intracellular antibody capture technology: towards the high-throughput selection of functional intracellular antibodies for target validation. Methods *34*, 200-214.

Wiesmann, C., Barr, K.J., Kung, J., Zhu, J., Erlanson, D.A., Shen, W., Fahr, B.J., Zhong, M., Taylor, L., Randal, M.*, et al.* (2004). Allosteric inhibition of protein tyrosine phosphatase 1B. Nat Struct Mol Biol *11*, 730-737.

Wu, T.T., and Kabat, E.A. (1970). An analysis of the sequences of the variable regions of Bence Jones proteins and myeloma light chains and their implications for antibody complementarity. J Exp Med *132*, 211-250.

You-Ten, K.E., Muise, E.S., Itie, A., Michaliszyn, E., Wagner, J., Jothy, S., Lapp, W.S., and Tremblay, M.L. (1997). Impaired bone marrow microenvironment and immune function in T cell protein tyrosine phosphatase-deficient mice. J Exp Med *186*, 683-693.

Yuan, B., and Sierks, M.R. (2009). Intracellular targeting and clearance of oligomeric alpha-synuclein alleviates toxicity in mammalian cells. Neurosci Lett *459*, 16-18.

Yudushkin, I.A., Schleifenbaum, A., Kinkhabwala, A., Neel, B.G., Schultz, C., and Bastiaens, P.I. (2007). Live-cell imaging of enzyme-substrate interaction reveals spatial regulation of PTP1B. Science *315*, 115-119.

Zabolotny, J.M., Bence-Hanulec, K.K., Stricker-Krongrad, A., Haj, F., Wang, Y., Minokoshi, Y., Kim, Y.B., Elmquist, J.K., Tartaglia, L.A., Kahn, B.B.*, et al.* (2002). PTP1B regulates leptin signal transduction in vivo. DevCell *2*, 489-495.

Zinker, B.A., Rondinone, C.M., Trevillyan, J.M., Gum, R.J., Clampit, J.E., Waring, J.F., Xie, N., Wilcox, D., Jacobson, P., Frost, L.*, et al.* (2002). PTP1B antisense oligonucleotide lowers PTP1B protein, normalizes blood glucose, and improves insulin sensitivity in diabetic mice. Proc Natl Acad Sci U S A *99*, 11357-11362.